This electronic thesis or dissertation has been downloaded from the King's Research Portal at https://kclpure.kcl.ac.uk/portal/

Towards understanding how post-translational modifications influence the decision making process of p53

Davies, Jonathan

Awarding institution:
King's College London

The copyright of this thesis rests with the author and no quotation from it or information derived from it may be published without proper acknowledgement.

END USER LICENCE AGREEMENT

Unless another licence is stated on the immediately following page this work is licensed

under a Creative Commons Attribution-NonCommercial-NoDerivatives 4.0 International

licence. https://creativecommons.org/licenses/by-nc-nd/4.0/

You are free to copy, distribute and transmit the work

Under the following conditions:

- Attribution: You must attribute the work in the manner specified by the author (but not in any way that suggests that they endorse you or your use of the work).
- Non Commercial: You may not use this work for commercial purposes.
- No Derivative Works - You may not alter, transform, or build upon this work.

Any of these conditions can be waived if you receive permission from the author. Your fair dealings and other rights are in no way affected by the above.

Take down policy

If you believe that this document breaches copyright please contact librarypure@kcl.ac.uk providing details, and we will remove access to the work immediately and investigate your claim.

Download date: 25. Dec. 2024

Towards understanding how post-translational modifications influence the decision-making process of p53

A thesis submitted to

King's College London

For the degree of

Doctor of Philosophy

Presented by

Jonathan Hugh Davies

March 2024

Primary supervisor: Dr. Manuel Müller

Secondary supervisor: Dr. Alex Brogan

Who has seen the wind?
Neither I nor you:
But when the leaves hang trembling,
The wind is passing through.

Who has seen the wind?
Neither you nor I:
But when the trees bow down their heads,
The wind is passing by.

- Christina Rossetti

Acknowledgements

I dread to think how this thesis would read if I had not had the guidance, encouragement, and support of my primary supervisor, Dr. Manuel Müller. I am grateful to him for giving me the opportunity carry out this research, and all the support he provided along the way. Additionally, thank you to my secondary supervisor, Dr. Alex Brogan, for his advice and support.

Thank you to Dr. Karola Gerecht, Dr. Sofia Margiola, and Dr. Jasmine Wyatt for the training they provided in key techniques. Thank you as well to the Müller group as a whole, and the people in 120A, for their advice and friendship.

Most of the p53 variants referred to in this thesis were prepared by Dr. Sofia Margiola, Mateusz Hess, and Sonja Schneider, and their work is greatly appreciated.

I was assisted for 3 months by Maria Hancu, who carried out some of the early assays probing the pS15-pT18 crosstalk in p53. The data were incredibly useful for demonstrating an initial proof-of-principle and streamlining the assay process. Her work is greatly appreciated.

During my PhD, I undertook a 3-month placement at the Parliamentary Office of Science and Technology (POST). Thank you to Dr. Lydia Harriss for her support during that placement, and everyone at POST. It was a fantastic experience. Thank you, again, to Dr. Manuel Müller for supporting me in my application.

Thank you to Dr. Joanna Fox and Dr. Clemens Mayer for agreeing to co-examine this thesis, and to the EPSRC for funding the research.

Thank you to Hank Marvin, whose dulcet guitar tones formed the sonic backdrop to most of my writing.

Thank you to my family and my partner, Fliss, for their support. I could not have done it without you all.

Contents

1 Acknowledgements **3**

2 Abbreviations **8**

3 Abstract **11**

4 Introduction **12**

4.1 p53: the guardian of the genome 12

4.2 p53 structure and function 13

4.2.1 Overview 13

4.2.2 N-terminal domain 14

4.2.3 Tetramerization domain 15

4.2.4 C-terminal regulatory domain 16

4.2.5 DNA-binding domain 16

4.3 Mutations in cancer 20

4.4 Post-translational modifications of p53 20

4.4.1 Modifications of the N-terminal domain and proline-rich region . . 21

4.4.2 Modifications of the DNA-binding domain 25

4.4.3 Modifications of the linker and tetramerization domain 26

4.4.4 Modifications of the C-terminal regulatory domain 26

4.4.5 PTM crosstalk 28

4.5 Accessing site-specifically modified p53 34

4.5.1 Writer enzymes 35

4.5.2 Protein semi-synthesis 36

4.5.3 Genetic code expansion 37

4.6 Aims of this thesis 41

5 Accessing AcK120 p53 through genetic code expansion **44**

5.1 Introduction . . . 44

5.2 Results . . . 45

5.2.1 Production of unmodified p53 . . . 45

5.2.2 Expression of $p53_{K120ac}$ as an inclusion body . . . 46

5.2.3 Expression of soluble $p53_{K120ac}$ . . . 54

5.3 Conclusion . . . 59

6 Towards a p53-based transcription assay using fluorescent RNA aptamers *in vitro* **62**

6.1 Introduction . . . 62

6.2 Results . . . 64

6.2.1 iSpinach fluoresces in the presence of DFHBI . . . 64

6.2.2 $p53_{rec}$ does not induce transcription from naked DNA *in vitro* . . . 66

6.3 Conclusion . . . 68

7 Recreating the early stages of p53 activation *in vitro* **70**

7.1 Introduction . . . 70

7.2 Results . . . 72

7.2.1 p53 undergoes post-translational modification in nuclear extracts 72

7.2.2 Antibody validation . . . 80

7.2.3 Cofactor titration . . . 80

7.2.4 Data normalisation strategy development . . . 82

7.2.5 Reconstitution of known PTM cascades . . . 85

7.2.6 Exploration of cell stress conditions . . . 90

7.2.7 Using ADR-stressed A549 extracts to probe p53 "kill switches" . 92

7.3 Conclusion . . . 94

8 Outlook **96**

9 Materials and Methods **100**

9.1 Western blotting . . . 100

9.2 Polymerase chain reaction . . . 102

9.3 Plasmids and constructs . . . 102

9.4 Site-directed mutagenesis . . . 104
9.5 Calcium competent cell preparation . . . 105
9.6 Expression and refolding of unmodified p53 . . . 106
9.6.1 p53 expression via autoinduction . . . 106
9.6.2 Inclusion body preparation . . . 106
9.6.3 p53 purification from inclusion body . . . 107
9.6.4 Analytical RP-HPLC . . . 107
9.6.5 High-resolution mass spectometry . . . 108
9.6.6 p53 refolding . . . 108
9.6.7 Glutaraldehyde crosslinking . . . 109
9.7 Ulp1 expression and refolding . . . 110
9.8 Expression of $p53_{K120ac}$ inclusion bodies in DH10B cells . . . 111
9.9 Expressing $p53_{K120ac}$ inclusion bodies in BL21 cells . . . 111
9.9.1 Expression trial comparing "bulk" and "spike" acetyllysine addition 112
9.10 Expression and purification of soluble $p53_{K120ac}$ . . . 113
9.10.1 Expression . . . 113
9.10.2 Purification . . . 113
9.11 Expression trial comparing arabinose addition before or with IPTG addition 114
9.11.1 H6SUMO-p53 and H6SUMO-$p53_{SS}$, non-amber suppressed . . . 115
9.11.2 H6SUMO-$p53_{K120ac}$, amber suppressed, arabinose added before IPTG 115
9.11.3 H6SUMO-$p53_{K120ac}$, amber suppressed, arabinose added with IPTG 115
9.12 Expression trial comparing the solubility of H6SUMO-$p53_{K120ac}$ versus H6SUMO-$p53_{SSK120ac}$ . . . 116
9.13 Human cell culture . . . 116
9.13.1 Cell treatment with cisplatin or adriamycin . . . 116
9.13.2 Human cell harvesting . . . 117
9.13.3 Nuclear and cytoplasmic extract preparation . . . 117
9.14 *In vitro* transcription using T7 RNA polymerase . . . 118
9.15 *In vitro* transcription using HeLa nuclear extracts . . . 118
9.16 Reverse transcription . . . 119
9.17 Agarose gel electrophoresis of RNA . . . 119
9.18 Agarose gel electrophoresis of DNA . . . 119

9.19 Optimised crosstalk assay 120
9.20 Initial crosstalk assay 120
9.21 Broad crosstalk screen 120
9.21.1 Mild stripping 121
9.21.2 Harsh stripping 121
9.21.3 GuHCl stripping 121
9.22 Optimising cofactor concentrations for crosstalk assays 121
9.23 *In vitro* kinase assay using CK1 121
9.24 Densitometric and statistical analysis 122

10 Supplementary Materials **123**

Abbreviations

ALLN	N-acetyl-Leu-Leu-Norleucinal
APS	Ammonium persulfate
ATM	Ataxia-telangiectasia mutated
ATR	Ataxia telangiectasia and Rad3 related
BAX	BCL2 associated X, apoptosis regulator
BNIP3	BCL2 Interacting Protein 3
BSA	Bovine serum albumin
CBP	CREB-binding protein
CDK9	Cyclin-dependant kinase 9
CHK2	Checkpoint kinase 2
CK1	Casein kinase 1
CSN	COP9 signalosome
DEPC	Diethyl pyrocarbonate
DFHBI	3,5-difluoro-4-hydroxybenzylidene imidazolinone
DMEM	Dulbecco's Modified Eagle Medium
DMSO	Dimethyl sulfoxide
DNA-PK	DNA-dependant protein kinase
DUSP26	Dual-specificity phosphatase 26
DYRK2	Dual specificity tyrosine-phosphorylation-regulated kinase 2
E4F1	E4F transcription factor 1
E6AP	Ubiquitin-protein ligase E3A
EDTA	Ethylenediaminetetraacetic acid
EMSA	Electrophoretic Mobility Shift Assay

FBXO11	F-box protein 11
GSK3β	Glycogen synthase kinase-3 beta
GST	Glutathione S-transferase
HATU	Hexafluorophosphate Azabenzotriazole Tetramethyl Uronium
HF	Hydrofluoric acid
HIPK2	Homeodomain interacting protein kinase 2
HIPK4	Homeodomain interacting protein kinase 4
HPV	Human papillomavirus
IKKβ	Inhibitor of nuclear factor kappa-B kinase subunit beta
LRKK2	Leucine-rich repeat kinase 2
MAPK	Mitogen activated protein kinase
MDM2	Mouse double minute 2 homolog
MLS2	RING finger protein 184
MOPS	3-morpholinopropane-1-sulfonic acid
PBS	Phosphate-buffered saline
PIASy	Protein inhibitor of activated STAT protein gamma
PBRM1	Polybromo 1
PUMA	p53 upregulated modulator of apoptosis
PKCδ	Protein kinase Cδ
PP1A	Protein-phosphatase 1A
PP2A	Protein-phosphatase 2A
PP1C	Protein-phosphatase 1C
PRMT5	Protein Arginine Methyltransferase 5
PTM	Post-translational modification
PVDF	Polyvinylidene fluoride
RNA	Ribonucleic acid
RP-HPLC	Reverse-phase high-performance liquid chromatography
SDS	Sodium dodecyl sulfate
SDS-PAGE	Sodium dodecyl sulfate–polyacrylamide gel electrophoresis
SIRT3	Sirtuin 3
SWI/SNF	SWItch/Sucrose Non-Fermentable
TAF1	TATA-box binding protein associated factor 1

TCE	Trichloroethylene
TEMED	N,N,N',N'-tetramethylethylenediamine
TFA	Trifluoroacetic acid
TFIID	Transcription factor II D
TRAPP	TRAnsport Protein Particle

Abstract

p53 is a critical tumour suppressor protein that is inactivated in around 50 % of cancers. Following DNA damage, p53 directs the cell to repair the damage, stop growing, or self destruct. p53 is decorated by a range of post-translational modifications that modulate its ability to induce distinct responses to stress. This represents a "decision making process" that can be the difference between life and death, where survival of the cell and survival of the patient are potentially mutually exclusive. Despite decades of research, the mechanisms that determine specific cell fates induced by p53 remain elusive.

Site-specifically modified p53 variants are incredibly useful tools for elucidating the roles of PTMs in p53 regulation, being applicable to a range of *in vitro* assays. Our lab has unique access to p53 phosphorylated on the N-terminus. This thesis describes the generation of p53 acetylated at K120 using genetic code expansion. Though complete purification was not achieved, this variant was used as a positive control in subsequent assays. This thesis also describes the development of an *in vitro* transcription assay and an assay to interrogate PTM crosstalk interactions. Though *in vitro* transcription was not achieved, the latter assay successfully reconstituted two well-described crosstalk interactions in p53: the promotion of T18 phosphorylation by S15 phosphorylation and the promotion of K373 acetylation by phosphorylation of S15 and S20. This assay allows for PTM crosstalk to be interrogated in a complex, biologically relevant environment with site-specifically modified p53 as a predefined input. The assay has the potential to be modified to interrogate p53 crosstalk under different stress conditions, making it a powerful tool in our quest to understand how p53 is regulated by PTMs.

Overall, this thesis represents an important step towards understanding how p53 is regulated by PTMs, particularly how PTMs promote the addition of other PTMs, the cascades that determine cell fate.

Introduction

4.1 p53: the guardian of the genome

Around half of cancers possess mutations in one gene: TP53.[1] TP53 encodes a protein, "p53", that plays a key role in suppressing the development of cancer, such that people who inherit a non-functional p53 gene (Li-Fraumeni syndrome) have an approximately 75 % or 100 % chance of developing cancer if they are male or female respectively.[2] p53 was discovered in 1979, almost simultaneously, by multiple research groups in the USA, France and the UK as a protein that associated with simian virus 40 large T-antigen.[3] It has since been the subject of intense research, with a PubMed search for "p53" yielding over 100,000 results as of March 2024.

Under normal cellular conditions, p53 is expressed but its levels are kept low by the E3 ligase MDM2, which ubiquitinylates lysine residues on the C-terminus of p53, leading to its degradation by the proteosome.[4,5] Under conditions of cellular stress, such as DNA damage, p53 rapidly undergoes post-translational modification, leading to accumulation in the nucleus where it acts as a transcription factor (Fig. 4.1).[6] In the case of DNA damage, p53 may activate genes involved in DNA repair (e.g., DDB2), cell cycle arrest (e.g., p21), or apoptosis (e.g., BAX) depending on the type and severity of the damage. This allows for the repair or removal of damaged cells that are, or may soon become, cancerous. Because p53 is capable of inducing a range of different cell fates, its activity is fine-tuned through post-translational modification.[7,8] Other types of stress, such as hypoxia,[9] serum starvation,[10] or loss of cell matrix adhesion[11] may also activate p53, and p53 is capable of inducing apoptosis through transcription-independent mechanisms.[12] A more detailed description of p53 function and regulation is presented in the following sections, with a focus on p53's role as a transcription factor in response to DNA damage.

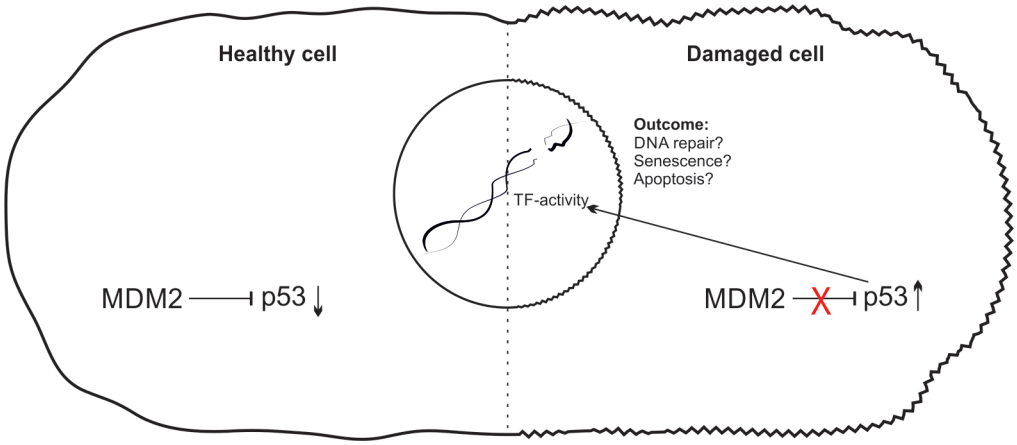

Figure 4.1: Schematic comparing p53 activity in a healthy versus damaged cell. In a healthy cell, p53 is suppressed by MDM2-mediated ubiquitinylation. Following DNA-damage, p53 accumulates, activates, and translocates to the nucleus where it acts as a transcription factor (TF), inducing the expression of genes that can lead to a range of cell fates.

4.2 p53 structure and function

4.2.1 Overview

p53 is 393 amino acids in length, with a mass of 43.7 kDa. It comprises two ordered domains: the DNA-binding domain and, connected via a short C-terminal linker, a tetramerization domain. Flanking these regions are the intrinsically disordered C-terminal regulatory domain and N-terminal domain (Fig. 4.2).[13] The N-terminal domain contains a transactivation domain subdivided into two subdomains, TAD1 and TAD2. Intrinsic disorder is a common feature of transcription factors and proteins situated at the center of protein interaction networks as it allows interactions to be made with a diverse range of other proteins.[13,14,15]

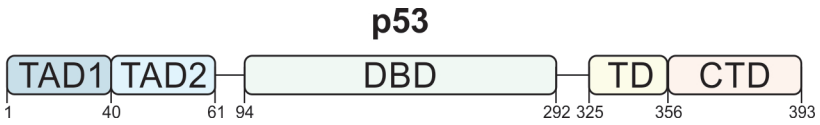

Figure 4.2: p53 scheme. Overall scheme of p53, showing the two transactivation domains (TAD1, TAD2), DNA-binding domain (DBD), tetramerization domain (TD) and C-terminal domain (CTD).

4.2.2 N-terminal domain

The N terminal domain (residues 1-94) is divided into a transactivation domain (TAD) and a proline-rich region. The TAD is subdivided into two subdomains, TAD1 (residues 1-40) and TAD2 (residues 40-61), and is the site of many key protein-protein interactions.[13] Under normal cellular conditions, TAD1 acts as the binding site for MDM2. This interaction takes place within a hydrophobic cleft on MDM2 and involves residues 15-29 of p53, which adopt an α-helical conformation upon binding to MDM2 (Fig. 4.3).[16,17] Following DNA damage, the N-terminal domain of p53 is rapidly phosphorylated, modulating the affinity of the TAD for different proteins. For example, T18 phosphorylation of p53 reduces the affinity of the TAD to MDM2 by about 20-fold,[17,18] allowing p53 to accumulate by preventing its degradation by MDM2. Phosphorylation of the TAD also promotes the interaction with p300/CBP,[19,20] a histone acetyltransferase that stabilizes and activates p53 through acetylation of key residues on the C-terminus.[21] With a suppressor (MDM2) and activator (p300) both competing for the same binding site on p53, the concentrations of both binding partners, as well as the phosphorylation status of the p53 N-terminus, are key factors in the stabilisation, accumulation and activation of p53 following cell stress.[13,22] The TAD also mediates interactions with components of the transcription machinery.[23,24,25]

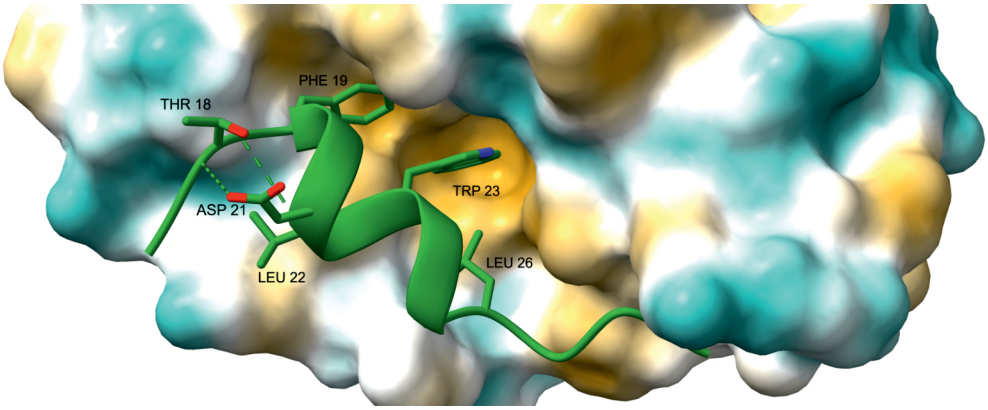

Figure 4.3: The p53-MDM2 interface. Crystal structure of a peptide corresponding to residues 17-29 of p53 bound to MDM2. Shown are residues of p53 that form key interactions with MDM2, as well as Thr18 and Asp21, which interact via hydrogen bonds. PDB 1YCR.[16]

4.2.3 Tetramerization domain

The tetramerization domain (residues 325-356) is a short, well-folded domain responsible for the formation of p53 tetramers. Tetramers of p53 are best described as dimers of primary dimers, with dimerisation occurring co-translationally and tetramers forming post-translationally.[13,26] Each monomer is made up of a β-sheet and α-helix linked by a sharp turn at G334.[27] Dimers form through formation of antiparallel interactions between the β-sheets of each monomer and antiparallel helix packing,[28] and tetramers form through hydrophobic interactions via the helix interfaces of each dimer (Fig. 4.4).[29] tetramerization promotes p53 binding to its consensus sequence[30] and may also promote nuclear retention of p53 by masking part of the C-terminal nuclear export signal.[31] There is evidence that regulation of the oligomeric state of p53 is a mechanism for regulating p53 activity: when p53 mutants that can only form dimers are expressed in H1299 cells, p53 remains in the cytosol and induces growth arrest. In contrast, expression of p53 capable of forming tetramers induces apoptosis.[32] Oligomerisation state can also be regulated by other proteins, for example 14-3-3 protein binding to the p53 C-terminus promotes tetramer formation. This interaction is strengthened by C-terminal phosphorylation of p53 at residues S366, S378 and T387.[33]

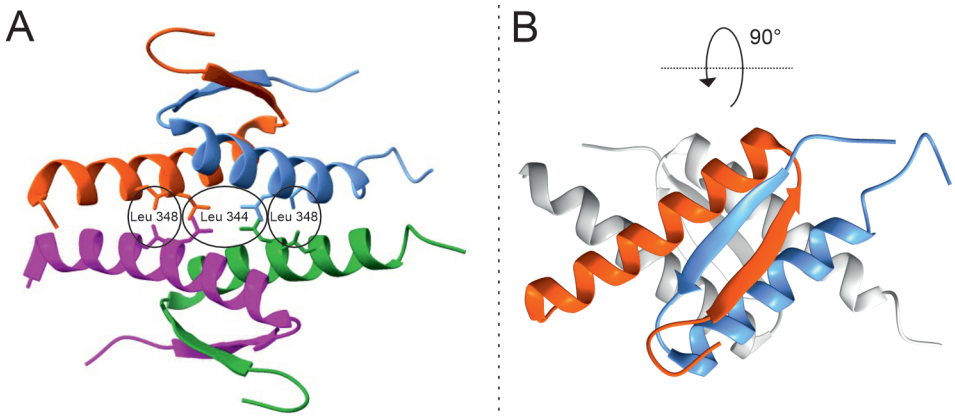

Figure 4.4: The tetramerization domain. A: Crystal structure showing the interface between p53 dimers with key residues highlighted. B: A different orientation highlighting the primary dimer, including the angle of rotation relative to A. Figure adapted from [13]. PDB: 8UQR.

4.2.4 C-terminal regulatory domain

The C-terminal regulatory domain (residues 356-393), like the N-terminal domain, is intrinsically disordered, but adopts secondary structure upon binding to protein partners.[34,35] This domain contains numerous positively-charged residues that bind DNA in a sequence-independent manner through electrostatic interactions with the phosphate backbone.[36] This enables p53 to "slide" across DNA, with the DNA-binding domain (covered in the next section) binding specifically to p53 response elements when they are encountered.[37,38] The C-terminal regulatory domain contains six lysine residues (370, 372, 373, 381, 382, and 386) that are subject to post-translational modifications that modulate its interactions with proteins and DNA, as well as p53 degradation.[39] These will be discussed in detail in section 4.4.4.

4.2.5 DNA-binding domain

The DNA-binding domain (residues 94-292) consists of an immunoglobulin-like β-sandwich and a DNA-binding surface that contains three loops (L1, L2 and L3). L1 forms part of a loop-sheet-helix motif that docks into the major groove of DNA, while L2 and L3, stabilised by a zinc ion that is coordinated by a histidine and three cysteine residues (C176, H179, C238, and C242).[40,41] The DNA-binding domain is relatively unstable, with a melting temperature of 44-45 °C.[42]

As p53 diffuses along the DNA strand in a non-specific manner (mediated by the C-terminal regulatory domain), the DNA-binding domain scans the DNA for its binding motif by frequent association and disassociation.[37] The p53 response element reads as two palindromic repeats of 5'-RRRCWWGYYY-3', where R represents a purine base (A/G), W represents A/T and Y represents a pyrimidine base (T/C), separated by up to 13 bases.[43] The most common central (CWWG) motif is CATG, and the strongest-binding sites have short (0-1bp) linkers.[44]

A crystal structure of the p53 DNA-binding domain bound to target DNA shows that two monomeric DNA-binding domains form dimers at each half site, forming tetramers even in the absence of a tetramerization domain. R248 on the L3 loop forms a key interaction with the minor groove. R273 interacts with the phosphate backbone and forms a salt bridge with D281, which also interacts with DNA via water. R280 forms a

key interaction with the conserved guanine in the half site, while K120, A276 and C277 interact with DNA in a sequence-specific manner, allowing modulation of target gene recognition (Fig. 4.5).[45,13]

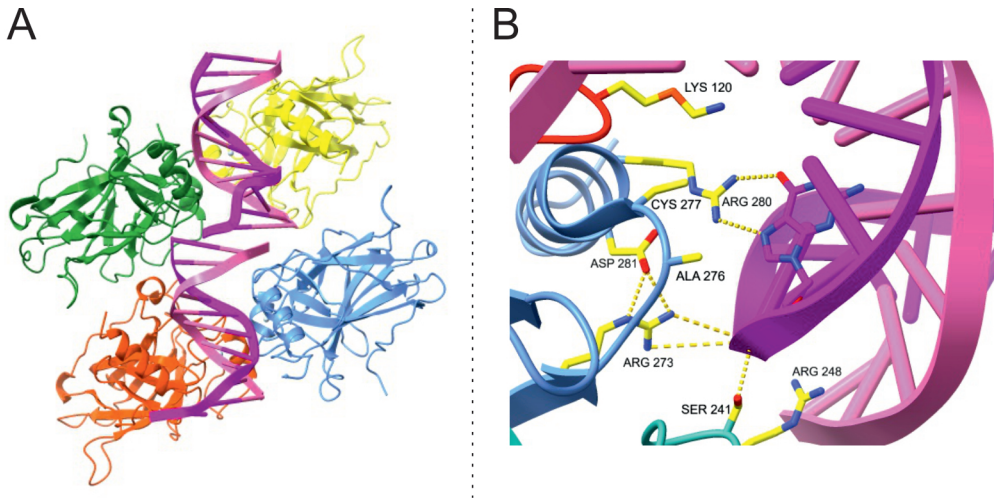

Figure 4.5: p53 bound to DNA. A: p53 binding to DNA as a tetramer. B: p53 binding to DNA as a monomer with key amino acids and interacions highlighted. PDB: 2AHI.

p53 and chromatin

p53 binds to DNA within the context of chromatin, and changes to chromatin influence the ability of p53 to bind to its response elements. In turn, p53 is capable of recruiting proteins that modify chromatin.[46] The fundamental unit of chromatin is the nucleosome: 1.65 turns (147bp) of DNA wrapped around an octomeric histone core. Two copies each of four core histones (H2A, H2B, H3 and H4) assemble into an octomer. A fifth histone, H1, coordinates the DNA at the point at which it links neighbouring nucleosomes (Fig. 4.6).[47,48] The packing of the nucleosomes in chromatin provides an additional layer of gene regulation, and this packing is controlled by post-translational modification of the histones. For example, PTMs that cause a net reduction in positive charge, such as phosporyl or acetyl groups, can weaken the interactions between the nucleosome and DNA, leading to decompaction of chromatin. Chromatin decompaction is largely associated with increased gene expression as the DNA becomes more accessible to the cell's transcription machinery.[49] Histone methylation is associated with both activation and repression of transcription. For example, trimethylation at lysine 4 of H3 (H3K4me3) promotes the recruitment of nucleosome remodelling factor (NURF), which binds to histones and mediates nucleosome sliding. This process is associated with an increase in transcriptional activity, especially in genes involved with development.[50] In contrast, trimethylation at lysine 9 of H3 (H3K9me3) can lead to recruitment of heterochromatin

protein 1 (HP1), which oligomerizes and non-covalently links nucleosomes, leading to a tightly packed chromatin structure that is inaccessible to the transcription machinery.[51] The list of histone PTMs is extensive,[52] and they work through a variety of mechanisms, exerting their effects directly via the interaction of histones with DNA and indirectly via the recruitment of proteins to nucleosomes. The tightly packed, transcriptionally repressive form of chromatin is called "heterochromatin"; the loosely packed, transcriptionally permissive form of chromatin is called "euchromatin".

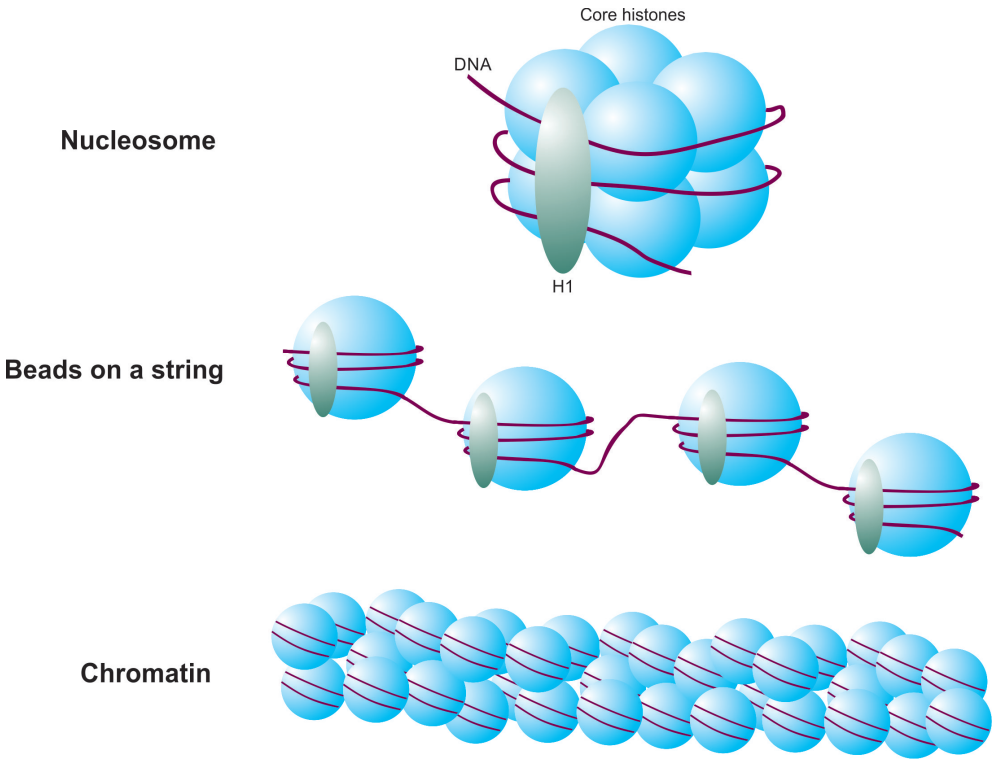

Figure 4.6: Shown are the different levels of DNA packaging: nucleosome, where DNA wraps around a core histone octomer, co ordinated by histone H1; "beads on a string", where multiple nucleosomes are connected via linker regions of DNA; and chromatin, where nucleosomes come together in a tightly packed structure.

p53 is capable of acting as a pioneer factor, binding to structurally inaccessible regions of chromatin.[53] Though p53 can bind DNA that is rendered accessible by chromatin, it has been shown to bind more favourably to DNA with high nucleosome occupancy, with p53 binding leading to nucleosome displacement.[54,55] Upon binding to chromatin, p53 can recruit histone acetyltransferases (HATs) such as CBP and adapter proteins such as TRAPP, which forms complexes with many different HATs and is associated with DNA repair.[56] This recruitment is dependant on prior C-terminal acetylation of p53.[57,58] A 2010 study investigated the ability of p53 to bind to its promoter sequence rotated in six different positions around the nucleosome and found that p53 binds most favourably when DNA is bent into the major groove in the CATG fragment, exposing the minor groove to solvent and protein binding.[59] A similar "bent" DNA conformation had been previously observed in crystal structures of p53 bound to DNA.[60]

4.3 Mutations in cancer

The majority of p53 mutations are missense substitutions (63 %), with nonsense substitutions (11 %) and frameshift deletions (5 %) being the next most common.[61,62] Most mutations occur in the DBD around several "hotspot" residues that together comprise 25-30 % of p53 mutations (Fig. 4.7).[63,64] The effect of these mutations on p53 vary, but can be broadly defined as either "contact" mutations, meaning they prevent the binding of p53 to target genes, or "structural" mutations, meaning they cause a conformational change in p53 that inactivates it another way, such as by destabilization.[65] Most p53 mutations are loss of function, though some mutations are gain of function and confer oncogenic properties onto p53.[66]

4.4 Post-translational modifications of p53

p53 function is regulated, in part, through a diverse range of post-translational modifications that decorate its surface, a few of which have been briefly described in the previous section. Phosphorylation, acetylation, and ubiquitinylation represent the most abundant PTMs in p53, however other modifications such as methylation, SUMOylation, neddylation, and ISGylation are present on p53. Additionally, p53 undergoes modification to its

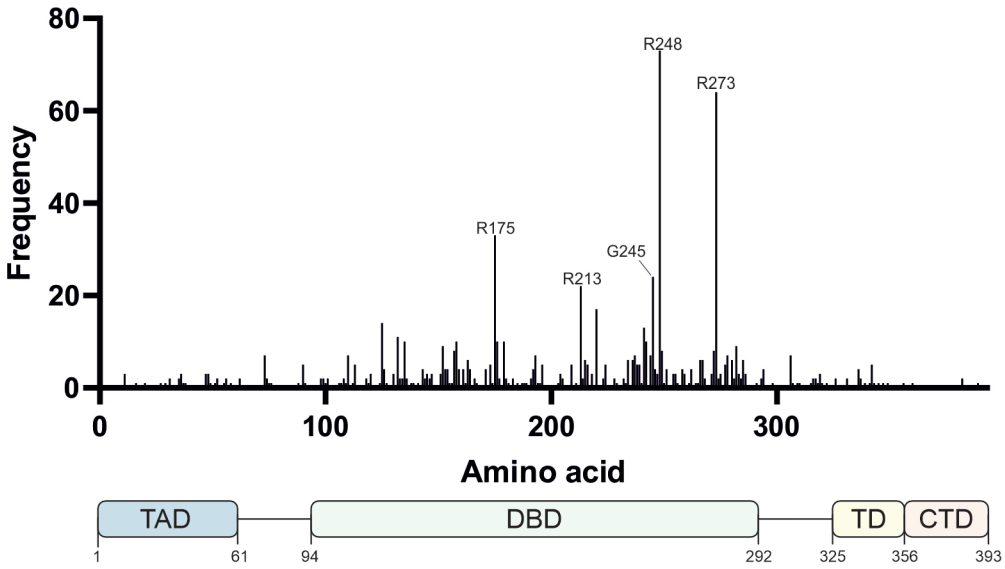

Figure 4.7: p53 residue mutation frequencies. Most oncogenic mutations in p53 occur in the DNA-binding domain (residues 94-292). The top five most frequently mutated residues in cancer are labelled. Data obtained from COSMIC. Also shown is a scheme of the domain structure of p53 aligned with the mutation data.[61,62]

protein backbone through the formation of isoaspartate on the N-terminus.[67] This section will describe the modifications that occur on each domain of p53 and how they influence p53 function (Fig. 4.8).

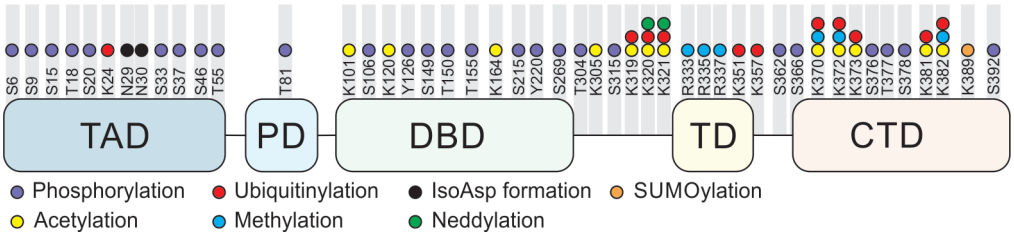

Figure 4.8: A summary of PTM events described on p53. Figure adapted from [39].

4.4.1 Modifications of the N-terminal domain and proline-rich region

Phosphorylation is the predominant PTM present on the N-terminus, with one residue (K24) a target for ubiquitinylation (Fig. 4.9A).[39,68] The N-terminal domain contains 10 residues where phosphorylation has been observed: S6, S9, S15, T18, S20, S33, S37, S46, T55, and T81.[39] Phosphorylation at many of these residues has been seen to occur

rapidly (0-5 hours) in cells after exposure to calpain inhibitors, adriamycin, IR or UV and, for the most part, promote the accumulation and activation of p53.[69,70,18,71,72] One exception is T55, which is constitutively phosphorylated in unstressed cells by TATA box binding protein-associated factor 1 (TAF1), promotes p53 degradation,[73,74,75] and can be dephosphorylated by PP2A.[74] Of these 10 phosphorylations, S15 and T18 are some of the more well-understood. Phosphorylation of S15 by is a key step in the activation of p53, with S15A mutant p53 showing a significantly reduced ability to induce expression of Bax, MDM2 or p21.[76] S15 has been shown to be phosphorylated by DNA-PK, ATM and ATR kinases[77,78,79] and is dephosphorylated by Wip1, a p53-target gene, and PP1C.[80,81] S15 phosphorylation is a prerequisite for T18 phosphorylation by CK1, which promotes p53 accumulation by inhibiting the interaction with MDM2.[82,20,83]

The individual roles of S6, S9, S20, S33, and S37 are less well-understood. These residues have been shown to be phosphorylated by multiple kinases, including CHK2 (S20), CK1 (S9), HIPK4 (S9), GSK3β (S33), CDK9 (S33), and DNA-PK (S37).[84,85,72,86,87,88,89] Dephosphorylation has been observed at S20 by DUSP26 and at S37 by DUSP26, PP1A, and PP2A.[90,81,89] Phosphorylation at these resides, along with S15 and T18, has been shown to promote the interaction of p53 with p300/CBP, leading to p53 acetylation.[20] S33, S46, and T81 are followed by a proline, and their phosphorylation has been shown to promote the binding of the peptidyl-prolyl isomerase Pin1, an enzyme that specifically isomerizes pSer/pThr-Pro motifs.[91,92,93] Pin1 knockout has been shown to lead to a reduction in p21, MDM2 and Bax transcription following DNA damage in a p53-dependant manner.[91,92,94] C-Jun N-terminal kinase (JNK) phosphorylation of T81 may promote complex formation between p53 and p73 promote the induction of p53 target genes.[71,95] S46 phosphorylation has been shown to increase the affinity of p53 for pro-apoptotic promoters such as p53AIP1 and BAX.[96,97] Though S46 phosphorylation has been reported to occur 4 hours after exposure of cells to UV or adriamycin, along with other N-terminal phosphorylations,[69] it has also been reported to only occur after long-term (24 hours) exposure to genotoxic stress, following translocation of DYRK2 to the nucleus.[98] As well as DYRK2, S46 can be phosphorylated by ATM, HIPK2, PKCδ, and p38 MAPK, and dephosphorylated by Wip1.[39,99,100,101,102]

These PTMs all affect the side chains of amino acids, however backbone modifications have also been observed on the N-terminus of p53. Residues N29 and N30 are capable

of spontaneous deamidation to succinimide, though this occurs in N29 much faster than in N30.[67] Succinimide hydrolyzes to isoaspartate or aspartate at an approximate 2:1 ratio. Protein l-isoaspartyl methyltransferase (PIMT) is capable of methylating the side-chain carboxyl of isoaspartate, forming a methyl-ester that rapidly decomposes back to succinimide, allowing a proportion of isoaspartate to be converted to aspartate as part of a repair process (Fig. 4.9B).[67,103] Interestingly, PIMT-mediated methylation of IsoAsp29 and IsoAsp30 may promote p53 degradation via MDM2, as the methylated intermediate has a greater affinity for MDM2 than isoaspartate and asparagine.[67]

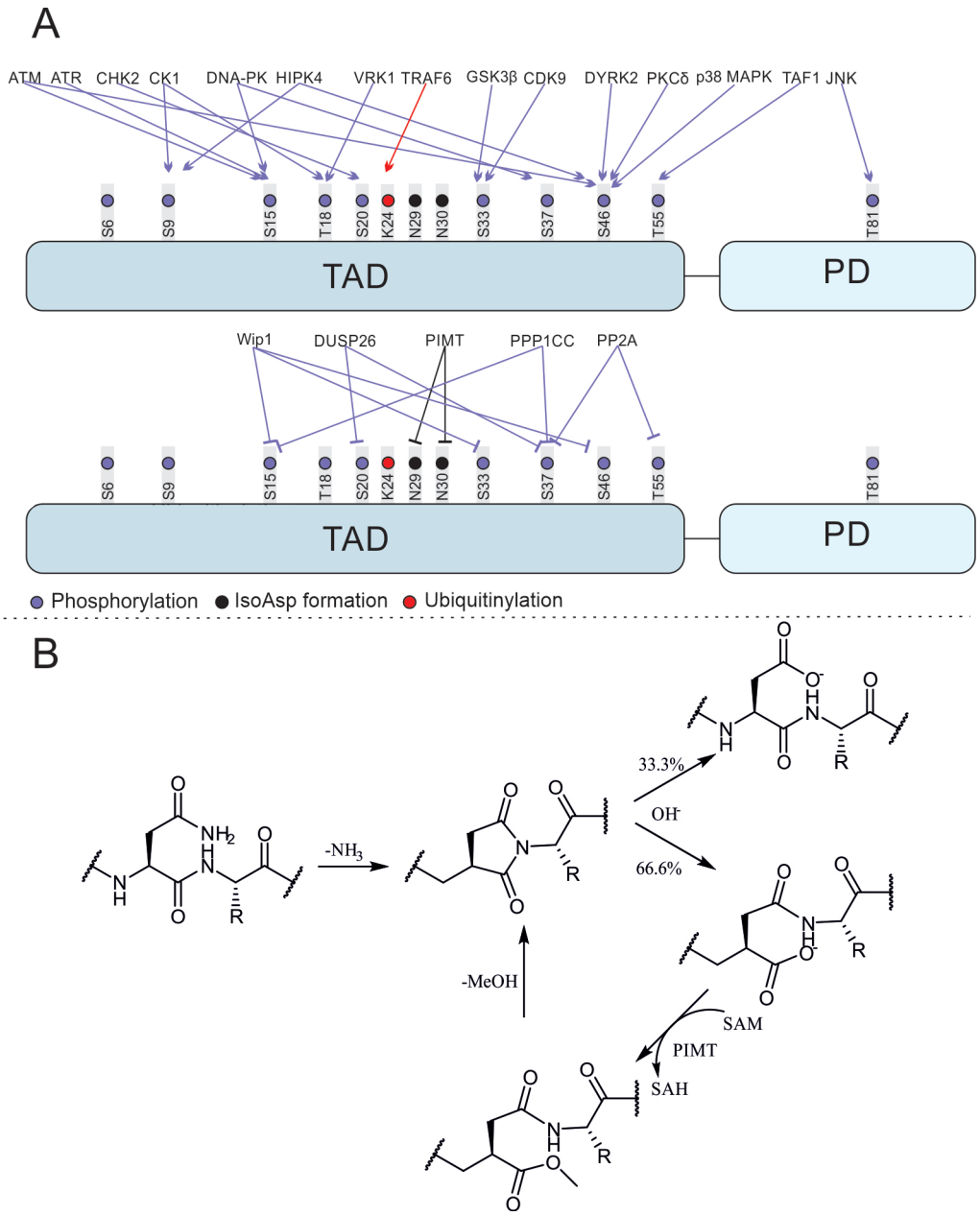

Figure 4.9: Isaspartate formation and summary of N-terminal PTMs. A: Summary of PTMs present on the N-terminus, including corresponding writers (top) and erasers (bottom). B: Mechanism of isoaspartate formation in proteins. Spontaneous deamidation of asparagine leads to formation of isoaspartate or aspartate, with the former able to undergo methylation by PIMT, allowing for decomposition back to succinamide.

4.4.2 Modifications of the DNA-binding domain

In contrast to the N-terminus, phosphorylation of the DNA-binding domain often has a repressive effect on p53 activity. S149, T150, and T155 phosphorylation by CSN has been shown to lead to p53 degradation,[104,105] while phosphorylation of S215 by Aurora-A has been shown to abrogate DNA binding and transcription of p53 target genes.[106] S269 phosphorylation may inhibit p53 activity by reducing its thermo-stability.[107,108] Phosphorylation of Y126 and Y220 by Src may lead to p53 degradation by promoting its interaction with Herc5, an E3 ligase that conjugates the ubiquitin-like modifier ISG15.[109,110] Not all phosphorylations on the DNA-binding domain are repressive: S106 phosphorylation by Aurora-A has been shown to inhibit the interaction of p53 with MDM2 (Fig. 4.10).[111]

There are three described acetylation sites on the DNA-binding domain: K101, K120, and K164 (Fig. 4.10). Of these, K120 is by far the most well-described. K120 can be acetylated by Tip60, MOF and MOZ and its acetylation has been shown to promote the induction of apoptotic genes such as PUMA and BAX.[112,113] Mechanistic insights into how K120 acetylation promotes apoptosis were provided by the purification of p53 DNA-binding domains site-specifically acetylated at K120, produced using genetic code expansion.[114,115,116] This will be described in detail in section 4.5.3.

The effect of acetylation at K101 and K164 are less well-understood, but both are acetylated by p300/CBP (Fig. 4.10).[117,118,119] Based on work carried out in mice, K164 acetylation may promote cell-cycle arrest and senescence,[118] and K101 acetylation may promote ferroptosis.[119]

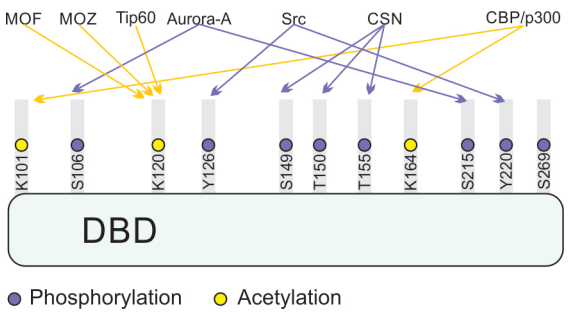

Figure 4.10: A summary of PTMs present on the DNA-binding domain, including corresponding writers.

4.4.3 Modifications of the linker and tetramerization domain

The predominant PTMs present on the linker domain and tetramerization domain are ubiquitinylation and ubiquitin-like modifiers, with the linker region also containing phosphorylation sites and the tetramerization domain containing methylation sites (Fig. 4.11).[39]

In the linker, T304 phosphorylation by Leucine-Rich Repeat Kinase 2 (LRRK2) has been demonstrated *in vitro*, and may promote p53 translocation to the nucleus.[120] S315 phosphorylation by CDK9 has been shown to lead to degradation.[121,88] Ubiquitinylation of the linker at K319, K320, and K321 by E4F1 has been observed in U2OS cells. Interestingly, p53 ubiquitinylated at these residues seems to localise on chromatin, with E4F1 expression promoting the induction of genes involved in growth arrest, such as p21.[122] K320 and K321 are also targets of neddylation, the conjugation of the ubiquitin-like modifier Nedd8, by FBXO11. FBXO11 knockout has been observed to increase the expression levels of p21 without affecting p53 levels, suggesting that neddylation at these residues may suppress p53 activity without promoting degradation.[123] Acetylation has been observed at K305 by p300/CBP following DNA damage in MCF-7 cells and may influence the ability of p53 to induce transcription, though precisely how is unclear as substitution of K305 with alanine or glutamine (acetyllysine mimetic) appears to reduce p53 transcriptional activity, while K305R appears to promote it.[124] K320 acetylation via PCAF occurs in response to DNA damage,[70,125] and may promote cell survival.[126,127] Recently, K320 acetylation was found to suppress the expression of BNIP3, a protein that promotes mitophagy.[128] Deacetylation of K320 by SIRT3 has been observed.[129]

Relatively few modifications have been observed on the tetramerization domain, with most PTMs that affect tetramerization occurring on the C-terminal regulatory domain.[130] p53 methylation by PRMT5 has been observed at R333, R335, and R337 and may promote nuclear import and binding to the p21 promoter.[131] p53 ubiquitinylation at K351 and K357 by MLS2 has been shown to promote nuclear export instead of degradation.[132]

4.4.4 Modifications of the C-terminal regulatory domain

The C-terminal regulatory domain is notable for its two clusters of three lysines (K370, K372, K373; and K381, K382, K386), all of which undergo acetylation, ubiquitinylation, and methylation. Between these two clusters are three residues (S376, T377 and S378)

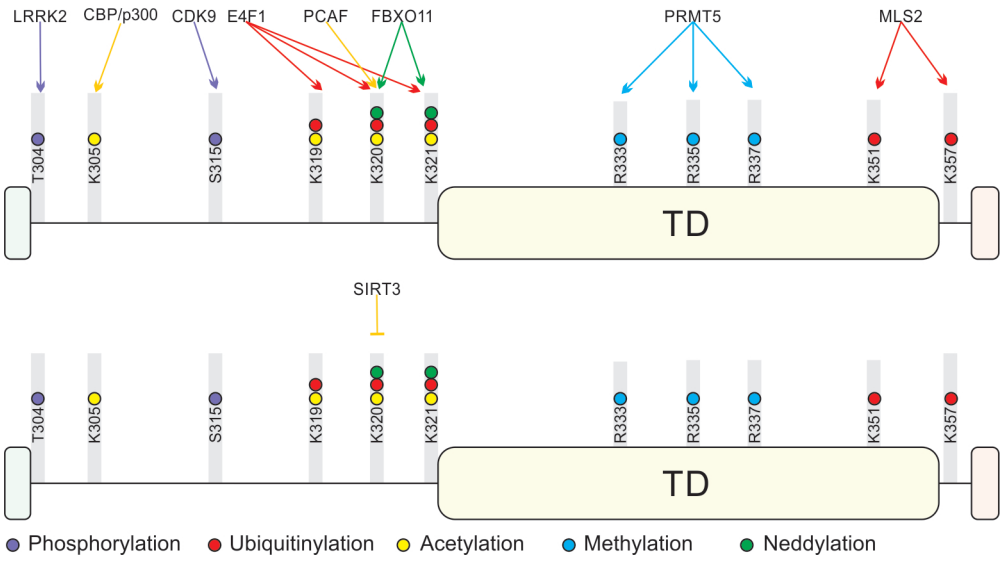

Figure 4.11: A summary of PTMs present on the linker and tetramerization domain, including corresponding writers (top) and erasers (bottom).

that undergo phosphorylation. In addition, the penultimate residue of p53 (S392) can also be phosphorylated (Fig. 4.12).[39]

Acetylation of p53 at K370, K372, K373, K381, K382, and K386 was first reported in 1997.[133] Despite being discovered over 26 years ago, there is still much uncertainty around the precise role of these acetylation sites.[134] Acetylation at these six residues is carried out by p300/CBP, and may increase p53s stability by preventing MDM2-mediated ubiquitinylation at the same sites and inhibiting the interaction with MDM2.[39,135,136,125] Interestingly, mutation of all C-terminal lysines to arginine in mouse embryonic stem cells has been shown to have a limited impact on p53 degradation, however transcription induction was suppressed.[137] p21 expression was found to be unaffected by simultaneous mutation of C-terminal lysines and K120 to arginine in transfected H1299 cells.[117] Though these results may suggest that acetylation is dispensable for p53 activity, deletion of the C-terminal regulatory domain in mouse models leads to dramatic and lethal phenotypes, with an increase in p53 activity.[138,139] In 2016, Wang *et al.* reported that, in its unacetylated form, the C-terminus acts as a docking site for the acidic domain of SET while bound to DNA, with SET preventing the recruitment of p300/CBP and subsequent acetylation of H3K18 and H3K27 on p53 target promoters. Mutation of C-terminal lysines to glutamine ($p53^{KQ/KQ}$) in mouse embryonic fibroblasts prevented the interaction with SET, leading to an increase in the expression of p53 target genes.[140] $p53^{KQ/-}$ mice

display increased expression of p53-target genes without elevated p53 levels compared to $p53^{WT/-}$ mice, suggesting that acetylation of the C-terminus predominantly regulates p53 activity rather than its stability.[141]

C-terminal acetylation has been shown to promote interactions of p53 with bromodomain-containing proteins. Bromodomains are evolutionary-conserved domains that selectively bind to acetylated lysines.[142] Following DNA binding, p300/CBP has been shown to bind to K382-acetylated p53 via its bromodomain, leading to acetylation of histones in the p21 promoter.[58,57,143] K373 and K382 acetylation has been shown to recruit TAF1, the largest subunit of TFIID, to the p21 promoter, leading to transcription *in vitro*.[144] K382-acetylated p53 has also been shown to recruit PBRM1, a subunit of a chromatin remodelling complex (SWI/SNF), to the p21 promoter.[145]

C-terminal lysines are also targets for other PTMs, including methylation and SUMOylation. Methylation has been observed at K370, K372, and K382 by Smyd2, Set7/9, and Set8 respectively.[146] K370 and K382 methylation may repress p53 activity, as depletion of the relevant methyltransferases enhances transcription of p53-target genes and apoptosis.[147,148] K372 methylation may promote p53 activity by suppressing the methylation of K370 and promoting the acetylation of K373 and K382,[148,149,150] though Set7/9 deletion in mouse models has been observed to not affect the induction of apoptosis or cell-cycle arrest following DNA damage.[151,152] K370 demethylation has been observed by LSD1.[153] SUMOylation of K389 by PIASy may suppress p53 activity by blocking C-terminal acetylation and promoting nuclear export.[154,155]

Constitutive S376 phosphorylation by GSK3β has been observed in unstressed cells, and dephosphorylation may promote the interaction of p53 with 14-3-3, a family of proteins that promotes p53 tetramer formation.[156,157] Phosphorylation of T377 (by LRKK2)[120] and S378 (by PKC, dephosphorylated by PP1 and PP2A),[33,158] and S392 (by IKKβ) in contrast, may promote this interaction.[159,160]

4.4.5 PTM crosstalk

"PTM crosstalk" covers a range of interactions between post-translational modifications,[161] some of which have been alluded to already. For this thesis, "crosstalk" will refer to the ability of one or more PTMs to influence the addition, function or removal of one or more other PTMs, with a focus on intra-protein PTM crosstalk in p53.

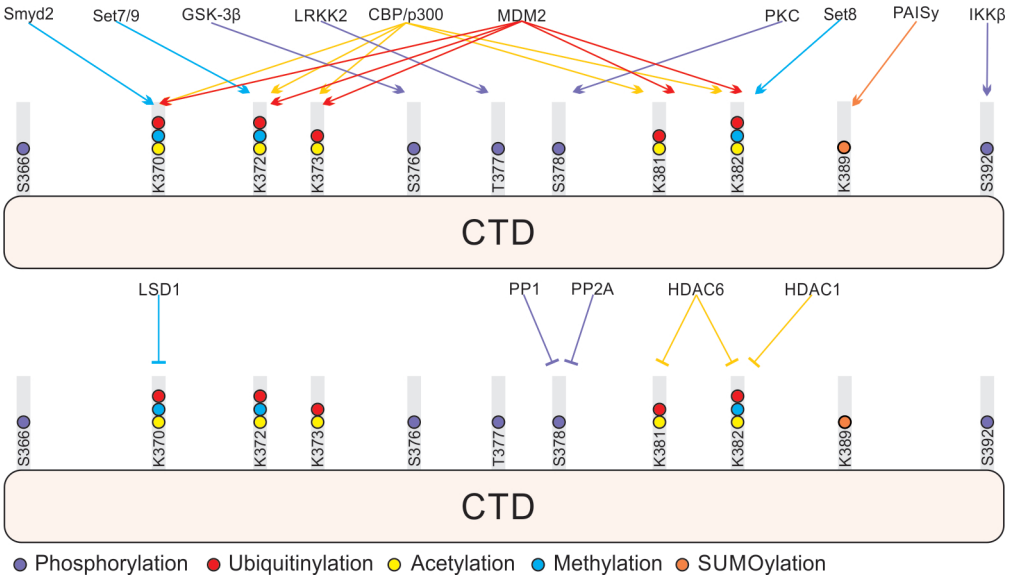

Figure 4.12: A summary of PTMs present on the C-terminus, including corresponding writers (top) and erasers (bottom).

The simplest form of PTM crosstalk occurs when writer enzymes for different modifications compete for the same residue. For example, many lysine residues on the C-terminal regulatory domain of p53 are targets for both acetylation and ubiquitinylation, with each modification precluding the addition of the other. Similar competition can also take place when modifications occur on different residues if the writer enzymes compete for the same binding site on the substrate. In p53, p300 and MDM2 compete for binding to the TAD1 domain, with phosphorylation of T18 inhibiting the interaction with MDM2 while promoting the interaction with p300.[17,18]

The p53 N-terminus is the site of many phosphorylations that display crosstalk. (Fig. 4.13) Some of these crosstalk interactions, such as the dependence of T18 phosphorylation by CK1 on prior S15 phosphorylation, are well-described. This dependence occurs due to CK1's consensus sequence, pSer/Thr-X-X-(X)-Ser/Thr, which requires a pre-phosphorylated serine or threonine 3 residues upstream of the substrate residue.[162,69,82] For other crosstalk interactions, the literature paints a less clear picture. A similar dynamic has been observed with CK1 phosphorylation of S9, which may be dependant on prior S6 phosphorylation.[72,86] In 2003, Saito *et al.* used an alanine scanning approach to probe the crosstalk relationships between phosphorylation events on the N-terminus of p53. They observed that S9 phosphorylation was abrogated in S6A p53. Interestingly, S6 phosphorylation was also abrogated in S9A p53. An S15A mutant of p53 showed abro-

gated S9, T18, and S20 phosphorylation, while S20A mutant p53 showed abrogated T18 phosphorylation. S33A mutant p53 showed abrogated S37 phosphorylation. S15, S33 and S46 phosphorylation were not abrogated by any mutations other than their own.[69] A 2005 study observed abrogation of S15 phosphorylation in S37A p53,[163] however this was not observed in prior or later studies.[69,164] In 2008, it was observed that mutagenesis of S37 to either alanine or aspartic acid led to abrogation of phosphorylation at S33, with S33 phosphorylation still observed in WT p53.[164] This is in contrast to prior studies which suggest S37 phosphorylation is dependant on prior S33 phosphorylation, and not *vice versa*.[69,165] The 2008 results suggest that both the phospho-null mimetic (S33A) and the phospho-mimetic (S33D) lead to abrogation of S37 phosphorylation,[164] a result that is difficult to interpret. There is *in vitro* evidence that S33 phosphorylation by GSK3β, which requires a phosphorylated serine four residues upstream of the substrate residue (Ser-X-X-X-pSer),[166] is dependant on prior phosphorylation of S37.[85] Altogether, there remains much uncertainty around the crosstalk relationships on the N-terminus and precisely how the phosphorylation cascades occur.

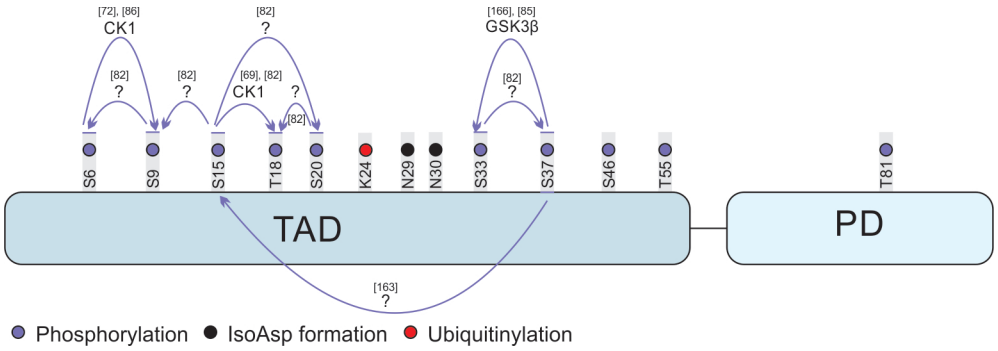

Figure 4.13: Summary of observed crosstalk interactions on the N-terminus, with proposed relevant enzymes. Arrows show where one modification promotes the addition of another. The endpoint modification is indicated by the colour of the arrow. The modification at the start of the interaction is indicated by the colour of the horizontal line at the base of the arrow.

On the C-terminus, phosphorylation may regulate C-terminal acetylation. Combined T377A/S378A mutants have been observed to show enhanced acetylation at K373 and K382, with combined T377D/S378D mutants showing reduced levels of K373 and K382 acetylation. Combined S366D/T387D mutants showed enhanced K373 and K382 acetylation, with no reduction in K373 and K382 acetylation observed for combined

S366A/T387A mutants.[167] However, like with N-terminal crosstalk relationships, the evidence is mixed: S378A mutation has been shown to promote K373 acetylation, along with mutation of S315 to either alanine or aspartic acid.[163] Evidence from mouse embryonic fibroblasts (MEFs) suggests that SET7/9 methylation at K369 (equivalent to K372 in human p53) may promote acetylation at K117, K317, K370 and K379 (equivalent to K120, K320, K373 and K382 in human p53, respectively) by promoting interactions with Tip60.[150] SUMOylation of K386 may preclude acetylation of nearby residues due to steric hindrance (Fig. 4.14).[154]

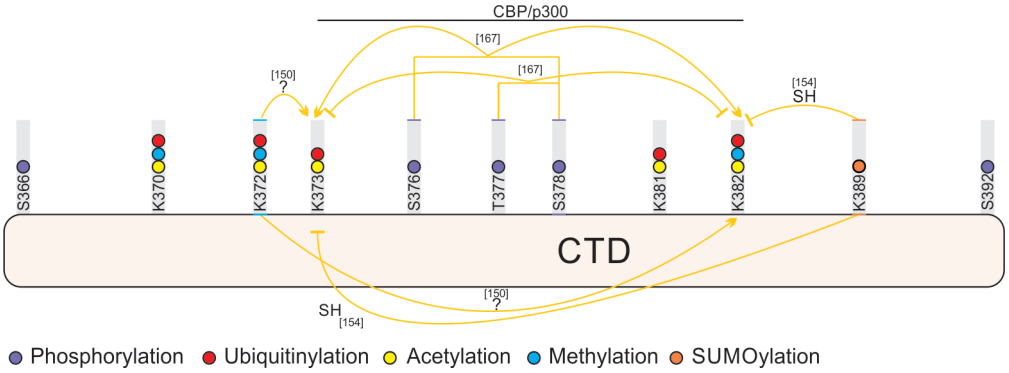

Figure 4.14: Summary of observed crosstalk interactions on the C-terminus, with proposed relevant enzymes. "SH" indicates steric hindrance. Arrows show where one modification promotes the addition of another, blunt arrows show where one modification inhibits the addition of another. The endpoint modification is indicated by the colour of the arrow. The modification at the start of the interaction is indicated by the colour of the horizontal line at the base of the arrow. Where starter modifications are connected by straight lines, crosstalk has only been demonstrated by mutagenesis of those residues in combination.

PTM crosstalk interactions spanning multiple domains

Some crosstalk interactions span multiple domains of p53 (Fig. 4.15). One example is the interaction between N-terminal phosphorylation and C-terminal acetylation, mediated by CBP/p300. N-terminal phosphorylation promotes p53's interaction with CBP/p300, which acetylates p53 on its C-terminus.[20,168]

p300 consists of several domains: the nuclear receptor interaction domain (RID), kinase-inducible domain (KIX), cisteine-histidine-rich region 1 (CH1)/Taz1, CH3/Taz2, and the interferon-response binding domain (IBiD). Between Kix and CH3/Taz2 is the catalytic core of p300, which comprises the bromodomain, CH2 and histone acetylatrans-

ferase (HAT) domain.[169,170] Kix, Ch1/Taz1, CH3/Taz2 and IBiD have been shown to interact with the N-terminal domain of p53.[19] Of the p300 domains that interact with p53 TAD1, CH3/Taz2 binds the tightest, followed by Taz1.[20,171]

Teufel *et al.* systematically assessed the binding affinities of Kix, CH1/Taz1, CH3/Taz2 and iBid for differentially phosphorylated N-terminal p53 peptides. They found that CH3/Taz2 and Taz1 binding is also affected the greatest extent by p53 N-terminal phosphorylation. In particular, phosphorylation at T18, which they found increased the affinity of CH3/Taz2 and Taz1 for p53 by 4.9- and 7-fold respectively.[20] Though one 2009 study suggests that pT18 p53 peptides show reduced affinity for CH3/Taz2 compared to unphosphorylated peptides,[171] the weight of evidence leans in the opposite direction. A similar (5-fold) increase in affinity between CH3/Taz2 and pT18 p53 TAD peptides, compared to unphosphorylated TAD, was observed in another study by Jenkins *et al.*[172] CH3/Taz2 of p300 has been shown to interact directly with T18 of p53 via hydrophobic interactions with the methyl group of T18. The increase in binding following T18 phosphorylation may be caused by interactions with two nearby arginine residues on p300 (R1731 and R1832). R1731A and R1732A mutants have been shown to bind the unphosphorylated TAD domain of p53 with similar affinity to that of wild-type CH3/Taz2. However, both mutants show twofold weaker affinity to the T18-phosphorylated TAD domain compared to the wild-type CH3/Taz2 sequence.[173] Phosphorylation of p53 at S15 has also been shown to increase the affinity of CH3/Taz2 by a factor of 6.3, while the affinity of CH1/Taz1 was increased by a factor of 3. Phosphorylation at S20 of p53 has been shown to increase the binding affinity of CH3/Taz2 and CH1/Taz1 by a factor of 4.3 and 6.0 respectively. Phosphorylation at S33 and S37 of p53 increases the affinity for CH1/Taz1 and CH3/Taz2 by 3.4- and 3.9-fold.[20]

It should be noted that many of the studies comparing the affinity of p53 for p300 domains made use of N-terminal p53 peptides that varied in length, with length of the p53 peptide drastically affecting its affinity for p300 domains. Initial work by Polley *et al.* calculated a K_D of $2.8 \pm 1.4 \times 10^{-5}$ M for p53 (1-39) binding to Taz1.[174] This is drastically lower than what Teufel *et al.* later calculated for p53 (1-57), 770 ± 50 nM.[20] Jenkins *et al.* directly compared the affinity of p53 (1-39) and p53 (1-57) for Taz2 and found that the 1-57 peptide had around 10x greater affinity for Taz2, compared to the 1-39 peptide.[172] A 13-61 peptide, as used by Lee *et al*, binds Taz2 and Taz1 with similar

affinity to the 1-57 peptide.[175]

Though individual N-terminal phosphorylation events can influence binding of p53 to p300 domains, the effect becomes more dramatic when multiple sites are phosphorylated.[20,172] For example, in a study comparing the binding affinities of various mono- and di-phosphorylated p53 (1-39) peptides with the Taz2 domain of p300,[172] p53 (1-39) phosphorylated at T18 and S20 was shown to have significantly greater affinity for CH3/Taz2 than either mono-phosphorylated peptide, likewise with p53 (1-39) phosphorylated at both S15 and S37. However, p53 phosphorylated at both S15 and S20 showed a similar affinity for CH3/Taz2 as p53 mono-phosphorylated at S15, and triple phosphorylation at S15, T18 and S20 showed a similar affinity to the di-phosphorylated peptides.[172] A 2010 paper by Lee *et al.* suggested a "rheostat" model, whereby the affinity of p53 for p300 is increased by increasing the number of phosphorylated residues on the N-terminus.[175] They observed that double-phosphorylation of p53 (13-57) at S15/T18, S15/S20, T18/S20 and S33/S37, and p53 (13-61) double-phosphorylated at S33/S46 and S37/S46 led to between 8.0- and 16.7-fold increase in affinity for CH3/Taz2 and between 4.6- and 11.8-fold increase in affinity for CH1/Taz1 compared to unphosphorylated p53 peptide. Fold changes in affinity for monophosphorylated p53 peptides for CH3/Taz2 and Taz1 compared to unphosphorylated peptides ranged from 0.9 (pT55 to CH3/Taz2) to 4.4 (pS46 to CH1/Taz1).[175] In agreement with prior work,[172] double phosphorylation increased the affinity of p53 for p300 more than the monophosphorylated peptides.[175] In contrast to previous work,[172] triple phosphorylation increased the affinity of p53 for p300 more than the constituent double-phosphorylated peptides. For p53 (13-57) phosphorylated at S15, T18, and S20, Lee *et al.* reported a fold-increase in affinity of of 22.2 and 11.4 for CH3/Taz2 and CH1/Taz1 respectively. The constituent double-phosphorylated peptides that showed the greatest fold-increase in affinity for CH2/Taz2 was pS15/pT18, with a fold-increase of 8.4 compared to unphosphorylated p53 (13-57). For CH1/Taz1, pS15/pS20 showed the greatest fold-increase in affinity compared to unmodified p53 (13-57), 16.7. A similar result was observed for p53 peptides triple-phosphorylated at S33, S37 and S46.[175] The "rheostat" model is bolstered by the earlier observation that hepta-phosphorylation of the p53 N-terminal peptides increases its affinity by 40- and 80-fold for CH3/Taz2 and CH1/Taz1 respectively, compared to unphosphorylated p53 peptides.[20]

These experiments carried out with peptides suggest that N-terminal phosphorylation

increases the affinity of p53 to p300. However, direct observation of subsequent acetylation is not possible on the peptide level when the crosstalk interactions span the length of a protein as large as p53. Recently, this crosstalk was directly observed *in vitro* using full-length p53 site specifically phosphorylated at S15 and S20 and purified p300.[168] These site-specifically modified p53 variants are powerful tools for the study of crosstalk interactions, especially when the interactions span distances longer than those accessible with peptides.

The crosstalk relationships that regulate modifications on the DNA-binding domain are poorly understood. As well as the observation that K369 methylation may induce K120 acetylation by promoting the interaction with Tip60,[150,119] mutation of S15 and S20 to aspartic acid has been shown to enhance the interaction of p53 with monocytic leukemia zinc protein (MOZ), an acetylatransferase that also acetylates p53 at K120. Mutation of S46 to aspartic acid, in contrast, reduced the interaction of p53 with MOZ.[176]

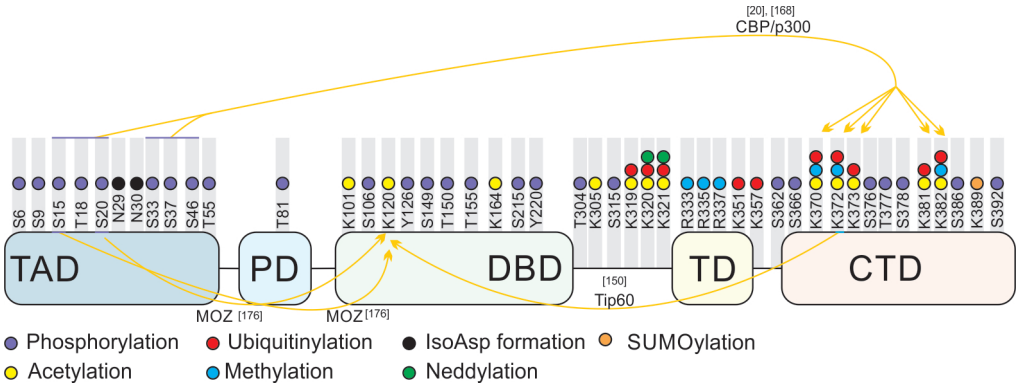

Figure 4.15: Summary of observed crosstalk interactions that span p53 domains, with proposed relevant enzymes. Arrows show where one modification promotes the addition of another. The endpoint modification is indicated by the colour of the arrow. The modification at the start of the interaction is indicated by the colour of the horizontal line at the base of the arrow.

4.5 Accessing site-specifically modified p53

Much of what we understand about the role of p53 PTMs relies on mutagenesis studies that either remove the capacity of a residue to be modified (typically through alanine mutation) or mimic the charge and length of a modified residue's side chain.[39] While significant advances have been made using mimetics, without case-by-case validation that

the mimetic sufficiently resembles the modified amino acid, this could lead to uncertainty when interpreting results. For example, a 2022 study that compared site-specifically phosphorylated 14-3-3 to 14-3-3 with aspartic acid at the same residue (S58) found differences in their oligomeric states at physiological 14-3-3 concentrations.[177] Mimetics are also irremovable, making it challenging to characterise the role of erasers in modulating protein function.

Site-specific modification overcomes many of these challenges. PTMs can be installed using writer enzymes, if the enzymes are known to install PTMs at only one or a few sites on a protein. This can be achieved via co-expression or *in vitro* using recombinant enzymes. Alternatively, PTMs can be installed using protein semi-synethsis or genetic code expansion, which do not require the writer enzyme for installation.

For p53, writer enzymes, protein semi-synthesis and genetic code expansion have been used to probe the effect of site-specific modification.[115,116,168]

4.5.1 Writer enzymes

One strategy for generating p53 bearing specific PTMs is to use the writer enzymes themselves, either *in vitro* or *in vivo* using co-expression. For example, Barlev *et al.* used purified CBP to acetylate recombinant p53, expressed in *E. coli*. They found that acetylated p53 bound TRAPP to a higher degree when it was acetylated compared to p53 that had been incubated with CBP, without acetyl-CoA.[57] Many writer enzymes can modify more than one residue on the same protein, limiting the choice of variants that can be produced using this method. If the modified residues are known in advance, site-directed mutagenesis can be used to generate more specific p53 variants. For example, Dumaz *et al.* observed that DNA-PK phosphorylates recombinant p53 *in vitro* at S15 and S37. By mutating S15 or S37 to alanine, the authors were able to generate monophosphorylated p53 at the residue that was not mutated. With this approach, they demonstrated that S15 phosphorylation promoted T18 phosphorylation by CK1 *in vitro*.[82] PTMs can be accessed *in vivo* by co-expressing the relevant writer enzyme with p53. For example, Bulavin *et al.* generated p53 phosphorylated at S33 and S46 by transfecting p53-negative cells with vectors expressing p53 and p38.[165] While these approaches have generated useful insights, the diversity of variants that can be produced with these methods is limited, as writer enzymes often modify more than one residue. Co-expression strategies will

also not generate homogeneously modified p53, as the endogenous writer enzymes are still present. Methods that enable the production of pure, homogeneous, site-specifically modified p53 would facilitate a deeper, more granular understanding of the role of PTMs in p53.

4.5.2 Protein semi-synthesis

Broadly speaking, protein semi-synthesis is carried out in three steps: Firstly, solid-phase peptide synthesis (SPPS) of a peptide containing a pre-modified amino acid. Secondly, the expression of a truncated form of a protein that lacks the chemically synthesised sequence; thirdly, ligation of the protein and peptide to yield the full-length protein bearing a specific PTM.[178]

SPPS involves immobilization of the C-terminal amino acid, protected on its N-α group by *tert*-butyloxycarbonyl (Boc) or fluorenylmethyloxycarbonyl (Fmoc), to a resin. Iterative cycles of N-α deprotection via TFA or piperidine (for Boc or Fmoc respectively) followed by coupling of the next amino acid, washing excess reagents between steps, allows for the synthesis of a pre-defined peptide sequence. Coupling is achieved by activation of the amino acid with a carbodiimide (e.g. N,N'-diisopropylcarbodiimide) in the presence of a nucleophilic catalyst such as oxyma or HATU. Cleavage from the resin is achieved via HF or TFA for Boc and Fmoc-SPPS respectively.[178,179]

Native chemical ligation requires that the N-terminal peptide fragment has a C-terminal α-thioester, with the C-terminal fragment carrying an N-terminal cysteine. Nucleophillic attack of the cysteine-sulphydryl group on the thioester results in *Trans*-thioesterification, followed by an *S*-to-*N* acyl shift to yield a native amide bond.[180]

p53 site-specifically phosphorylated at S15, S20, and both S15 and S20, has been produced using protein semi-synthesis (Fig. 4.16). Due to lack of a cysteine residues, this required mutation of M40 (located between the two TADs) to cysteine. It also required refolding of p53 following native chemical ligation. *In vitro* acetylation assays using p300 showed that p53 acetylation was enhanced about 1.5-fold, 2.2-fold, and 2.3-fold in when p53 was phosphorylated at S15, S20, and both S15 and S20 respectively.[168]

Protein semi-synthesis is ideal for insertion of modifications within the first 40 or so amino acids of a protein, though small proteins can be produced by the separate synthesis and ligation of multiple peptides.[181] C-terminal modifications can be accessed by taking

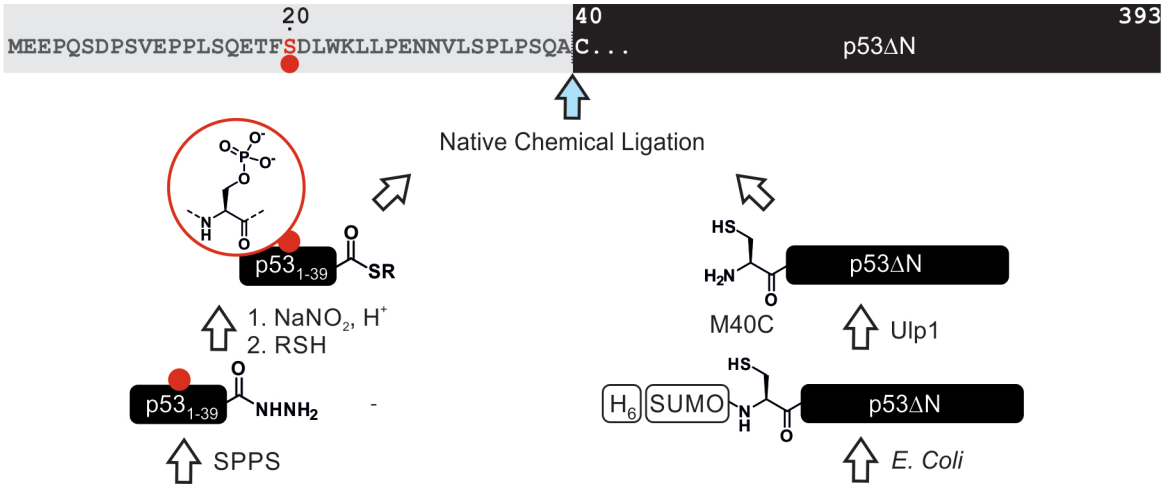

Figure 4.16: A semisynthetic strategy to produce site-specifically phosphorylated p53 at S20. Using SPPS, the p53 N-terminus (1-39) is synthesised with phosphoserine installed at position 20. Truncated p53 bearing a methionine corresponding to position 40 of full-length p53 is expressed in *E. coli* as a H6SUMO fusion. Following Ulp1 cleavage of H6SUMO, the synthetic peptide is ligated to the truncated p53 using native chemical ligation, producing full-length p53 phosphorylated at S20.

advantage of intein splicing, which occurs via thioester intermediate. By trapping the thioester intermiediate with a small molecule thiol and reacting it with a synthetic peptide bearing an N-terminal cysteine, site-specific modification is possible. The first instance of this was in 1998, when Muir *et al.* produced site-specifically phosphorylated C-terminal Src kinase (CSK).[182]. Since then, many other site-specifically modified proteins have been produced using this method.[183] For modifications in the middle of large proteins, protein semi-synthesis is less ideal as it would require the synthesis and ligation of multiple peptides.

4.5.3 Genetic code expansion

Genetic code expansion is a versatile and powerful method for introducing non-canonical amino acids (NCAAs) into proteins, particularly when the modifications are in the middle of large proteins. Briefly, genetic code expansion involves reassigning a codon (typically the amber stop codon, UAG) to an NCAA.[184] During translation, the ribosome mediates the coupling of amino acids in a sequence defined by triplet codons on mRNA. This is enabled by the prior coupling of amino acids to their corresponding tRNA via aminoacyl-tRNA synthetase.[185] When the ribosome reaches a stop codon, a release factor (RF)

binds, leading to the disassociation of the nascent peptide strand from the ribosome.[186]

In methogenic bacteria, the triplet that corresponds to the amber stop codon (UAG) in *E. Coli* encodes pyrollysine.[187,188] Using directed evolution approaches, the aminoacyl-tRNA synthetase can be engineered to load NCAAs on to the tRNA complementary to UAG. The NCAA can be incorporated selectively into a protein-of-interest by mutation of the desired codon to UAG and expressing the protein-of-interest alongside the engineered aminoacyl-tRNA synthetase and tRNA in *E. Coli*.[189] UAG is the least common stop codon in *E. Coli*, which minimises disruption of native *E. coli* genes.[186,190] This method is particularly convenient when the engineered synthetase and tRNA are already available.

As well as the the full-length modified protein, genetic code expansion often yields a truncated variant where the reassigned codon is read as an ordinary stop codon (Fig: 4.17).[184] Genetic code expansion is therefore less well-suited to the incorporation of multiple NCAAs than protein semisynthesis due to the increased number of truncated variants. However, a strain of *E.coli* with release factor 1 knocked out has been used to incorporate multiple NCAAs using genetic code expansion.[191]

Genetic incorporation of PTMs can lead to unique challenges depending on the PTM being incorporated. For example, bulky or negatively-charged amino acids may be unable to cross the cell membrane.[192] In *E. coli*, negatively-charged amino acids can cross cell membranes via the transporter DppA if they are part of a dipeptide. In the cytoplasm, the dipeptide can be cleaved by endogenous nonspecific peptidases, releasing the negatively-charged amino acid. This strategy has been used to genetically encode phosphotyrosine and a nonhydrolyzable analog of phosphotyrosine into multiple recombinant proteins.[193] If the NCAA is structurally very similar to an endogenous amino acid, this can lead to challenges when engineering the synthetase. Engineering a synthetase that specificially incorporates methyllysine has been challenging for this reason, as lysine is very similar in structure and highly abundant in cells.[194] This issue has been circumvented by genetic incorporation of a Boc-protected methyllysine, followed by deprotection post-translationally. This enabled the site-specific methylation of histone H3 at K9.[194] Using genetic code expansion, the effect of acetylation,[115] ubiquitinylation,[195] and methylation[196] on p53 have been probed. These experiments are described in more detail in the following sections

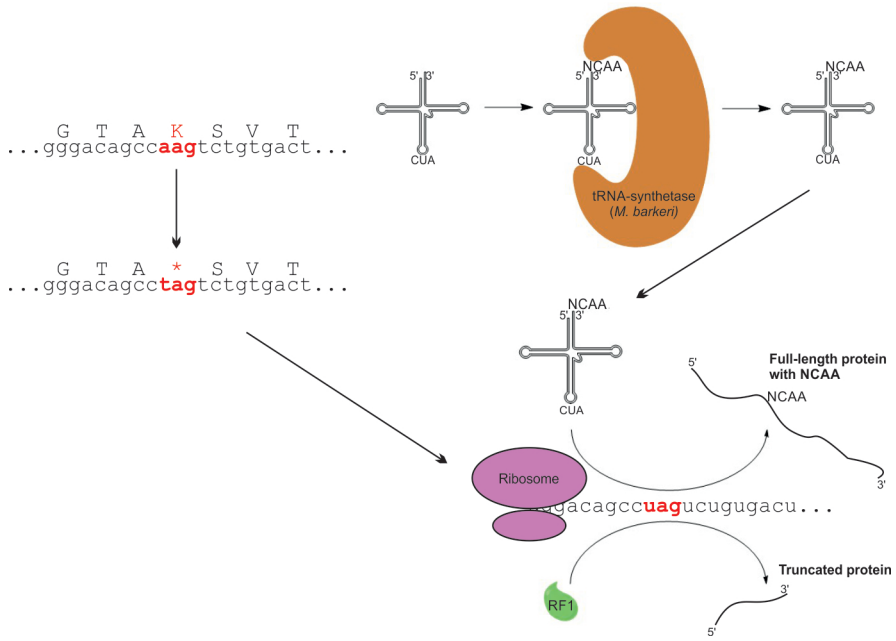

Figure 4.17: Genetic code expansion. Mutation of the desired residue (in this case, a lysine) to the amber stop codon allows for the subsequent incorporation of an NCAA at that position. Using an engineered tRNA synthetase from *M. barkeri*, a non-canonical amino acid (NCAA) can be conjugated to a tRNA corresponding to the amber stop codon. This allows for incorporation of the NCAA into the protein strand during translation. Because of the use of a stop codon, release factor 1 (RF1) binding may still occur leading to a truncated protein.

Site-specific acetylation of p53

Arberly *et al.* described the production of full-length p53 with stabilising mutations (M133L/V203A/N239Y/N268D), as well as the isolated DBD, with acetylated lysine incorporated at position 120.[115,197] Incorporation of acetyllysine into full-length p53 and the p53 DBD was confirmed by western blot using an anti-acetyllysine antibody. Acetylation of the DBD, but not full-length p53, was also confirmed by mass spectrometry. Using the site-specifically acetylated DBD, the authors investigated the ability of the K120-acetylated DBD to bind DNA at physiological salt concentrations. They found that, without K120 acetylation, p53 does not discriminate between its promoter sequences and random oligonucleotides at an ionic strength of 150 mM. Upon increasing the ionic strength, non-target binding was weakened, whereas promoter binding is unaffected. Similarly, K120 acetylation led to increased specificity by decreasing the affinity for random DNA and some weaker promoters, though the exact mechanism is complex. Access to K120 acetylated p53 DBD also enabled characterisation of the structural impact of K120

acetylation.[115,116] K120 sits on the L1 loop, which can induce dissociation of p53 from DNA via a conformational switch that can be modulated via mutation.[198] The crystal structure of the K120-acetylated DBD bound to DNA shows that K120 acetylation increases the flexibility of the L1 loop and induces this conformational switch when p53 binds to random or consensus DNA, but not the Bax promoter. When bound to the consensus or Bax promoter, K120 acetylation leads to K120 facing into the protein core rather than interacting with DNA (Fig. 4.18).[116]

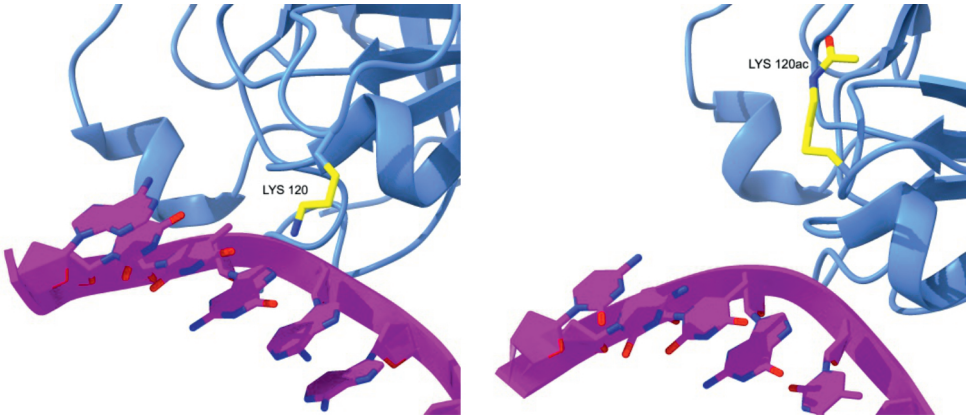

Figure 4.18: The effect of K120 acetylation on the L1 loop conformation. Unacetylated K120 (left, PDB: 4HJE) and K120-acetylated (right, PDB: 5BUA) p53 are shown bound to the Bax promoter. K120 acetylation causes K120 to face away from DNA and into the protein core.

Site-specific mono-ubiquitinylation of p53

Recently, Julier *et al.* used genetic code expansion to produce full-length p53 mono-ubiquitinylated at K120. The authors chose an otherwise wild-type sequence, forgoing stabilising mutations.[195,197,115] Ketolysine (KeK) was incorporated at K120 of p53, while genetic code expansion was also used to incorporate a Boc-protected Nϵ-aminooxy-L-lysine on the C-terminus of ubiquitin (Fig. 4.19). Incorporation of both ketolysine into p53 and Boc-protected Nϵ-aminooxy-L-lysine into ubiquitin respectively was confirmed by western blotting and mass spectrometry. Following deprotection, ubiquitin was conjugated to p53 at KeK120 via oxime ligation. The authors found that monoubiquitinylation at K120 did not affect the ability of p53 to bind the p21 promoter, suggesting that the structural integrity of p53 was maintained.[195]

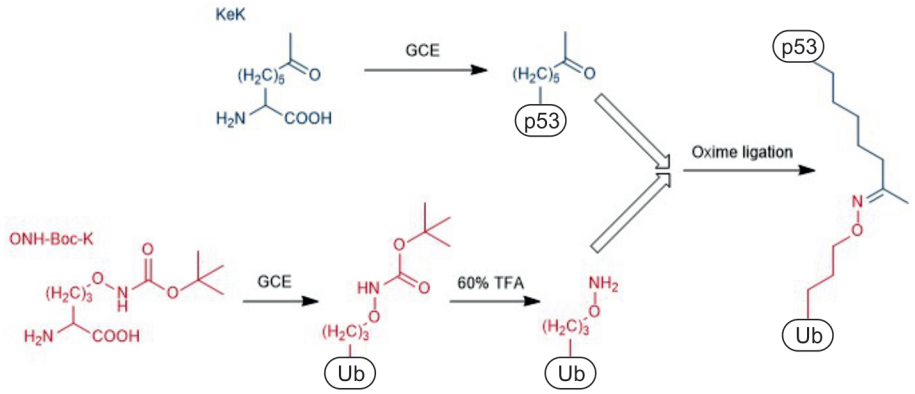

Figure 4.19: Site-specific ubiquitinylation of p53 by Julier *et al.* Using genetic code expansion (GCE), ketolysine (KeK) was incorporated into p53 at position 120 and Boc-protected Nϵ-aminooxy-L-lysine (ONH-Boc-K) was incorporated into ubiquitin. Following TFA deprotection of ubiquitin, the two proteins were joined by oxime ligation, yielding p53 mono-ubiquitinylated at K120. Figure adapted from [195].

Site-specific methylation of p53

Wang *et al.* described the genetic incorporation of mono- and di-methyllysine into full-length p53[196] without stabilising mutations.[196,195,197,115] The authors genetically encoded a precursor of allysine (AlK), Nϵ-(4-azidobenzoxycarbonyl)-δ, ϵ-dehydrolysine (AcdK), into p53 at K372. Following expression, AcdK was reduced with a phosphine generating δ, ϵ-dehydrolysine, which spontaneously hydrolyses to the aldehyde form, AlK. AlK was then converted to mono- or di-methyllysine by reductive amination with methylamine or dimethylamine respectively (Fig. 4.20). Alk was not genetically encoded directly because of concerns over its toxicity to cells. Mono- and di-methylation of p53 was confirmed by western blotting. In *in vitro* assays with Tip60, the authors showed K372 mono- and di-methylated p53 both showed elevated K120 acetylation, as determined by western blotting. This experiment provided direct evidence for a crosstalk between C-terminal methylation and acetylation on the DBD of p53.[196]

4.6 Aims of this thesis

Using protein semi-synthesis, our lab has unique access to p53 site-specifically phosphorylated on residues up to 40 amino acids from the N-terminus. The aims of this thesis are broadly twofold: firstly, expanding our access to site-specifically modified p53 beyond the

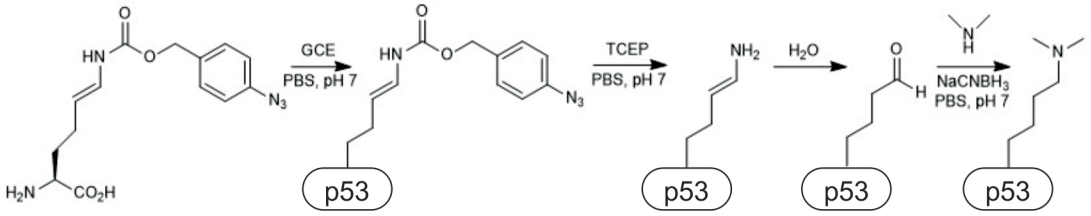

Figure 4.20: Genetic incorporation of dimethylysine into p53 by Wang *et al.* Acdk was incorporated into p53 using genetic code expansion (GCE). After expression, AcdK was reduced with TCEP (Staudinger reduction). Following self-cleavage of the *para*-aminobenzyloxycarbonyl group and enamine hydrolysis, reductive amination with dimethylamine in the presence of sodium cyanoborohydride yielded dimethyllysine. Figure adapted from [196].

first 40 amino acids using genetic code expansion, and secondly characterising the effect of site-specific p53 modification using *in vitro* assays to measure transcription and PTM crosstalk. Achieving these aims would lead to a deeper understanding of the role p53 PTMs play in life and death decisions in cells. Long term, this work aimed to contribute to an understanding of what really "decides" cell fate following stress. If, in an otherwise unstressed cell, p53 gained PTMs that promoted apoptosis, would apoptosis ensue or would the cell "correct" the PTM status of p53?

For genetic code expansion, the aim was to initially produce p53 acetylated at K120. This has already been successfully produced elsewhere with superstable p53 mutations,[115] and I initially aimed to produce K120-acetylated p53 without these mutations. I also aimed to develop an *in vitro* transcription assay similar to those developed previously,[199] using fluorescent RNA aptamers for transcript quantification. The effect of K120 acetylation on DNA binding is well-described,[115,116] so K120-acetylated p53 would serve as an ideal initial variant to validate the *in vitro* transcription assay. Following initial experiments with K120-acetylated p53, I then aimed to produce p53 bearing less well-characterised modifications, such as K101 and K164 acetylation, and use the *in vitro* transcription assay to assess their impact on DNA binding and transcription.

I also aimed to develop an assay to probe PTM crosstalk in p53 using nuclear extracts similar to those used in *in vitro transcription*. By exposing cells to different stress conditions before nuclear extract preparation, the effect of stress on PTM cascades could also be investigated. Initially, I aimed to use semisynethetic p53 variants produced in

the Müller lab by Dr. Sofia Margiola, Mateusz Hess, and Sonja Schneider to validate the assay, probing known crosstalk interactions such as the dependance of T18 phosphorylation on prior S15 phosphorylation and the effect of N-terminal phosphorylation on C-terminal acetylation. Having validated that the assay can recreate known crosstalk phenomena, I then aimed to investigate the effect of N-terminal phosphorylation on the accumulation of modifications that induce apoptosis, such as K120 acetylation and S46 phosphorylation. PTM crosstalk on the DNA-binding domain is very poorly understood, and I aimed to use any acetylated variants produced by genetic code expansion in the crosstalk assay.

Accessing AcK120 p53 through genetic code expansion

5.1 Introduction

Acetyllysine was first incorporated into recombinant proteins via amber suppression in 2008, when Neumann *et al.* described the directed evolution of *M. Barkeri* pyrrolysine tRNA synthetase to enable the site-specific incorporation of Nϵ-acetyllysine into myoglobin.[114] This engineered synthetase was subsequently used to incorporate acetyllysine into multiple proteins,[200] including p53 at position 120.[115] In this instance, p53 was expressed bearing four stabilising mutations (M133L, V203A, N239Y, N268D).[197,115] Acetyllysine incorporation was confirmed by western blotting for the DBD and full-length protein, and mass spectrometry also confirmed acetyllysine incorporation in the DBD.[115]

I initially aimed to produce AcK120 p53, hereon referred to as $p53_{K120ac}$, without stabilising mutations by expressing it in inclusion bodies and refolding, an approach similar to that used to generate semisynthetic phosphorylated p53.[168,201] This approach used autoinduction has an expression strategy.[168] Autoinduction takes advantage of carbon catabolic repression in *E. coli*: when grown in the presence of glucose and lactose, *E. coli* preferentially takes up glucose, with glucose suppressing the uptake of lactose.[202] Transformed *E. coli* are grown in the presence of glucose and lactose, such that the glucose will deplete during the log-phase of growth, at which point lactose is taken up allowing for expression through a lactose-inducible T7 promoter.[203] Expression via autoinduction often leads to several times greater yields than manual induction with IPTG.[203] Autoinduction has been successfully used with genetic code expansion to express site-specifically modified proteins, though these proteins did not require refolding.[204,205,206]

A key challenge with amber suppression is the formation of a truncated species at the mutated residue.[184] For p53, the truncated species would lack the majority of the DNA-binding domain. Removal of the truncated species was to be achieved using a heparin column, something we already used when purifying refolded unmodified p53. If successful, a longer term aim would have been to combine amber suppression with protein semisynthesis by using amber suppression to produce site-specifically modified truncated p53 with an N-terminal cysteine and ligating it to a site-specifically modified synthetic peptide using native chemical ligation. This would greatly expand the diversity of variants available.

5.2 Results

5.2.1 Production of unmodified p53

Downstream assays probing the effect of K120 acetylation would require unmodified p53 for comparison, so unmodified p53 was produced recombinantly in *E.coli*. Hereon, this form of p53 will be referred to as "$p53_{rec}$". Initial attempts to express and purify $p53_{rec}$ were successful, albeit with high (37.2 %) levels of methionine oxidation after inclusion body purification (Fig. 5.1). Methioinine oxidation is difficult to avoid, and the effect it has on downstream assays is unknown. Because of this, we try to keep methionine oxidation levels between 20-30 % before refolding to ensure approximate homogeneity. Expression was attempted using varying concentrations of L-methionine, a scavenger for oxygen species, in the culture media. Expression was successful for all L-methionine conditions, based on the appearance of a 53 kDa band after autoinduction. Inclusion body purification followed by RP-HPLC led to a large peak after 17 minutes, and HRMS analysis indicated that all L-methionine conditions led to similar levels of oxidation (26.6-29.9 %), all within a range considered acceptable (Fig. 5.2).

$p53_{rec}$ from the least-oxidised samples (those cultured with 50 mg/L L-methionine) were refolded and purified using a heparin column. Size-exclusion chromatography generated a large peak after 14 minutes (F14), preceded by a smaller peak that appears as a hump just before the F14 peak at around 12 minutes (F12). The oligomerisation state of the F12 and F14 fractions was assessed using glutaraldehyde crosslinking, with tetrameric p53 observed in the F14 fraction using SDS-PAGE and stain-free imaging (Fig. 5.3).

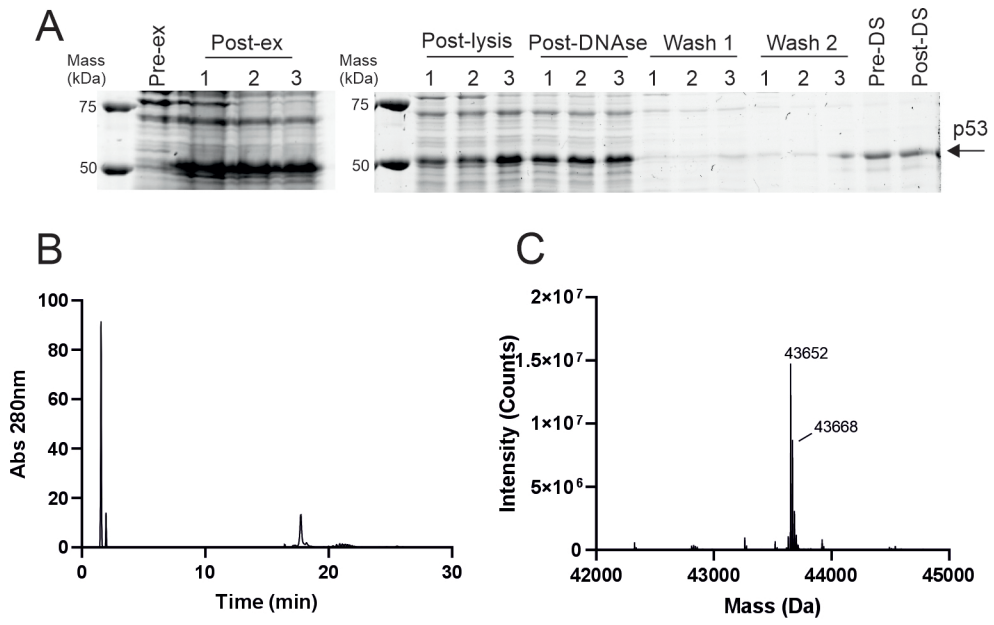

Figure 5.1: Initial attempt at expressing p53$_{rec}$. A: Expression and purification of p53$_{rec}$. Expression was carried out in three flasks that were loaded on to the gel separately. Stain-free imaging shows the appearance of a 53 kDa band post-autoinduction (post-ex) that was not present pre-autoinduction (pre-ex). p53$_{rec}$ is present post-lysis and post DNAse treatment. Minimal p53$_{rec}$ was lost during the subsequent two wash steps (Wash 1, Wash 2), or by desalting (DS). B: Analytical RP-HPLC trace of p53$_{rec}$ post-desalting showing a peak at around 17 minutes. C: HRMS of the 17 minute RP-HPLC peak shows the expected mass for p53 (43652 Da) and oxidised (+16) p53 (43668 Da).

5.2.2 Expression of p53$_{K120ac}$ as an inclusion body

Having carried out production and refolding of p53$_{rec}$, I attempted to produce p53$_{K120ac}$ using genetic code expansion. A plasmid containing a Nϵ-acetyllysyl-tRNA synthetase (pACYC) and a plasmid containing genes for tRNA$_{CUA}$ and myoglobin (pBR322) were obtained from Prof. Jason Chin.[114] The myoglobin gene was replaced with the gene for p53 using NEB HiFi DNA assembly, with codon 120 of p53 subsequently mutated to TAG using site-directed mutagenesis. This yielded a plasmid system where p53, mutated to TAG at position 120 (K120$_{TAG}$), was under the control of an araBAD promoter, while the tRNA and tRNA synthetase were constituatively expressed.

Initial attempts to express p53$_{K120ac}$ via autoinduction indicated that DH10B cells undergoing amber suppression grow slower compared to non-amber suppressed DH10B cells, with no p53 expression observed after 16 hours. Extending the expression period

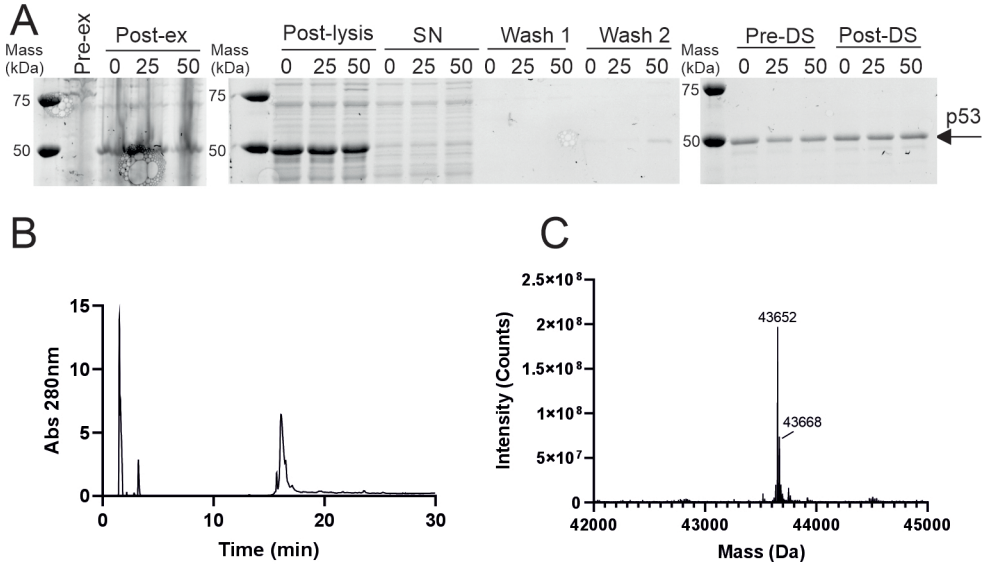

Figure 5.2: Expression and purification of p53$_{rec}$ A: Expression and purification of p53$_{rec}$ with the addition of 0, 25, or 50 mg/L L-methionine (indicated by 0, 25, and 50 respectively). Stain-free imaging shows the appearance of a 50 kDa band post-autoinduction (post-ex) that was not present pre-autoinduction (pre-ex). p53$_{rec}$ is present post-lysis, but not in the supernatant (SN) following centrifugation. Minimal p53$_{rec}$ was lost during the subsequent two wash steps (Wash 1, Wash 2), or by desalting (DS). B: Analytical RP-HPLC trace of p53$_{rec}$ post-desalting showing a peak at around 17 minutes. C: HRMS of the 17 minute RP-HPLC peak shows the expected mass for p53 (43652 Da) and oxidised (+16) p53 (43668 Da). For B and C, data shown is for p53$_{rec}$ expressed in the presence of 50 mg/L L-methionine.

to 24-48 hours led to the expression of full-length p53, detectable by western blot, with levels peaking at 24 hours (Fig. 5.4). DH10B cells are often used for arabinose induction as they are unable to catabolise L-arabinose.[207]

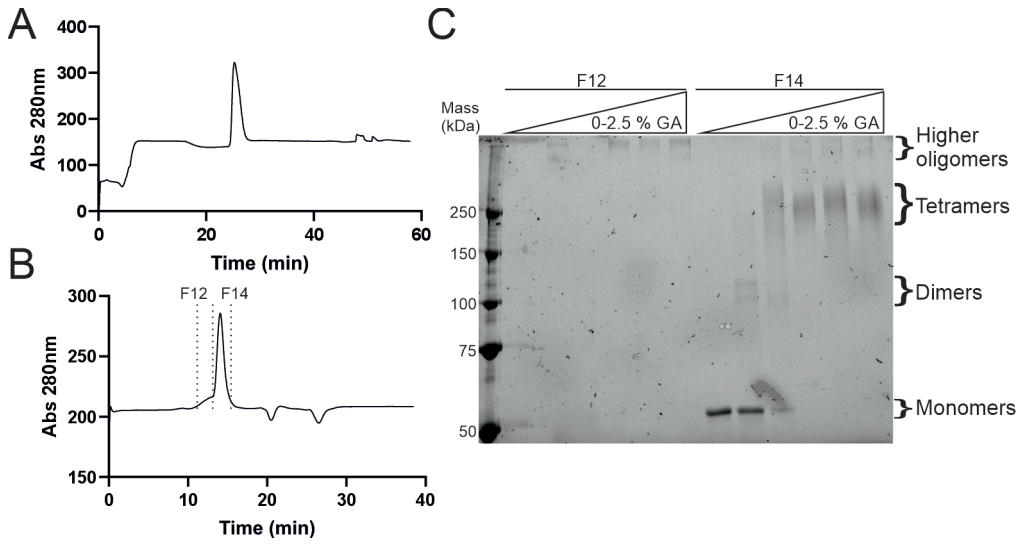

Figure 5.3: p53$_{rec}$ refolding A: RP-HPLC (280 nm) following heparin column purification of refolded p53$_{rec}$ generated a single peak. B: Size exclusion chromatography generated a large peak corresponding to tetrameric p53$_{rec}$ (F14) and a small peak at 12 minutes (F12). Glutaraldehyde (GA) crosslinking reactions were carried out on F12 and F14 to assess the oligomeric state of p53$_{rec}$ in each fraction, with tetrameric p53$_{rec}$ only present in F14.

Refolding p53 is inefficient: during preparation of p53$_{rec}$, only 12.8 % of the p53$_{rec}$ that entered the refolding process was successfully refolded. Methods were therefore sought to maximise the expression yield of p53$_{K120ac}$. An alternative plasmid system was obtained from Addgene that contained a Nϵ-acetyllysyl-tRNA synthetase under the control of an araBAD promoter and the tRNA constituatively expressed[208]. This was used in conjunction with a pET vector containing K120$_{TAG}$ p53, where p53 was under the control of a T7 promoter, lactose-inducible in BL21 cells. A trial comparing the two plasmid systems showed that blottable quantities of full-length p53 were only expressed in BL21 cells using the pEVOL/pET system (Fig. 5.5). It was unclear why the pACYC/pBR322 system utilizing DH10B cells did not yield p53 in blottable quantities in this instance, as it provided measurable quantities previously (Fig. 5.4B).

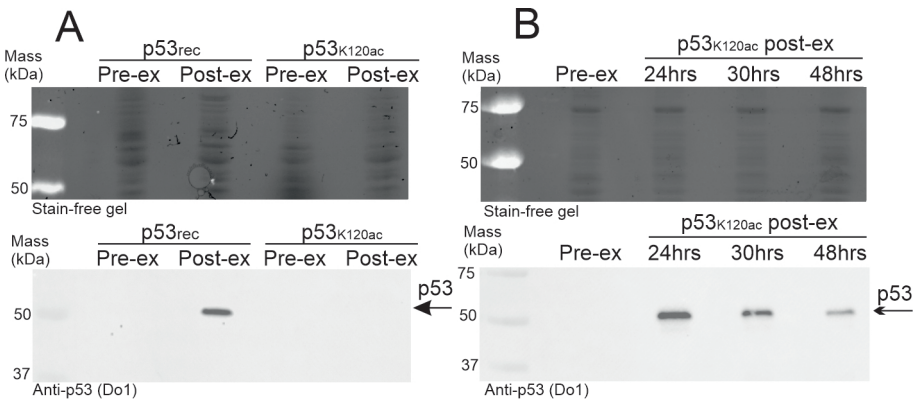

Figure 5.4: Expression of p53$_{K120ac}$. A: Expression of p53$_{K120ac}$ failed to yield blottable quantities after 16 hours autoinduction. Shown is a stain-free gel (top) and western blot (bottom) using anti p53 antibody (DO1). B: Expression of p53$_{K120ac}$ yielded full-length p53 after 24 hours autoinduction, with levels lower at 30 and 48 hours. Shown is a stain-free gel (top) and western blot (bottom) using anti p53 antibody (DO1).

Using the pACYC/pBR322 system in DH10Bs, it had been observed that p53 levels decreased when expression was attempted for longer than 24 hours. A hypothesis was generated that, after 24 hours, the acetyllysine may have become depleted. This may have led to production of full-length p53 being halted. This, combined with a degree of proteolytic degradation, may have led to a decrease in p53 levels over time. If this was the case, increasing the concentration of acetyllysine in the media may allow p53 to continue accumulating after 24 hours. The use of BL21 cells in the pEVOL/pET system was also considered to be an advantage, as BL21 cells are deficient in Lon and OmpT proteases. Expression levels after 24 and 48 hours were compared between cells expressing p53$_{K120ac}$ in the presence of 1-20 mM acetyllysine. For cells harvested after 48 hours, acetyllysine was added either all at once at the start of expression ("bulk") or in two doses, one at the start of expression and one 24 hours afterwards ("spike").

In the stain-free gel, p53 expression was only visible for p53$_{rec}$ using non-amber suppressed BL21s. Western blotting followed by densitometric analysis comparing the intensity of p53$_{rec}$ with the positive control indicated a yield of approximately 25 μg/100mL culture. Western blotting for p53 showed that 20 mM acetyllysine yielded the highest levels of expression after "bulk" acetyllysine addition, but still around 25-times lower levels of expression than the non-amber suppressed cells (approximately 1.0 μg/100mL). For "spike" acetyllysine addition, the highest levels of expression was observed after 24 hours

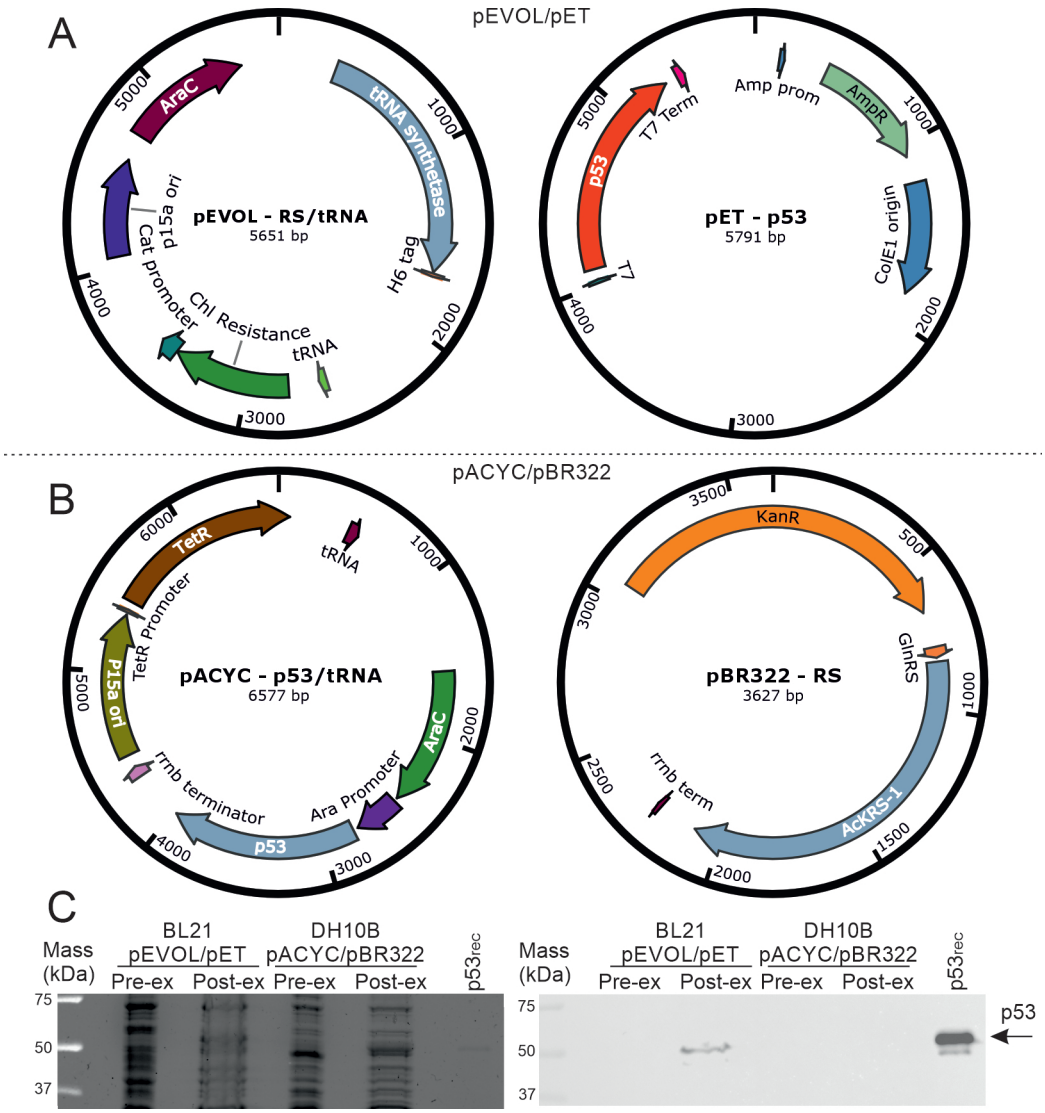

Figure 5.5: Comparison of plasmid systems for production of p53$_{K120ac}$ in *E. coli*. A: Plasmid maps showing the pEVOL/pET system. B: Plasmid maps showing the pACYC/pBR322 system. C: Expression trial using pEVOL/pET in BL21 cells and pACYC/pBR322 in DH10B cells. Full-length p53 was only detected in the BL21 cells using the pEVOL/pET system. Shown is a stain-free image of the SDS-PAGE gel (left) and a western blot (right) using an antibody against p53 (DO1).

grown with 2.5 mM acetyllysine (approximately 1.3 μg/100mL), with no detectable expression with 0.5 or 5 mM acetyllysine, and very low expression with 10 mM acetyllysine (approximately 0.1 μg/100mL). Adding more acetyllysine and switching to a protease-deficient cell line did not prevent the drop in p53 levels after 48 hours from occurring. Western blotting using an antibody against K120-acetylated p53 generated a clear band for the "spike" 5 mM acetyllysine sample, and a fainter band for the "bulk" 20 mM

acetyllysine sample (Fig. 5.6). After 24 hours, bands just below the 25 kDa marker were visible following western blotting with an anti-p53 (DO1) antibody. This may be the expected truncated species. Though this band appears approximately 10 kDa higher than the expected mass of the truncated species (12 kDa), p53 also runs approximately 10 kDa higher than its actual mass (43.7 kDa) following SDS-PAGE.

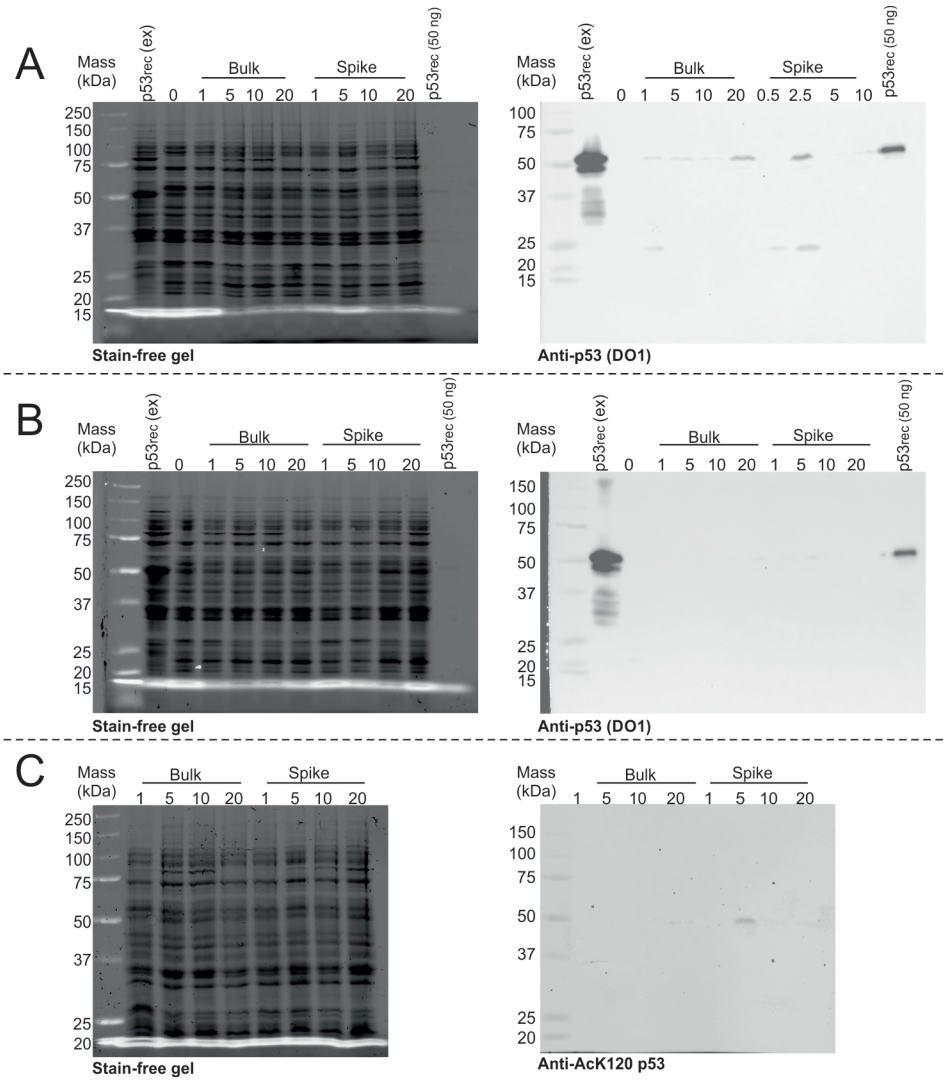

Figure 5.6: Expression of p53$_{K120ac}$ in the presence of 0-20 mM acetyllysine, added either at once at the start of autoinduction ("bulk") or in two-doses every 24 hours ("spike"). Also shown is p53$_{rec}$ expressed without amber suppression and a 50 ng p53$_{K120ac}$ control. Full-length p53 runs at 53 kDa, the truncated variant falls at around 25 kDa. SDS-PAGE (left) and western blots (right) using anti-p53 antibody (DO1) were carried out after 24 (A) and 48 (B) hours expression. After 48 hours, western blots were also carried out using an antibody against K120-acetylated p53 (C). Aliquots of culture were taken just before addition of the second acetyllysine dose in the "spike" samples.

I aimed to produce purified $p53_{K120ac}$ for analysis by mass spectrometry and precise quantification of yields to facilitate refolding. $p53_{K120ac}$ was expressed at a 10 x higher scale (1L) than previously for 24 hours in the presence of 2.5 mM acetyllysine, with $p53_{rec}$ also expressed as usual. Inclusion body purification was carried out to purify both proteins. Whereas $p53_{rec}$ was clearly distinguishable on a stain free gel following inclusion body purification, $p53_{K120ac}$ was not clearly distinguishable from other bands, and the inclusion body contained many more proteins. A western blot using an antibody against acetyllysine was carried out to see whether this was due to aggregation of endogenous *E. coli* proteins that had incorporated acetyllysine at native amber stop codon sites. The inclusion body for the amber suppressed sample did not appear to contain an abundance of such proteins (Fig. 5.7). The results suggest that $p53_{K120ac}$ may constitute a lower proportion of proteins in the inclusion body due to low levels of expression. Moreover, no acetylated protein was detected following desalting of the $p53_{K120ac}$ prep, including acetylated p53. It was concluded that other approaches should be explored for the production of $p53_{K120ac}$.

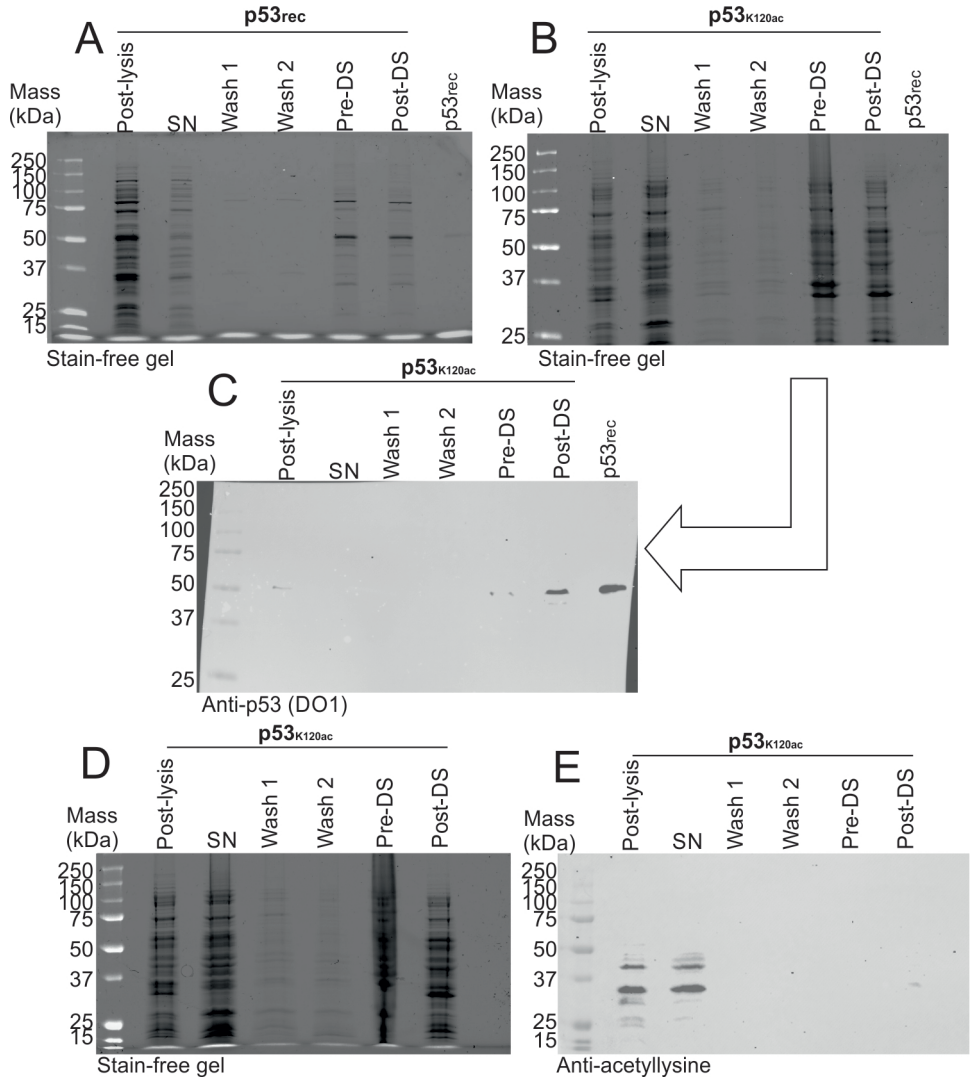

Figure 5.7: Inclusion body purification following p53$_{K120ac}$ and p53$_{rec}$ expression. Aliquots were taken of cells post-lysis, of supernatants after first centrifugation (SN), after wash steps (wash 1, wash 2), pre desalting (pre-DS), and post-desalting (post-DS). Full-length p53 runs at 53 kDa, the truncated variant falls at around 25 kDa. Shown are stain free gels of p53$_{rec}$ purification (A), p53$_{K120ac}$ purification (B), western blot of the p53$_{K120ac}$ purification gel using an anti-p53 (DO1) antibody (C), and a stain free gel of p53$_{K120ac}$ purification (D) taken prior to western blotting with an anti-acetyllysine antibody (E).

5.2.3 Expression of soluble p53$_{K120ac}$

Though western blot evidence indicated that p53$_{K120ac}$ was expressed, low yields suggested that purification and refolding from inclusion bodies may not be an effective strategy. Expression of soluble, folded p53$_{K120ac}$ would lower the threshold for acceptable yields by avoiding the inefficient refolding process. The K120$_{TAG}$ mutation was intro-

duced into p53, bearing a H6SUMO tag, in a pET vector. Additionally, four stability-increasing mutations were introduced that have been successfully used in the past for generating p53$_{K120ac}$: M133L, V203A, N239Y, N268D.[197,115] Hereon, superstable but otherwise unmodified H6SUMO-p53 will be referred to as "H6SUMO-p53$_{SS}$", while the K120-acetylated form will be referred to as "H6SUMO-p53$_{SSK120ac}$". Non-superstable K120-acetylated H6SUMO-p53 will be referred to as "H6SUMO-p53$_{K120ac}$". Expression of H6SUMO-p53$_{SSK120ac}$ and H6SUMO-p53$_{K120ac}$ were measured from 16-36 hours post induction with IPTG. Because IPTG has been shown to suppress induction through the pBAD promoter in *E. coli*,[209] the effect of adding arabinose from the start of growth culture versus simultaneously with IPTG was also compared. Western blotting using an anti-p53 antibody (DO1) showed the accumulation of full-length H6SUMO-p53 from 16 hours post-simultaneous induction with IPTG and arabinose. Western blotting with an antibody against K120-acetylated p53 did not yield any bands at the expected mass, however the presence of full-length H6SUMO-p53 suggested that acetyllysine had been incorporated. Expression was comparable between wild-type H6SUMO-p53$_{K120ac}$ and H6SUMO-p53$_{SSK120ac}$, though in both cases expression was higher in *E. coli* where expression was induced simultaneously with IPTG and arabinose than when arabinose had been present from the start of growth culture (Fig. 5.8).

The solubility of H6SUMO-p53$_{K120ac}$ versus H6SUMO-p53$_{SSK120ac}$ was assessed by lysis, centrifugation, and comparison of p53 levels in the supernatant versus the resuspended pellet. Approximately 42 % of H6SUMO-p53 was soluble, compared to 92 % for H6SUMO-p53$_{SS}$. For H6SUMO-p53$_{K120ac}$, approximately 61 % was soluble, compared to 88 % for H6SUMO-p53$_{SSK120ac}$, based on densitometric analysis. Though soluble expression of wild-type H6SUMO-p53$_{K120ac}$ may have been possible based on these results, it was decided that H6SUMO-p53$_{SSK120ac}$ would be expressed first. The presence of full-length H6SUMO p53 suggested acetyllysine had been incorporated (Fig. 5.9). As before, a species approximately 10 kDa higher than the expected mass of the truncated variant (25.4 kDa) was observed following western blotting with anti-p53 (DO1) antibody.

Expression and purification of H6SUMO-p53$_{SSK120ac}$ was attempted at a higher scale (3 L). Western blot analysis with both an anti-p53 antibody (DO1) and an antibody against K120-acetylated p53 showed successful expression of H6SUMO-p53$_{SSK120ac}$. His-Trap purification led to successful elution of H6SUMO-p53$_{SSK120ac}$, with an approxi-

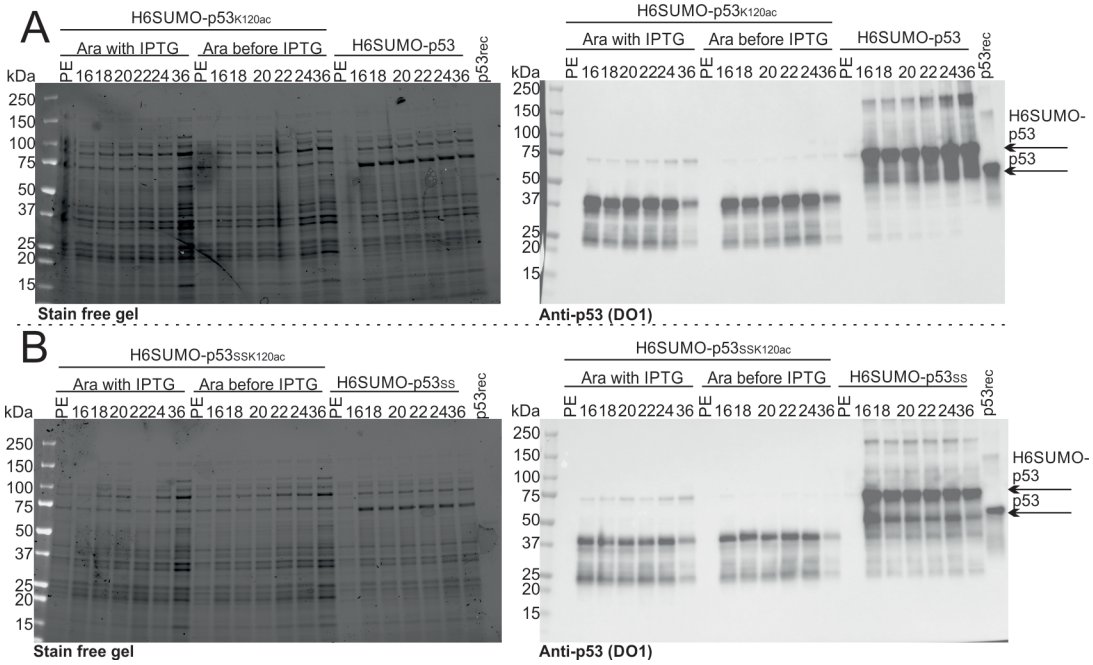

Figure 5.8: Expression trial with different timings of arabinose addition. H6SUMO-p53$_{K120ac}$ was expressed at 25 °C using amber suppression and the pEVOL/pET system in BL21 cells. Arabinose was added either simultaneously with IPTG (Ara with IPTG) or at the start of growth culture (Ara before IPTG). Aliquots were taken pre-expression (PE) and at time points indicated, shown in hours (16-36). A 50 ng p53$_{rec}$ control, lacking a H6SUMO tag, is also shown, running at 53 kDa. Full-length H6SUMO-p53 runs at 75 kDa, the truncated variant falls at 37 kDa. Shown are stain free gels and western blots against p53 (DO1) for p53$_{K120ac}$ (A) and H6SUMO-p53$_{SSK120ac}$ (B).

mately 25 % of the protein input eluting from the column. The H6SUMO tag was cleaved with Ulp1 overnight at 4 °C. No uncleaved p53 was detected following cleavage, though a precipitate was observed in the dialysis tubing. Dissolving this precipitate in 100 μL 1x SDS loading dye and western blotting indicated that the precipitate contained a wide array of proteins, including p53. Purification using a heparin column led to successful elution, but not complete purification. Densitometric analysis of the stain free gel, assuming that the faint band visible around 50 kDa is 100 % p53, suggests that, at most, p53 constituted approximately 2 % of the protein in the heparin column elute. Western blotting against an antibody targeting K120-acetylated p53 generated bands in each lane at the expected mass, suggesting that acetyllysine incorporation was successful (Fig. 5.10).

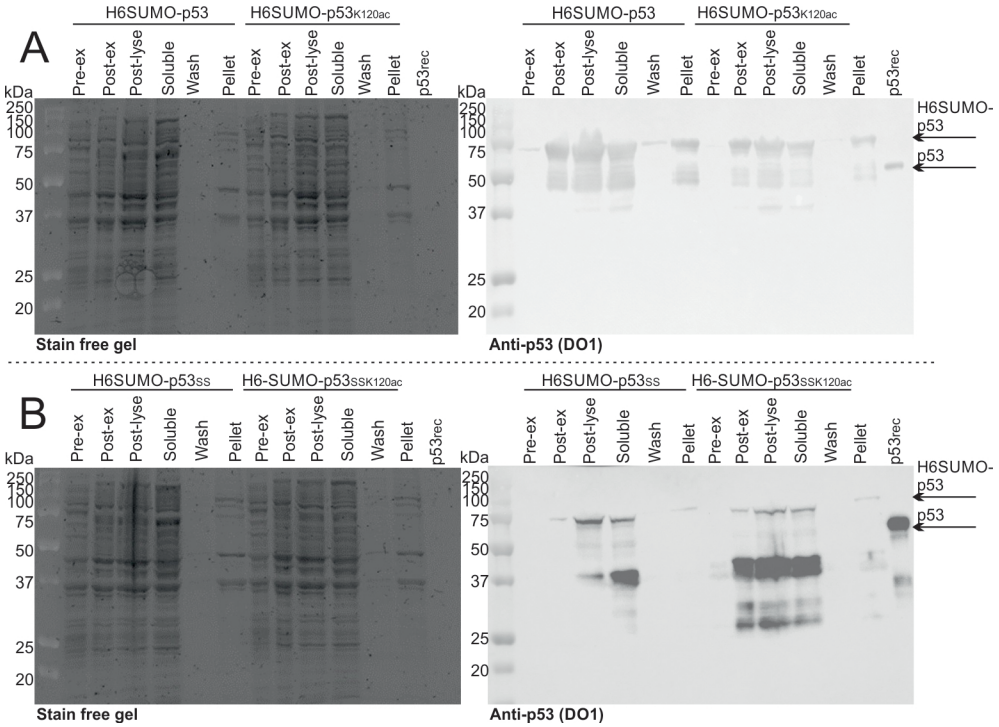

Figure 5.9: Solubility trial comparing H6SUMO-p53$_{K120ac}$ to H6SUMO-p53$_{SSK120ac}$. H6SUMO-p53$_{K120ac}$ was expressed at 25 °C using amber suppression and the pEVOL/pET system in BL21 cells. Aliquots were taken pre-expression ("Pre-ex"), post-expression ("Post-ex"), post lysis, of the supernatant post centrifugation ("soluble"), of the supernatant post pellet resuspension and centrifugation ("wash"), and post further resuspension of the pellet without centrifugation ("pellet"). A 50ng p53$_{rec}$ control is also shown. Full-length H6SUMO-p53 runs at 75 kDa, the truncated variant falls at 37 kDa. A: H6SUMO-p53$_{K120ac}$ expression, and non-amber suppressed (non-AS) p53$_{rec}$ expression. Shown is a stain-free gel (left) and western blot (right) using an antibody against p53 (DO1). B: H6SUMO-p53$_{SSK120ac}$ expression, and non-amber suppressed (non-AS) H6SUMO-p53$_{SS}$. Shown is a stain-free gel (left) and western blot (right) using an antibody against p53 (DO1).

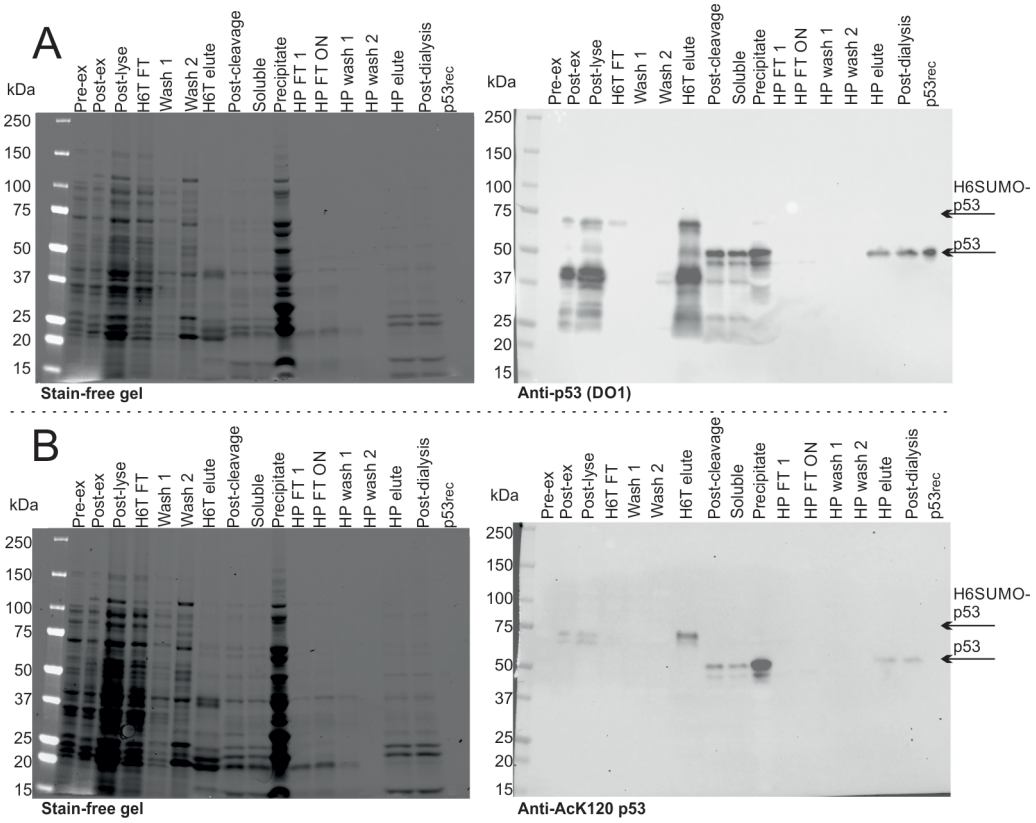

Figure 5.10: Expression and attempted purification of H6SUMO-p53$_{SSK120ac}$. H6SUMO-p53$_{K120ac}$ was expressed at 25 °C using amber suppression and the pEVOL/pET system in BL21 cells. Aliquots were taken pre-expression (Pre-ex), post-expression (Post-ex), post lysis, of the supernatant post centrifugation (soluble), of the supernatant post pellet resuspension and centrifugation (wash), and post further resuspension of the pellet without centrifugation (pellet). A 50 ng p53$_{rec}$ control is also shown. Full-length H6SUMO-p53 runs at 75 kDa, the truncated variant falls at around 37 kDa. Cleaved full-length p53 runs at around 53 kDa. A: Stain-free gel (left) and western blot using an anti-p53 (DO1) antibody (right) of aliquots taken during the purification procedure. B: Stain-free gel (left) and western blot using an antibody against K120-acetylated p53 (right) of aliquots taken during the purification procedure.

RP-HPLC generated multiple peaks, with one notably large peak after 14 minutes. HRMS analysis failed to detect any mass corresponding to p53 or monoacetylated p53 in the collected peaks. The heparin column elute was cleaned up further by passing it through a HisTrap to remove residual Ulp1 or cleaved H6SUMO. SDS-PAGE and stain-free imaging showed that, even after further cleanup, there were still proteins in the elute at similar or greater abundance than p53. Subsequent RP-HPLC analysis failed to yield any peaks corresponding to p53 (expected elution time 17 minutes) (Fig. 5.11).

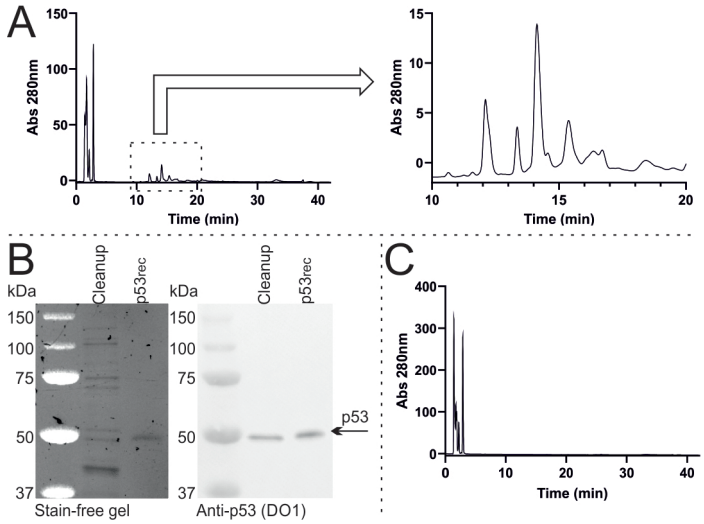

Figure 5.11: p53$SSK120ac$ cleanup A: RP-HPLC trace (Abs 280) following elution of $p53_{K120ac}$ from a heparin column. Shown is the trace from 0-42 minutes, including early peaks corresponding to salts (left) and the trace from 10-20 minutes only, showing peaks collected for HRMS. B: Stain free gel (left) and western blot using anti-p53 (DO1) antibody, including a 50 ng $p53_{rec}$ control, following cleanup via reverse nickel purification. C: RP-HPLC trace (Abs 280) following reverse nickel purification.

5.3 Conclusion

During the process of optimising the expression protocol, many different approaches were directly compared. Purification strategies (inclusion body vs soluble), plasmid systems (pBR322/pACYC vs pEVOL/pET), timing of addition of acetyllysine ("bulk" vs "spike") and, where multiple inducing sugars were used, the timing of their addition (arabanose before or with IPTG). The difference in solubility between "superstable" and wild-type recombinant p53 was also directly compared.

Plasmid systems: pBR322 vs pACYC

The switch to a pEVOL/pET system was initially motivated by the hypothesis that expression from the T7 promoter in BL21 cells would lead to greater yields than expression from the pBAD promoter in DH10B cells. Ultimately, however, the switch to pEVOL/pET occured because the pBR322/pACYC unexpectedly stopped producing detectable p53, despite initial success. Why pBR322/pACYC stopped producing detectable p53 is unclear, and it is difficult to conclude for certain that one system is "better" than the other.

Timing of addition of acetyllysine: "bulk" vs "spike"

The observation that p53 levels appeared to decrease after 24 hours expression led to the hypothesis that acetyllysine was being depleted in the media, leading to the formation of a truncated variant. Basal degradation of full-length p53 would then lead to a decrease in overall p53 levels over time. Interestingly, p53 was barely detectable after 48 hours even when cells were supplemented with additional acetyllysine after 24 hours, suggesting that the drop in p53 levels was not due to depletion of acetyllysine. It was also notable that there was no clear correlation between acetyllysine concentration and p53 levels, with the highest expression after 24 hours being observed in the presence of 2.5 and 20 mM acetyllysine. One approach that might be considered is spiking of additional arabinose, as metabolism of arabinose might also lead to full-length p53 expression halting due to a lack of tRNA synthetase expression. It may also be the case that, because most protein expression occurs during the exponential phase of growth, incubating the cells for longer at the stationary phase may not lead to an increase in protein expression, while protein degradation may still occur. In this case, harvesting the cells earlier may improve protein recovery.

Timing of addition of arabinose when used with IPTG

It has been reported that expression through the pBAD promoter is suppressed in the presence of IPTG,[209] and we considered that simultaneous induction with arabinose and IPTG might lead to low expression levels of the tRNA synthetase and a higher proportion of p53 being truncated. Expression levels in cells that were induced simultaneously

with IPTG and arabinose were compared with cells that were grown in the presence of arabinose and induced with IPTG. If IPTG-mediated suppression of tRNA synthetase expression was a limiting factor in full-length p53 expression, pre-incubation with arabinose might allow circumvent this by allowing the tRNA synthetase to accumulate before IPTG induction. The observation that expression of both H6SUMO-p53$_{K120ac}$ and H6SUMO-p53$_{SSK120ac}$ was higher when IPTG and arabinose were added simultaneously was unexpected, and may have been caused by metabolism of arabinose.

Insoluble vs soluble expression

Initial attempts to express p53$_{K120ac}$ as an inclusion body were successful, however isolation of the inclusion body did not lead to purification of p53 in any meaningful sense due to p53 making up a very small proportion of the inclusion body, which contained many other proteins. In contrast, when inclusion bodies were isolated following p53$_{rec}$ expression, they contained mostly p53. Soluble expression of H6SUMO-p53$_{K120ac}$ and H6SUMO-p53$_{SSK120ac}$ was achieved, though H6SUMO-p53$_{SSK120ac}$ was 1.5-2 times more soluble. H6SUMO-p53$_{SSK120ac}$ was successfully cleaved by Ulp1 following HisTrap purification, though even after heparin column purification p53$_{SSK120ac}$ was not adequately purified. Furthermore, without HRMS analysis of the expressed p53$_{SSK120ac}$, it is still unclear whether a proportion of the acetylated p53 produced was deacetylated in *E. coli*.

Conclusion

The aim, to produce p53 site-specifically acetylated at position 120, was achieved, though low yields and difficulties with purification precluded its full characterisation and application in functional assays. Nevertheless, aliquots of partially-purified p53$_{K120ac}$ were used as positive western blot controls in crosstalk assays (described in chapter 7). Considering that p53$_{K120ac}$ has already been expressed in superstable form,[115] the challenges described in this chapter should not be insurmountable. In retrospect, purifying by heparin column before H6SUMO cleavage may have been better as it would have immediately removed truncated p53. Approaches to improve the yields of proteins produced through amber suppression, such as using RF1-knockout cell lines,[191] are available.

Towards a p53-based transcription assay using fluorescent RNA aptamers *in vitro*

6.1 Introduction

p53 functions as a transcription factor, and its transcriptional activity is regulated in a large part by PTMs.[39] Cell extracts capable of transcribing exogenous DNA templates are useful tools for dissecting the mechanisms of transcription initiation.[210] Transcriptionally active nuclear extracts can be produced from HeLa cells through gentle lysis approaches that do not damage the nuclei, removal of the cytoplasmic material, and subsequent extraction of nuclear proteins from chromatin using a high salt buffer.[211] Transcription from a DNA template containing a p53 promoter has been demonstrated in HeLa cell nuclear extracts using p53 immunoprecipitated from insect cells expressing p53 using a recombinant baculovirus, or immunoprecipitated from HeLa cells infected with recombinant vaccinia virus expressing p53.[199,212,213] *In vitro* transcription from the p21 promoter has also been observed in nuclear extracts from rat embryonic fibroblasts (REFs) using both human p53 immunoprecipitated from insect cells and a temperature-sensitive mutant of murine p53 expressed in the cells from which the nuclear extracts were prepared.[214] The role of p53 PTMs have been investigated using *in vitro* transcription, with one study reporting that C-terminal dephosphorylation of recombinant p53 derived from insect cells abrogated transcription in nuclear extracts derived from rat liver.[215] *In vitro* transcription assays have also been used to probe the ability of p53 to repress gene expression.[216]

These studies measured p53-mediated induction of transcription from naked DNA

templates. However, many aspects of p53 activity require interactions with chromatin.[46] One 2001 study failed to detect transcription *in vitro* from naked DNA templates containing the p21 promoter when insect-derived recombinant p53 and p300 were added to HeLa nuclear extracts. In contrast, robust transcription was observed when the DNA templates were chromitinised. Transcription levels were robust when p53 and p300 were added, and modest when p53 or p300 were supplied alone.[58] A 2012 study also compared *in vitro* transcription from naked DNA with chromitinised DNA. For naked DNA, they observed robust transcription that was not affected by addition of p300 or acetyl-CoA. In chromatinised templates, p53 was only able to induce transcription if p300 and acetyl-CoA were present.[217]

For quantification, *in vitro* transcription often use radiolabelling approaches for detection of transcripts, though RT-PCR has also been used.[218] For the latter approach, depletion of the DNA template is necessary to prevent amplification of the reporter gene during PCR. This can be achieved by DNAseI treatment and Trizol extraction to purify RNA.[218] Another approach for quantification is the use of fluorescent RNA aptamers such as Broccoli and Spinach.[219,220] These aptamers fluoresce when in complex with DFHBI, a small molecule derived from the fluorophore utilized by green-fluorescent protein, and allow for rapid detection and quantification of RNA transcripts.[221] Though initially optimised for *in vivo* applications, RNA aptamers are also useful *in vitro* as they negate the need for radiolabelling or depletion of the DNA template.[222,223]

With these experiments, the aim was to develop a simplified tool to assess the effect of p53 PTMs on transcription. HeLa nuclear extracts and refolded $p53_{rec}$ were used in an *in vitro* transcription assay, with the eventual aim of carrying out the assay with $p53_{K120ac}$ and the phosphorylated variants available in our lab. Quantification was to be achieved through the use of iSpinach, an RNA aptamer that is optimal for *in vitro* applications due to its increased brightness, reduced salt-sensitivity, and increased thermal stability relative to Broccoli and Spinach.[224]

6.2 Results

6.2.1 iSpinach fluoresces in the presence of DFHBI

Plasmid templates containing 13 copies of a p53 promoter sequence (PG13) or 15 copies of a mutated promoter sequence that does not bind p53 (MG15) were purchased from Addgene[225] and their luciferase reporter genes were replaced by iSpinach RNA aptamer using NEB HiFi DNA assembly. This placed the iSpinach aptamer gene downstream of the PG13/MG15 sequence, which themselves were downstream of a T7 promoter (Fig. 6.1). The RNA aptamers were produced using an *in vitro* T7 transcription kit (Thermo Fisher). The RNA aptamers were both transcribed successfully as parts of transcripts that fell just below the 1000 nt marker on a denaturing RNA agarose gel. The expected transcript lengths were 905 nt for PG13 and and 827 nt for MG15. Purified RNA aptamers from both PG13 and MG15 showed robust fluorescence in the presence of DFHBI (excitation 444 nm, emission 520 nm, Fig. 6.2).

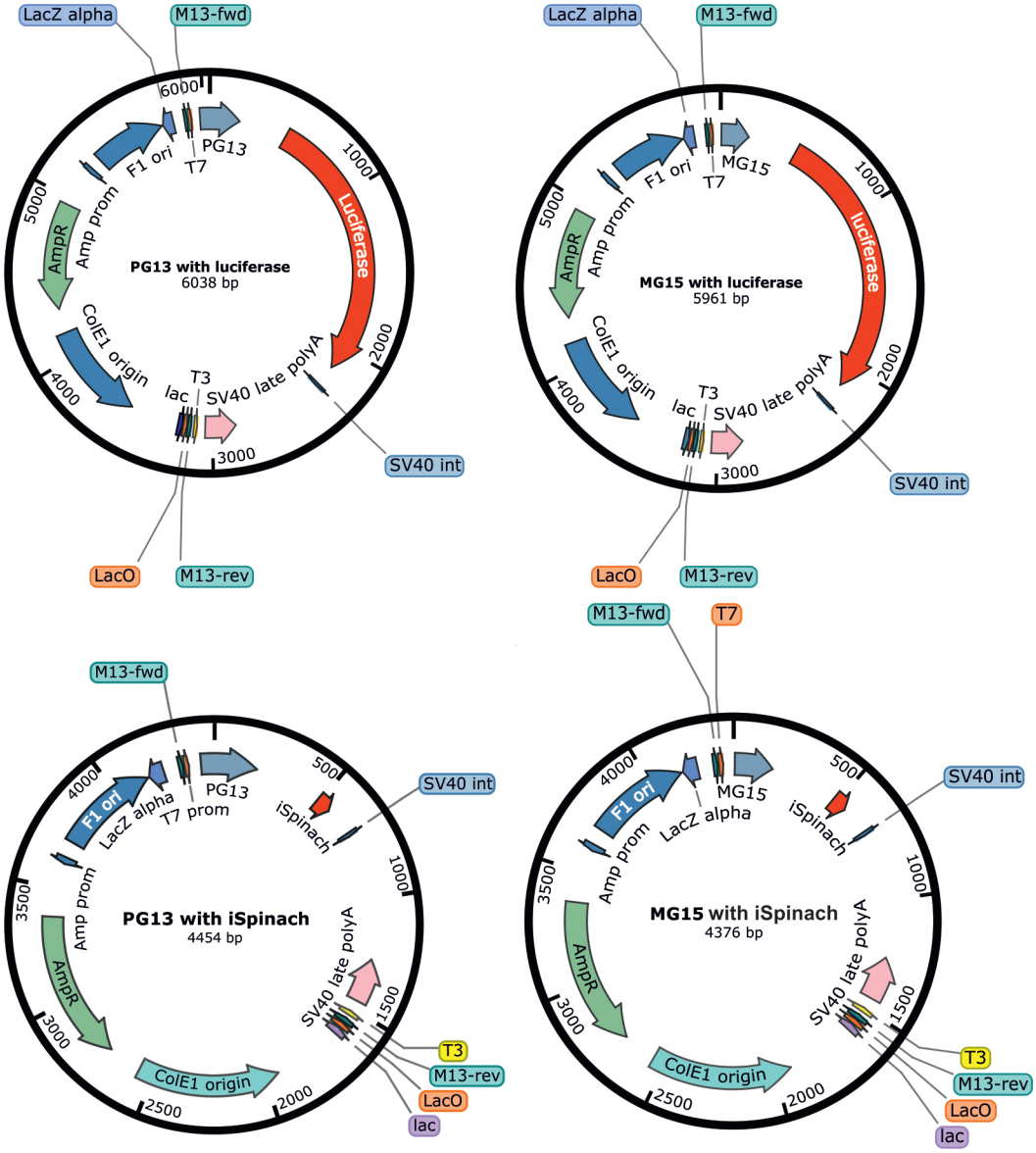

Figure 6.1: Luciferase- and iSpinach-containing PG13 and MG15 templates. Shown are the PG13 and MG15 templates containing luciferase (top), which was replaced by iSpinach (bottom).

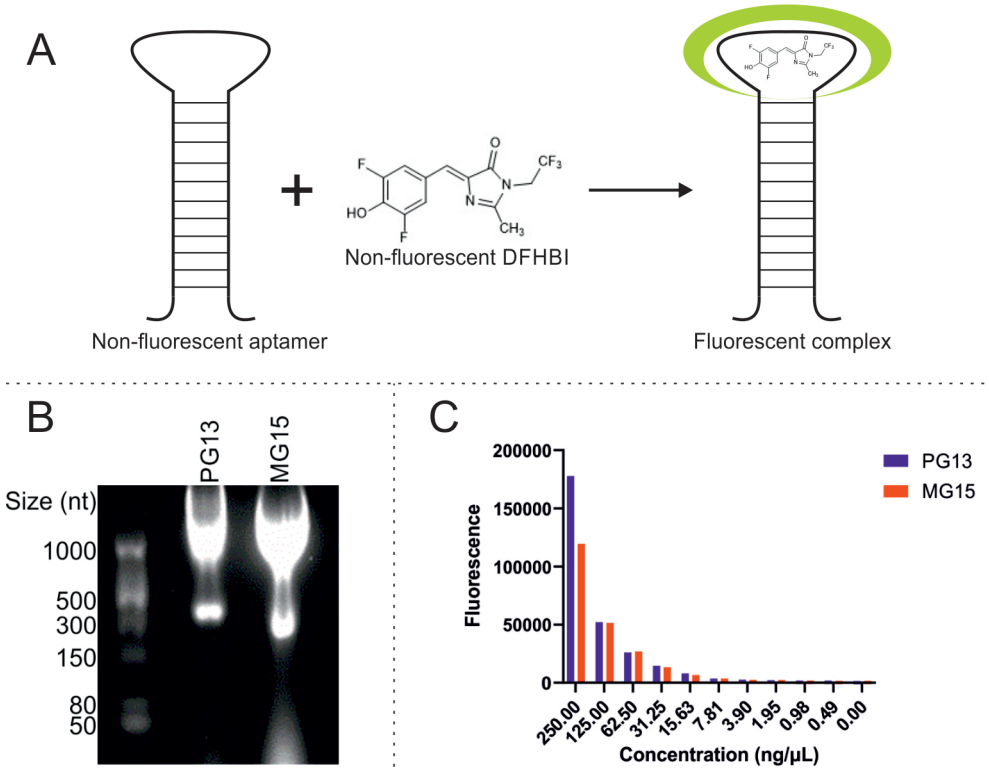

Figure 6.2: Fluorescence of the iSpinach aptamer in the presence of DFHBI. A: Schematic showing fluorescence occurring following complex formation between DFHBI and iSpinach. B: Denaturing RNA agarose gel following *in vitro* transcription using a T7 RNA polymerase kit (Thermo Fisher). Expected transcript lengths were 905 and 827 for PG13 and MG15 respectively. C: Fluorescence measurements of serially diluted T7-transcribed aptamers in the presence of 10 μM DFHBI (excitation 444 nm, emmission 520 nm).

6.2.2 $p53_{rec}$ does not induce transcription from naked DNA *in vitro*

HeLa nuclear extracts were prepared and validated by western blotting against nuclear (H3 histone) and cytoplasmic (β-tubulin) markers. The nuclear fraction was successfully enriched for nuclear proteins, as indicated by the very low presence of β-tubulin in the nuclear fraction (Fig. 6.3).

In vitro transcription using these extracts supplemented with $p53_{rec}$ failed to yield any detectable transcription, while fluorescence of the purified T7-transcribed aptamers was detected. Serial dilution of the T7-transcribed aptamers showed that fluorescence was detectable from an aptamer concentration of 15.6 ng/μL (Fig. 6.4A). To assess whether *in vitro* transcription occurred but was too low-yielding to produce detectable

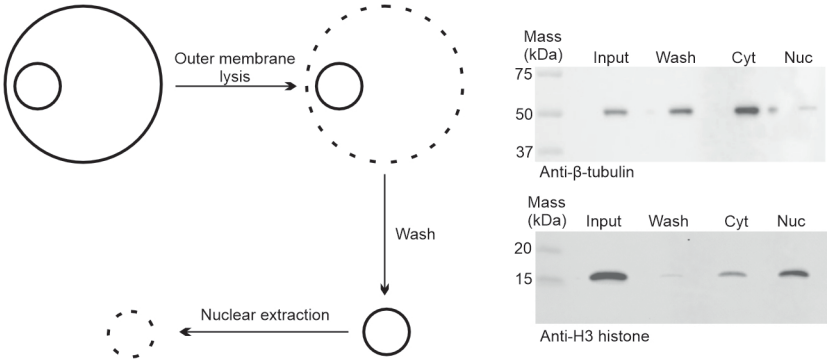

Figure 6.3: Nuclear extract preparation. Shown is a schematic of nuclear extraction preparation, along with western blots with nuclear and cytoplasmic markers (H3 histone and β-tubulin respectively). Lanes comprise the cells before lysis (input), after washing with NP-40-free buffer post outer-membrane lysis (wash), cytoplasmic extract (Cyt), and nuclear extract (Nuc).

fluorescence, RT-PCR was used. After the reaction, RNA was purified using a Monarch RNA purification kit followed by DNAseI digestion, cDNA synthesis and RT-PCR using primers complementary to iSpinach. The progress of RT-PCR reactions was monitored manually by taking aliquots of the reaction after 10, 20, 25, and 30 cycles. The T7-transcribed aptamers, which had also been reverse-transcribed, were faintly visible on an agarose gel after 10 cycles and robustly visible after 20 cycles. After 25 cycles, amplicons were visible in all reactions except those that contained both PG13 and $p53_{rec}$ (Fig. 6.4B).

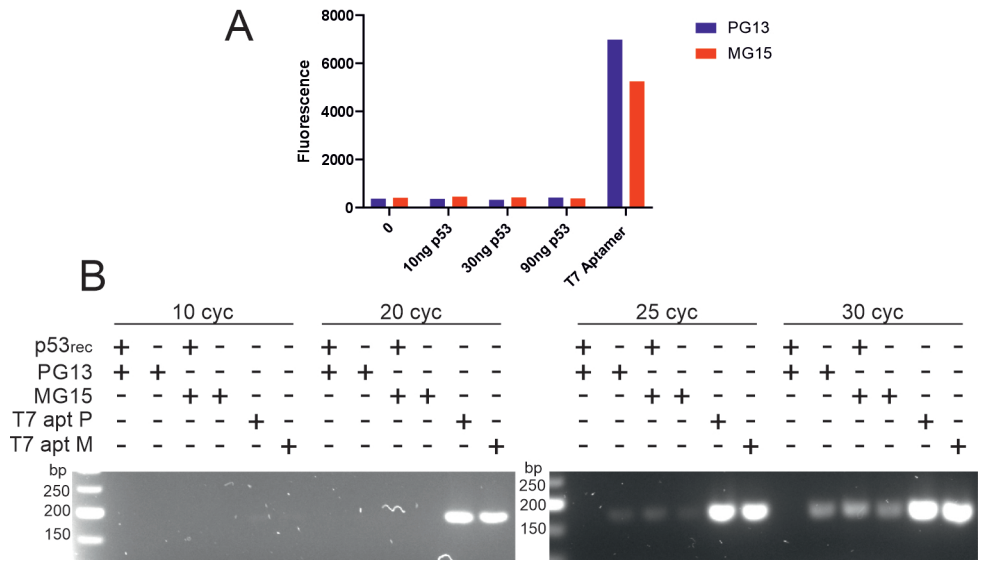

Figure 6.4: A: **Aptamer fluorescence and failed transcription.** Fluorescence measurements (excitation 444 nm, emmission 520 nm) following *in vitro* transcription in HeLa nuclear extracts. T7-transcribed aptamers were used as a positive control. B: Agarose gel following *in vitro* transcription in HeLa nuclear extracts, RNA purification, cDNA synthesis and RT-PCR. PCR reaction aliquots were taken at 10, 20, 25, and 30 PCR cycles (Cyc). Primers were complementary to cDNA synthesized from the iSpinach transcript.

6.3 Conclusion

It is unclear why no detectable transcription was observed in these assays, despite the approaches being very similar to some of those described in the literature. There are notable differences between the assays described in this chapter and those successfully carried out elsewhere. For example, these assays use $p53_{rec}$, which has no post-translational modifications. Previous assays used p53 purified from human or insect cells that potentially carry post-translational modifications. The assays reported here also use naked DNA as templates. Though robust transcription from naked DNA templates has been reported,[217] some studies have failed to detect transcription from naked DNA, only observing transcription from chromatinised templates.[58]

If the components of the transcription machinery are present in the nuclear extracts, a basal level of transcription might be expected to occur independently of p53. It is interesting to note that, following DNA depletion, cDNA synthesis, and PCR, bands were observed when either PG13 or MG15 were present without $p53_{rec}$. This suggests a

low degree of transcription is taking place independently of p53. When $p53_{rec}$ was present, this basal level of transcription occurs in the presence of MG15, but not PG13. It may be that, under these assay conditions, $p53_{rec}$ is binding to its promoter and preventing transcription. The question of whether p53 can directly repress the transcription of genes is controversial.[226] Even if direct transcriptional repression is occurring in this assay, it would be incorrect to conclude that the phenomenon necessarily occurs in nature. EMSA could be used to check whether p53 binds to the PG13 p53 binding site. Alternatively, *in vitro* transcription using a T7 polymerase in the presence of p53 might indicate whether p53 is bound to the PG13 promotor, if the presence of p53 prevents the T7 polymerase from transcribing past the p53 binding site.

In conclusion, it is unfortunate that *in vitro* transcription using $p53_{rec}$ was unsuccessful. Had transcription been detected, assays using semisynthetic p53 and chromatinised templates would have been attempted.

Recreating the early stages of p53 activation *in vitro*

7.1 Introduction

A more granular understanding of PTM crosstalk in p53 would allow us to unpick the individual steps in the PTM cascades that lead p53 to induce specific cell fates. In particular, how is the pro-apoptotic p53 state established? Many methods have been employed to study PTM crosstalk in other proteins, with much early work being carried out on histones.[227] Detecting co-occurrence of PTMs in cells, typically through mass spectrometry or western blotting, enables the initial discovery of potential crosstalk interactions. This is often facilitated through mutagenesis of residues to either alanine or a PTM mimetic and comparison of the PTMs that are installed on the different mutants. Following discovery in cells, *in vitro* assays using either synthetic peptides or site-specifically modified proteins containing pre-installed PTMs in combination with purified enzymes or functional cell extracts enable the validation of these crosstalk interactions (Fig. 7.1).[228,69,229]

For p53, much of what we know about PTM crosstalk is from work carried out in cells using mutagenesis,[39,69] with validation of crosstalk interactions often achieved using purified enzymes and p53 peptides.[82] Though nuclear extracts have been used to study PTM crosstalk in histones,[229] they have not been applied to crosstalk on p53.

Each of these approaches are complementary tools with unique advantages and disadvantages. Assays carried out in cells retain much of the complexity present in nature and can be useful for identification of crosstalk interactions, however identifying the enzymes responsible for the crosstalk can be challenging. For example, it is notable that, though a wide array of crosstalk interactions have been observed on the p53 N-terminus, very

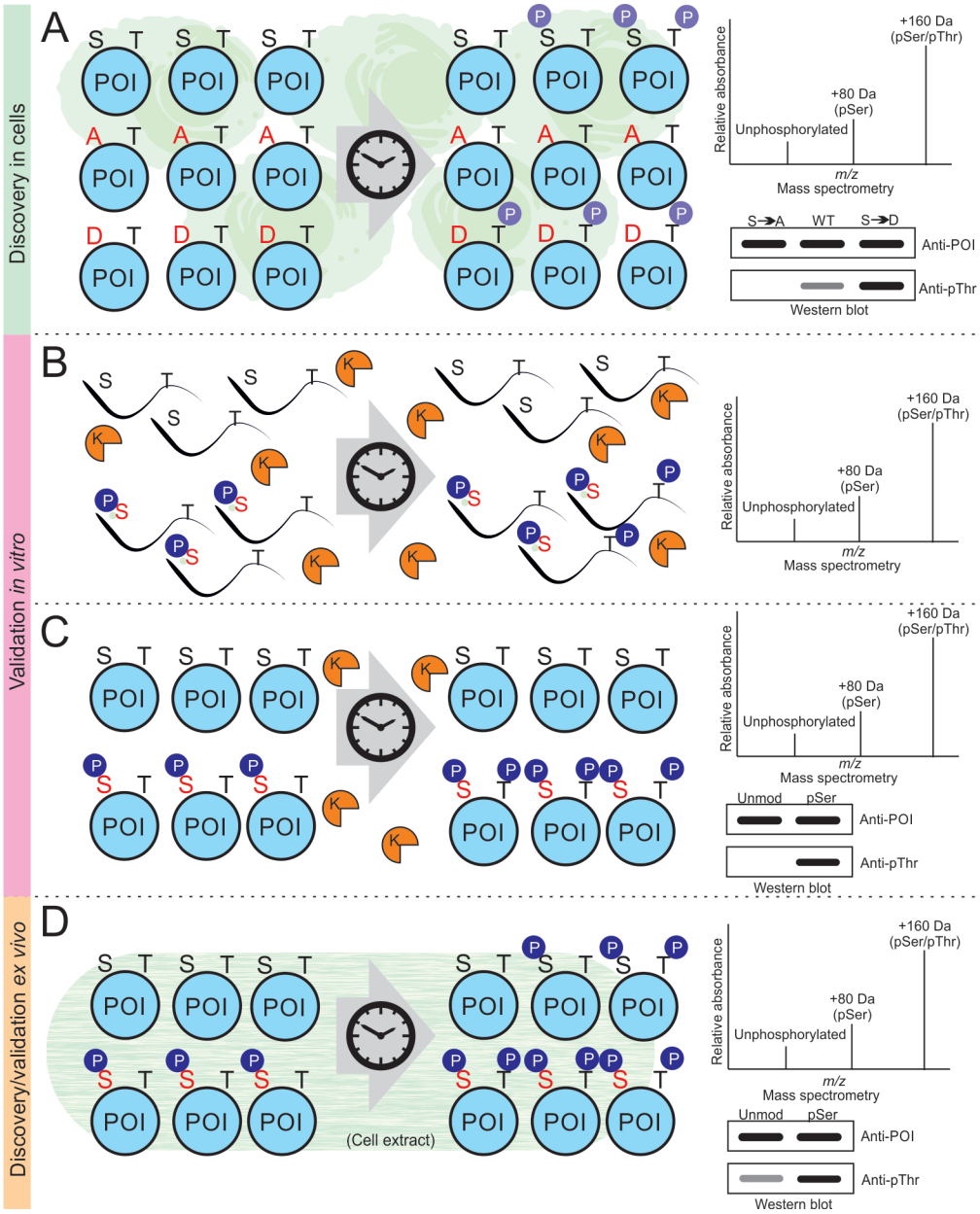

Figure 7.1: Overview of common approaches for probing PTM crosstalk. Shown are methods for probing a hypothetical crosstalk interaction where phosphorylation at a serine (S) promotes the phosphorylation of a nearby threonine (T). A: Following mutagenesis of Ser to Ala or Asp, the amount of Thr phosphorylation can be quantified by mass spectrometry or western blotting. B: Peptides bearing serine or phosphoserine are incubated with the relevant kinase with Thr phosphorylation quantified by mass spectrometry. Site-specifically modified proteins (C) can also be used, with western blotting another method of quantification. Site-specifically modified protein can also be used in cell extracts, allowing for the control over the experiment as with (C) while retaining a similar degree of biological relevance as (A).

few of the relevant kinases have been identified (Fig. 4.13, and references therein). *In vitro* assays using purified enzymes and p53 peptides or proteins allow for confirmation that p53 is a substrate for the enzyme present, and analysis of the impact of pre-installed PTMs on enzyme activity. While these types of assays are useful for probing specific interactions, they offer little information regarding the biological relevance of those interactions. For example, while ATM has been shown to phosphorylate p53 at S46 *in vitro*,[101] S46 phosphorylation was still observed in ATM-depleted cells, albeit slightly delayed.[230] Factors such as redundancy and subcellular location are lacking in these types of *in vitro* assays.

Bridging the gap between these two types of assays are those that employ functional cell extracts. Cell extracts retain much of the complexity of cell-based studies, while also giving the researcher more control over particular aspects of the experiment, such as the amount of substrate protein added. Specific quantities of site-specifically modified (or mutated) substrate can be "spiked" into the cell extract, and downstream PTMs can be detected using western blotting or mass spectrometry.[229] Cell extracts can be enriched for nuclear proteins, producing nuclear extracts similar to those used in *in vitro* transcription assays.

The experiments described in this chapter used site-specifically modified p53, generated via semisythesis, and nuclear extracts to probe p53 crosstalk interactions. Different stress regimes were applied to the cells prior to nuclear extract preparation to investigate whether PTM crosstalk can be modulated as a function of stress. These assays successfully reconstituted two well-described crosstalk interactions in p53. Specifically, the dependence of T18 phosphorylation on prior S15 phosphorylation and the positive effect of N-terminal phosphorylation on C-terminal acetylation.

7.2 Results

7.2.1 p53 undergoes post-translational modification in nuclear extracts

H1299 cells, chosen for their p53-negative status, were stressed for 24 hours with 20 μM cisplatin. This stress procedure was chosen based on prior work undertaken in the group.

Nuclear extracts were prepared from these cells and validated using nuclear (Histone H3) and cytoplasmic (β-tubulin) markers (Fig. 7.2A). $p53_{rec}$ or $p53_{S15ph}$ was spiked into the nuclear extracts, incubated for 0, 15, 30, 45, or 60 minutes at 30 °C and analysed by western blotting using an antibody against p53 (DO1, for overall p53 levels), pS15, and pT18. The anti-p53 (DO1) blot suggested that p53 levels were stable over the course of the experiment. Western blotting using an anti-pS15 antibody suggested S15 phosphorylation occurred at detectable levels in reactions containing $p53_{rec}$ after 30 minutes, peaking after 60 minutes. In the reactions containing $p53_{S15ph}$, pS15 levels appeared to stay relatively consistent. This suggested that widespread dephosphorylation was not occurring in these extracts. Western blotting using an anti-pT18 antibody led to the appearance of a band at the expected mass for p53 that increased in intensity over time in both $p53_{rec}$ and $p53_{S15ph}$. No band appeared in either the $p53_{rec}$ or $p53_{S15ph}$ controls, indicating that this band was not generated through non-specific binding to p53 (Fig. 7.2B). Based on these results, it seemed likely that the nuclear extracts contained active kinases that were phosphorylating p53.

It was unclear to what extent exposure to 20 μM cisplatin for 24 hours sufficiently stressed the cells. A screen was carried out during which H1299 cells were exposed to 0, 10, 20, 50, 100 and 1000 μM cisplatin for 0, 2, 6, 16, or 24 hours. Visual inspection under a microscope and western blotting for phosphorylated Akt1 were used as markers for cell stress. Akt1 is activated in response to DNA damage by phosphorylation and promotes cell survival, in part by promoting p53 degradation by MDM2. Akt1 activity has been shown to be inhibited by p53.[231] In p53-negative cells, we hypothesised that phosphorylated Akt1 would accumulate in response to DNA damage. A western blot for pS473 Akt1 was inconclusive, though cell death was observed from 6 hours in cells treated with 1 mM cisplatin (Fig 7.3). Cell death was only observed after 24 hours in cells treated with 100 μM cisplatin, while no visible cell death was observed in cells treated with 0, 10, 20, or 50 μM cisplatin (Fig 7.3A). Because treatment with 1 mM cisplatin led to visible cell death after 6 hours, nuclear extracts were prepared from H1299 cells treated with 1 mM cisplatin for 2 hours. The aim was to harvest the cells at a time when the DNA damage response was likely ongoing.

Having already demonstrated that nuclear extracts could phosphorylate p53 at S15 and T18, a broader screen of p53 PTMs was attempted. $p53_{rec}$, $p53_{S15ph}$, $p53_{S20ph}$ or

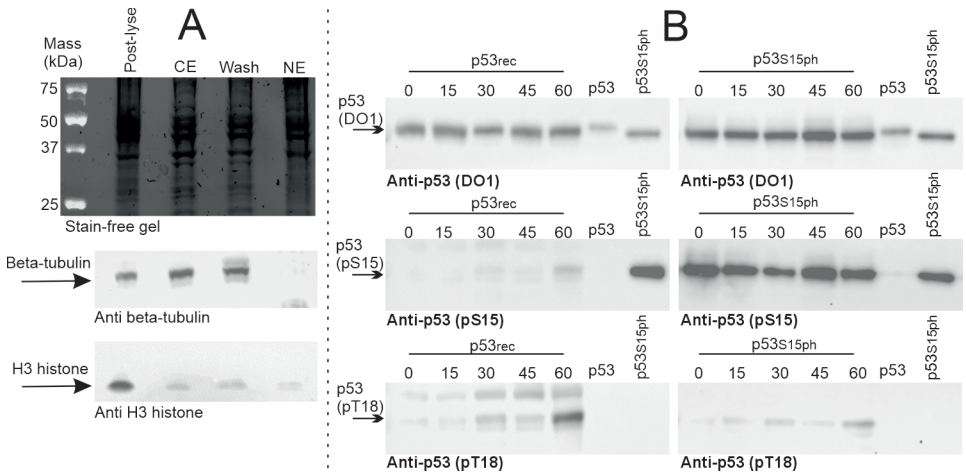

Figure 7.2: p53 phosphorylation occurs in nuclear extracts. A: Western blotting of fractions following H1299 nuclear extract preparation, where cells had been stressed for 24 hours by 20 μM cisplatin. Lanes comprise the cells immediately after lysis (post-lyse), cytoplasmic extract (CE), after washing with NP-40-free buffer post outer-membrane lysis (Wash), and nuclear extract (NE). β-tubulin and H3 histone were used as cytoplasmic and nuclear markers respectively. B: Crosstalk assays were carried out over the course of 1 hour, with reactions quenched at 0, 15, 30, 45, and 60 minutes (indicated by numbers). Accumulation of T18 phosphorylation was observed when nuclear extracts were spiked with either $p53_{rec}$ or $p53_{S15ph}$. $p53_{rec}$ also accumulated S15 phosphorylation. For stain-free gel images, see supplementary figures (Fig. 10.2).

$p53_{S15/S20ph}$ (double-phosphorylated) were incubated for 2 hours at 30 °C with nuclear extracts prepared from H1299 cells that were either unstressed or stressed with 1 mM cisplatin. Western blots were carried out using a general antibody against p53 (DO1), as well as a panel of p53 PTMs: pS15, pT18, pS20, AcK120, AcK373, AcK382. Because of the large number of western blots, multiple PVDF membrane stripping approaches were used, and their effectiveness assessed for future assays. Tandem mass spectrometry was also attempted to obtain a broad assessment of p53 PTMs in an unbiased manner. For this, quenched reactions were subjected to SDS-PAGE, and p53 was purified by cutting out the corresponding band following Coomassie blue staining. Unfortunately, no data were obtained with this method.

The antibodies against p53 (DO1) and AcK120 were both derived from mice, while antibodies against all other PTMs were derived from rabbits. Membranes were first probed with either anti-p53 (DO1) or anti-AcK120. "Mild" stripping using an acidic

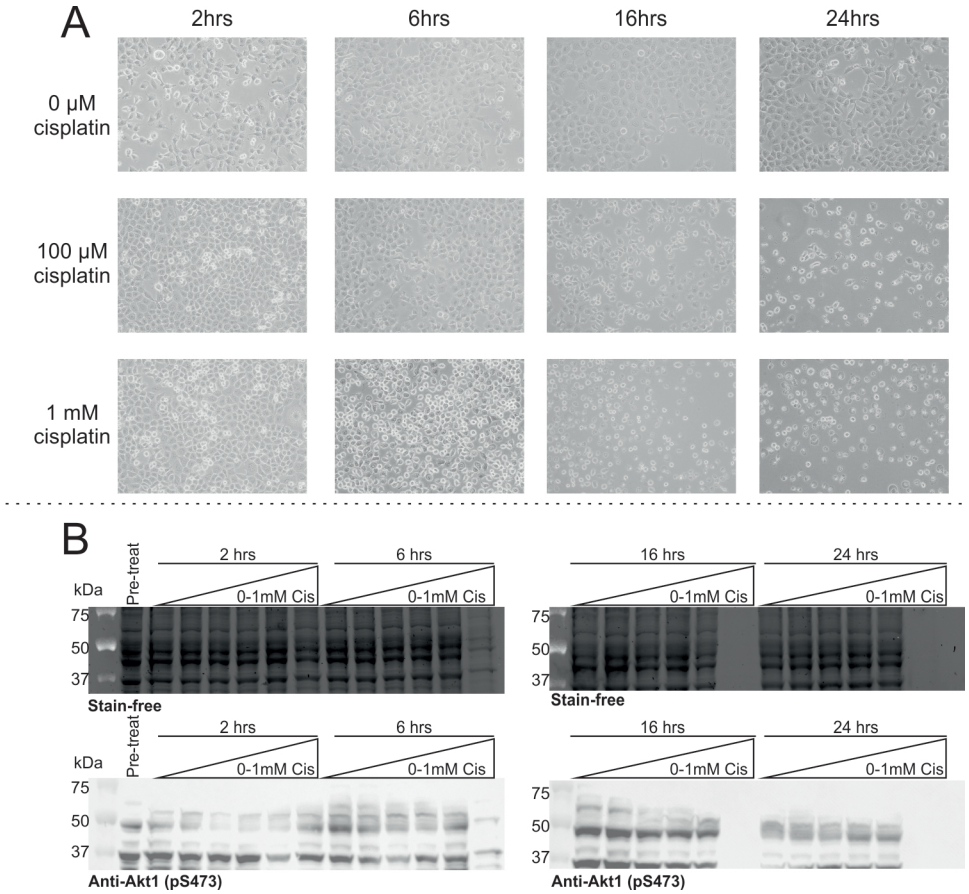

Figure 7.3: Cisplatin treatment screen. A: H1299 cells were treated with 0-1 mM cisplatin for 24 hours. Cell death was visible in the 1 mM-treated cells from 6 hours, while in the 100 μM-treated cells cell death was visible after 24 hours. B: Lysates from H1299 cells treated with 0, 10, 20, 50, 100, or 1000 μM cisplatin were blotted against pS473 Akt1. Shown are stain-free gels (top) and western blots (bottom). Western blotting generated many non-specific bands, with pAkt1 expected to fall at around 60 kDa. Cell images for 10, 20, 50 μM cisplatin treatments can be found in supplementary figures (Fig. 10.3).

SDS-containing buffer enabled each membrane to be re-probed against one of the antibodies derived from rabbits. Subsequent stripping and re-probing was carried out using "harsh" stripping methods that utilise hot (55 °C) SDS. The stripping/reprobing strategy employed in this experiment is shown in Figs. 7.4 and 7.5. For experiments carried out in unstressed extracts (Fig. 7.4), western blotting using a general anti-p53 antibody (DO1) showed highly variable signal for the different phosphorylated forms of p53, with no signal observed in reactions containing $p53_{S15/S20ph}$ and little signal observed in reactions containing $p53_{S20ph}$ (Fig. 7.4, top left blot). Mild stripping and reprobing this membrane with an antibody against pS15 p53 led to the bands from reactions and con-

trols containing $p53_{rec}$ and $p53_{S20ph}$ disappearing, while bands were visible in $p53_{S15ph}$ and $p53_{S15/S20ph}$-containing reactions and controls (Fig. 7.4, left blot second from the top). The fact that no signal was observed in $p53_{S20ph}$ and $p53_{S20ph}$-containing reactions suggested that no detectable S15 phosphorylation was occurring in these reactions. Harsh stripping of this membrane followed by re-probing with an antibody against pT18 p53 led to bands appearing in all time-points of the p53-containing reactions, including the 0 minute time-point, with no visible increase over time. For signal appearing in $p53_{rec}$, $p53_{S15ph}$, and $p53_{S15/S20ph}$ lanes, this was likely caused by incomplete stripping and retention of signal from the previous blot. For the bands appearing in $p53_{S20ph}$ reaction lanes, this was likely caused by non-specific binding of the primary antibody to $p53_{S20ph}$, as signal also appeared at similar intensity for the $p53_{S20ph}$ control (Fig. 7.4, left blot second from the bottom). This membrane was stripped using GuHCl and re-probed for an antibody targeting AcK373 p53. $p53_{rec}$ lanes showed very faint bands appearing at 30 and 60 minutes, with no signal observed for the $p53_{rec}$ control. $p53_{S15ph}$ lanes showed robust bands at all time points, with signal also appearing for the $p53_{S15ph}$ control. This suggested the signal for $p53_{S15ph}$ was likely caused by incomplete stripping of the membrane. Bands were observed at 30 and 60 minutes for both $p53_{S20ph}$ and $p53_{S15/S20ph}$-containing reactions, increasing over time, with no bands appearing in the respective control lanes. This suggested that these bands were likely not caused by incomplete stripping, and that they represented genuine K373 acetylation (Fig. 7.4, bottom left blot). A western blot was carried out on fresh membranes using antibodies targeting AcK120 p53. Bands were observed at all time-points in all reactions, including the reactions that did not contain p53. Because bands appeared in the reactions that did not contain p53, these bands were not indicative of K120 acetylation (Fig. 7.4, top right blot). This membrane underwent mild stripping and was re-probed using an antibody against pS20 p53 (Fig. 7.4, right blot second from the top). This led to robust bands for the reactions containing $p53_{rec}$ at all time points, with no band observed in the $p53_{rec}$ control, suggesting pS20 phosphorylation may have occurred very rapidly. Bands appeared for reactions containing $p53_{S15ph}$ and $p53_{S20ph}$ at all time-points, and in these cases bands were also observed in the corresponding controls. This suggested that, for $p53_{S15ph}$-containing reactions, these bands were indicative of nonspecific binding of the antibody. For $p53_{S15/S20ph}$, bands were observed in both the reactions and the corresponding control, though they

were visibly fainter than the bands for $p53_{S20ph}$-containing reactions and controls. This suggested that the S15 phosphorylation may be weakening the interaction between p53 and the anti-$p53_{S20ph}$ antibody. This membrane was harsh-stripped and re-probed using an antibody targeting AcK382 p53 (Fig. 7.4, right blot second from the bottom). No bands were observed in reactions or controls containing unmodified or $p53_{S15ph}$. Bands were observed in reactions containing pS20 and pS15/$p53_{S20ph}$, however they were also observed in the corresponding controls. This was likely caused by incomplete stripping of the previous primary antibody, which targeted $p53_{S20ph}$. The membrane was stripped with GuHCl and probed again with the antibody targeting AcK382 p53, leading to no visible bands (Fig. 7.4, bottom right blot).

The results obtained using 1 mM cisplatin-stressed nuclear extracts were similar, with the following differences: before probing with the antibody targeting AcK373 p53, the membrane was harsh stripped to remove the previous antibody targeting pT18 p53 (Fig. 7.5, left blot second from bottom). In unstressed extracts, the stripping at this stage was carried out using GuHCl. Harsh stripping led to bands being visible at all time-points for $p53_{rec}$, $p53_{S15ph}$, and $p53_{S15/S20ph}$. The $p53_{S15ph}$ and $p53_{S15/S20ph}$ control lanes also contained signal, indicating that the signal for $p53_{S15ph}$ and $p53_{S15/S20ph}$-containing reactions was caused by incomplete stripping. Bands were visible from 30 minutes in the $p53_{S20ph}$-containing reactions, with no band visible in the $p53_{S20ph}$ control, suggesting that K373 acetylation was likely occurring in these reactions. Stripping this membrane with GuHCl and re-probing with the antibody targeting AcK373 p53 led to visible bands in the $p53_{rec}$ and $p53_{S20ph}$-containing reactions, and no bands visible in any control lanes (Fig. 7.5, bottom left blot). This suggested that K373 acetylation was occurring when p53 was either unmodified or phosphorylated at S20. In contrast to the reactions carried out with unstressed nuclear extracts, no K373 acetylation was observed in the $p53_{S15/S20ph}$-containing reactions.

Robust K373 acetylation was subsequently observed in nuclear extracts derived from both unstressed and 1 mM cisplatin-stressed cells (Fig. 7.6). No clear difference in K373 acetylation was observed between the different forms of p53.

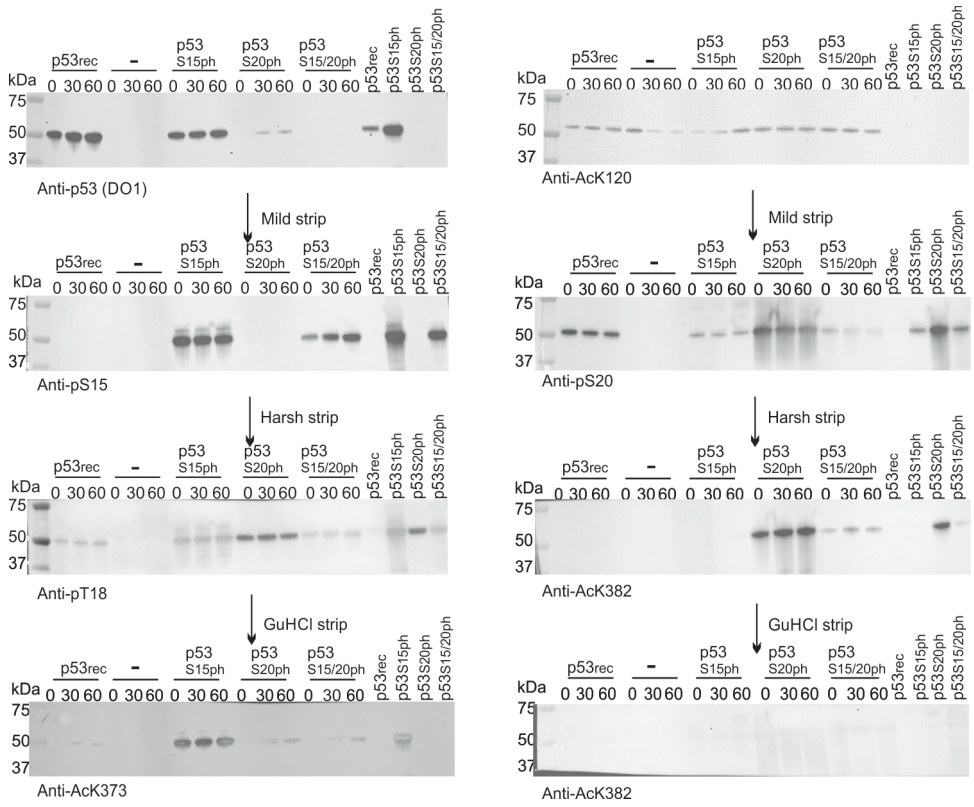

Figure 7.4: Broad PTM screen in unstressed nuclear extracts. $p53_{rec}$, $p53_{S15ph}$, $p53_{S20ph}$, and $p53_{S15/S20ph}$, as well as a negative control with no p53 were incubated for 0, 30 or 60 minutes (indicated by 0, 30, 60) with nuclear extracts derived from unstressed H1299 cells. Shown are the order in which membranes were probed with different primary antibodies, and the method with which they were stripped. Membranes were either stripped with acidified (pH 2) SDS-containing buffer (mild strip), a hot (55 °C) SDS-containing buffer (harsh strip), or a buffer containing 6M guanidine and β-ME (GuHCl strip). For stain-free gel images and replicates, see supplementary figures (Fig. 10.4).

From these data, it was decided that four main elements of the experimental design needed refining. Firstly, antibody occlusion and cross-binding was clearly taking place, particularly with the anti-p53 (DO1) antibody, which is required to confirm equal p53 levels. Antibody validation regarding epitope occlusion and cross-binding would give us more confidence that our observations represent true positive or true negative results. Secondly, a method for normalising data to allow for statistical analysis of data obtained from different blots was required. Thirdly, the reactions were being carried out at 30 °C. We considered that cooling the reactions to 16 °C may slow down the accumulation of PTMs and make detecting differences in the rate of PTM accumulation easier while also protecting p53 from unfolding. Fourthly, it was still unclear whether the "stressed"

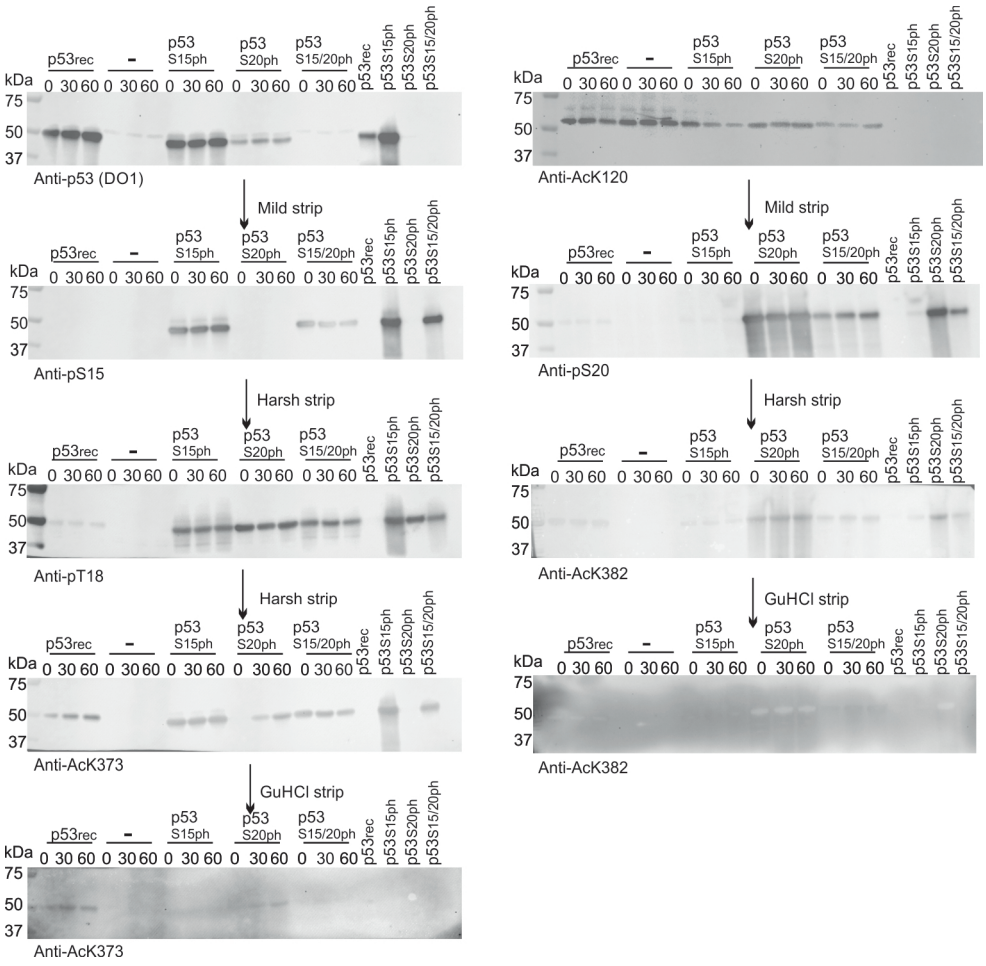

Figure 7.5: Broad PTM screen in stressed nuclear extracts. $p53_{rec}$, $p53_{S15ph}$, $p53_{S20ph}$, and $p53_{S15/S20ph}$, as well as a negative control with no p53 were incubated for 0, 30 or 60 minutes (indicated by 0, 30, 60) with nuclear extracts derived from H1299 cells that had been stressed for 2 hours with 1 mM cisplatin. Shown are the order in which membranes were probed with different primary antibodies, and the method with which they were stripped. Membranes were either stripped with acidified (pH 2) SDS-containing buffer (mild strip), a hot (55 °C) SDS-containing buffer (harsh strip), or a buffer containing 6M guanidine and β-ME (GuHCl strip). For stain-free gel images and replicates, see supplementary figures (Fig. 7.5).

H1299 extracts used in these experiments were appropriately stressed. Though cell death was observed in the 1 mM cisplatin-treated H1299 cells, it was not known whether death occurred via apoptosis or necrosis. The aim was to find a stress regime that, if it H1299 cells were $p53^{+/+}$, would induce a p53 response.

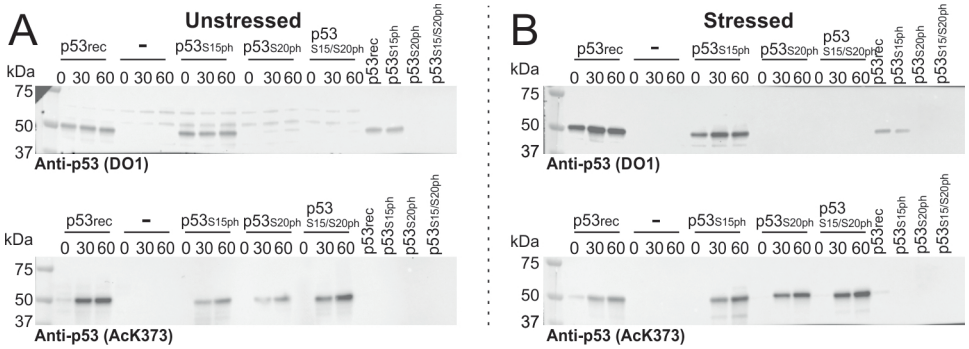

Figure 7.6: p53 acetylation occurs in nuclear extracts. $p53_{rec}$, $p53_{S15ph}$, $p53_{S20ph}$, and $p53_{S15/S20ph}$, as well as a negative control with no p53 were incubated for 0, 30 or 60 minutes (indicated by 0, 30, 60) with nuclear extracts derived from H1299. A: Assay performed in unstressed H1299 extracts. Shown is a western blot against p53 (DO1, top) and AcK373 p53 (bottom). B: Assay performed in H1299 extracts from cells stressed with 1 mM cisplatin for 2 hours. Shown is a western blot against p53 (DO1, top) and AcK373 p53 (bottom).

7.2.2 Antibody validation

SDS-PAGE was carried out on equal amounts of $p53_{rec}$, or semisynthetic $p53_{S15ph}$, $p53_{S20ph}$, or $p53_{S15/S20ph}$. Following transfer to PVDF, membranes were probed with antibodies against p53 (DO1), pS15, pT18 and pS20 (Fig. 7.7). As before, epitope occlusion was clearly visible when DO1 was probed against p53 phosphorylated at S20, alone or in combination with S15. Epitope occlusion was also observed when anti-pS15 antibody was probed against p53 phosphorylated at both S15 and S20, and with the anti-pS20 antibody when it was used to probe p53 phosphorylated at both S15 and S20. Faint cross-binding was observed when anti-pT18 antibody was probed against p53 monophosphorylated at S15 or S20. An alternative anti-p53 antibody, "Y5", was kindly provided by Abcam for evaluation of epitope occlusion (the precise epitope is not in the public domain). No epitope occlusion was observed when Y5 was probed against the aforementioned p53 variants, so this antibody was used in subsequent assays instead of DO1.

7.2.3 Cofactor titration

The assays performed previously contained 833 μM ATP, 10 μM AcCoA, and 10 μM SAM. For AcCoA and SAM, these concentrations were determined based on previous assays carried out in the literature using recombinant acetyltransferases and methyl-

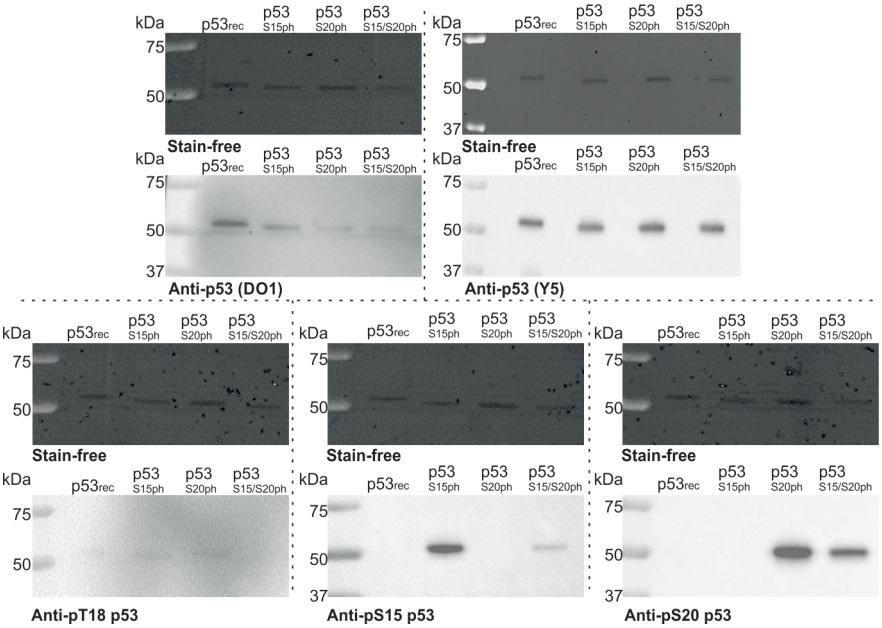

Figure 7.7: Antibody occlusion screen. Antibodies against p53 (DO1 and Y5), pS15, pT18, and pS20 were screened against 50 ng of $p53_{rec}$, $p53_{S15ph}$, $p53_{S20ph}$, or $p53_{S15/S20ph}$. Also shown are stain-free images taken before transfer.

transferases.[232,168,233,67] ATP was added to a much higher concentration because the intracellular concentration of ATP is typically in the low millimolar range, and 833 μM was the final concentration when the purchased ATP stock was used undiluted.[234,235]

Titrations were performed using p53 and nuclear extracts at 30 °C to find the optimal cofactor concentrations. The unmodified p53 used in these assays was produced recombinantly in *E. coli* and contained the M40C mutation present in the semisynthetic variants. Hereon, this will be referred to as $p53_{rec\Delta}$. Optimal cofactor concentrations were determined by western blotting for T18 phosphorylation in $p53_{S15ph}$, K373 acetylation in $p53_{rec\Delta}$, and K372 mono-methylation in $p53_{rec\Delta}$ (Fig. 7.8). Robust T18 phosphorylation was observed with 250 μM ATP, and appeared to peak at 500 μM ATP. K373 acetylation was observed even when no exogenous AcCoA was added, though acetylation peaked with the addition of 10 μM AcCoA. No signal was observed in the $p53_{rec\Delta}$ control when blotted for AcK373 p53, so this may have been caused by endogenous AcCoA being bound to acetyltransferases and remaining in the extract. Equal bands were observed across all SAM concentrations and time-points, with visibly lower signal in the $p53_{rec\Delta}$ control (Fig. 7.8). This may indicate very rapid methylation that peaks at residual endogenous SAM concentrations. It may also indicate that no detectable methylation occured, with the

antibody against MetK372 binding non-specifically to p53. In this case, the lower band intensity seen in the $p53_{rec\Delta}$ control lane may be caused by uneven transfer, something that had been observed previously.

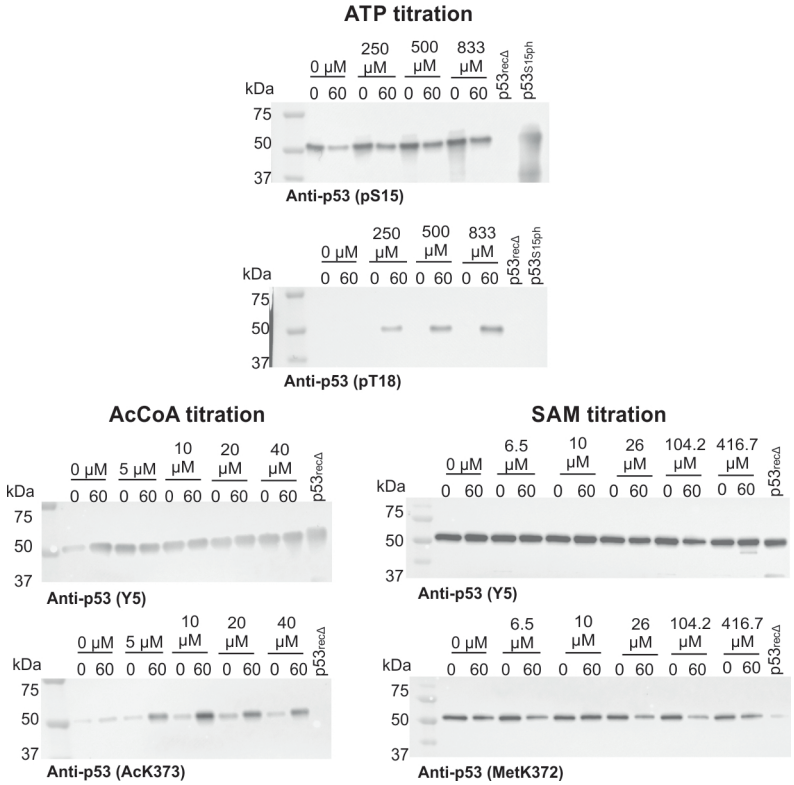

Figure 7.8: Cofactor titration Assays were performed using p53 in nuclear extracts, supplementing PTM cofactors at different concentrations. ATP titration assays were carried out using $p53_{S15ph}$, blotting for T18 phosphorylation. AcCoA and SAM titration assays were carried out using $p53_{rec\Delta}$, blotting for AcK373 and Met372 p53 respectively. Time points (0, 60) are shown in minutes. Also loaded are 50 ng p53 controls. Overall p53 levels in the ATP titration assays were determined using an anti-p53 (pS15) antibody. ATP titration data were collected by Maria Hancu. For stain-free gel images, see supplementary figures (Fig. 10.6).

7.2.4 Data normalisation strategy development

Nuclear extracts were prepared from H1299 cells that has been subjected to one of four stress regimes: unstressed, 20 μM cisplatin for 24 hours, 100 μM cisplatin for 6 hours, or 1 mM cisplatin for 2 hours. The known crosstalk relationship between pS15 and pT18 was probed to see if the accumulation of T18 phosphorylation was affected by stress. For these assays, anti-p53 (Y5) antibody was used to measure overall p53 levels. Assays

using unstressed, 20 μM, and 1 mM cisplatin-stressed nuclear extracts were carried out in triplicate, though it should be noted that replicates used the same batches of stressed nuclear extracts and p53, making them technical rather than biological replicates. Assays using extract from cells stressed with 100 μM cisplatin were not carried in triplicate due to lack of extract. Whereas the assays described in section 7.2.1 were carried out at 30 °C, these assays were carried out at 16 °C, as it was thought that slowing the reaction down might make the differences in the rate of pT18 accumulation easier to detect.

Robust accumulation of T18 phosphorylation was observed in extracts that had been spiked with $p53_{rec\Delta}$ or $p53_{S15ph}$ (Fig. 7.9). Visually, pT18 levels were consistently higher in assays containing $p53_{S15ph}$ than they were in assays containing $p53_{rec\Delta}$. However, the Y5 blot indicated that overall p53 levels also varied from lane-to-lane, often trending upwards over time (Fig. 7.9, top blots). Western blots varied in their overall levels of transfer, which would increase variation (Fig. 7.9, middle blots). Moreover, some western blots showed evidence of uneven transfer, with decreased signal towards the right hand side of the blot (Fig. 7.9, top left blot).

These issues made data analysis difficult. A normalisation strategy was devised whereby the signals for the anti-pS15/anti-pT18 western blots would be normalised against a band on each blot where the intensity should be constant. The band chosen was the 60-minute time-point of the assays spiked with $p53_{S15ph}$. The positive control bands were not used for normalisation because of the issues observed with uneven transfer, which tended to occur on the edges of the membrane and would artificially inflate the values if the transfer was poor across the positive control lanes. Because the 60 minute time point of $p53_{S15ph}$ had been used for normalisation, all the normalised band intensities for these lanes became 1, with zero standard deviation. Direct, pairwise comparison between the 60-minute band intensities between $p53_{rec\Delta}$ and $p53_{S15ph}$ would not be appropriate under these circumstances. However, because the differences are visually at their most stark after 60 minutes, it was still considered useful to analyse the data after 60 minutes. Shown in Fig. 7.9B is a graphical comparison of average, normalised band intensities for each blot at 0 and 60 minutes. Averaged, normalised band intensities at 60 minutes were analysed by one sample t test, comparing the means to 1. Naturally, for bands that were used for the normalisation, no p value could be obtained as the sample difference had no standard deviation. In all stress conditions, pT18 band intensities for

$p53_{rec\Delta}$ were significantly lower than 1 after 60 minutes (unstressed p=0.0061, 20 μM cisplatin p=0.004, 1 mM cisplatin p=0.0006). This, combined with the trend visible on the blot, suggests that $p53_{S15ph}$ becomes phosphorylated at T18 more than $p53_{rec\Delta}$. After 60 minutes, pS15 band intensities were significantly lower than 1 only in the reactions carried out in 1 mM cisplatin-stressed extracts.

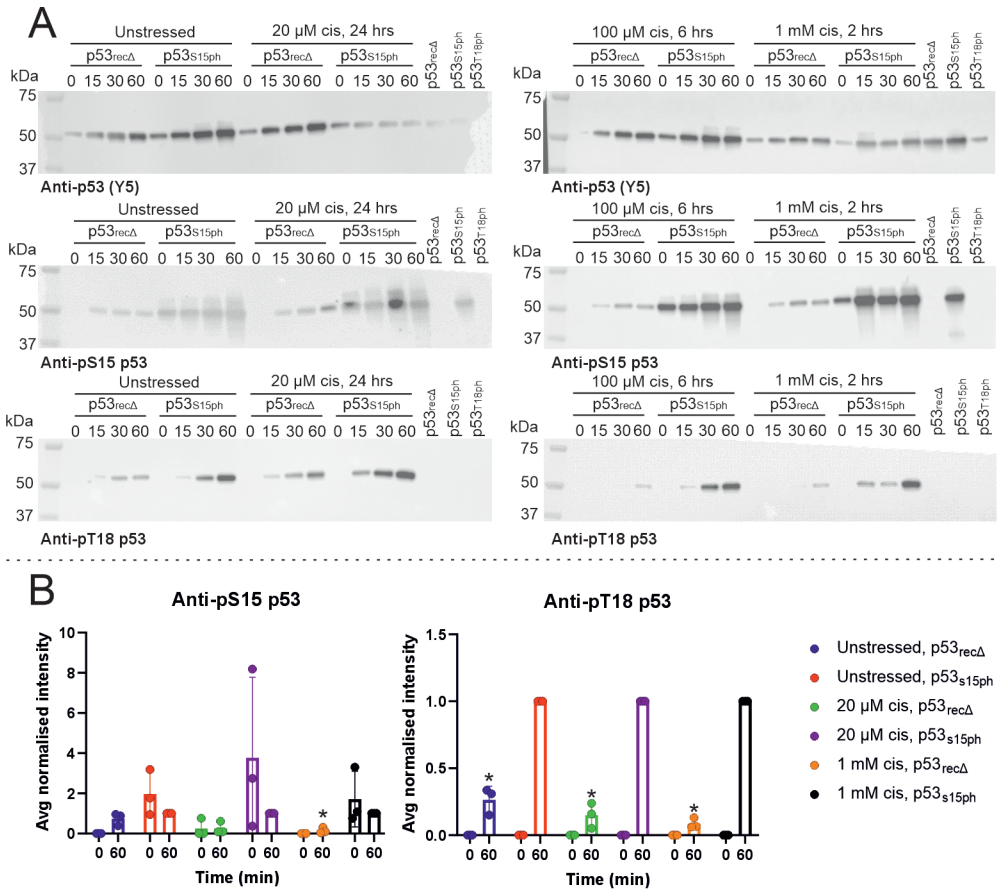

Figure 7.9: Probing the pS15-pT18 axis using cisplatin-stressed extracts at 30 °C. A: $p53_{rec\Delta}$ or $p53_{S15ph}$ were incubated for 0, 15, 30 or 60 minutes (indicated by 0, 15, 30, 60) with nuclear extracts derived from H1299 cells. Cells from which nuclear extracts were prepared were either unstressed or subjected to the following cisplatin treatments: 20 μM for 24 hours, 100 μM for 6 hours, 1 mM for 2 hours. Shown are western blots against p53 (Y5, top), anti-pS15 p53 (middle), and anti-pT18 p53 (bottom). Also shown are 50 ng positive controls for $p53_{rec\Delta}$, $p53_{S15ph}$, and $p53_{T18ph}$. B: Band intensities at 60 minutes were normalised by the 60 minute time point of pS15, averaged, and analysed one sample t test, comparing to 1. Statistically significant differences are indicated by an asterisks (*). Only data for t0 and t60 is shown for clarity. $\alpha = 0.05$, n = 3. Data collected by Maria Hancu. For stain-free gel images and replicates, see supplementary figures (Figs. 10.7) and 10.8).

Normalising by a band presumed to have consistent intensity may account for differences in transfer efficiency between blots, but would not account for uneven transfer within the same blot. Multiple approaches were tried to account for potential uneven transfer within the same blot, including staining post-transfer with Ponceau S; and re-imaging the gel post-transfer, assuming any un-transferred protein gets retained on the gel. Ponceau S staining typically yielded very faint bands, or none at all. Imaging the gel post-transfer did provide useful visual information, however they were not used for precise normalisation as they became very fragile and tended to break as they were prised off the filter paper.

It was concluded that some of the variation exhibited in these assays was better alleviated by making adjustments to the experimental procedure, rather than through normalisation, though normalisation by the 60 minute $p53_{S15ph}$ band would continue. In subsequent assays, time-point measurements would be taken by removing aliquots from single, larger reactions, rather than by preparing individual reactions for each time-point. Images of gels post-transfer allowed for a visual check that transfer occurred evenly.

7.2.5 Reconstitution of known PTM cascades

The effect of S15 phosphorylation on accumulation of T18 phosphorylation was probed using unstressed H1299 nuclear extracts at 16 °C. After 1 hour incubation, T18 phosphorylation levels were consistently higher across all three replicates when p53 was pre-phosphorylated at S15, compared to $p53_{rec\Delta}$, as determined by western blotting and densitometric analysis (Fig. 7.10A, left). For these, and subsequent, experiments, triplicates made use of separately-prepared batches of nuclear extracts, making them biological replicates (though the p53 used was not from separate batches). Band intensities on each blot were normalised by the band present after 60 minutes for the $p53_{S15ph}$-containing reactions. One sample t test comparing the mean of the normalised band intensities for $p53_{rec\Delta}$ after 60 minutes showed that the mean was significantly lower than 1 when blotting with an antibody against pS15 p53 ($p < 0.0001$) and pT18 p53 ($p = 0.0113$, Fig. 7.10B). No detectable phosphorylation occurred in unstressed H1299 cytoplasmic extracts (Fig. 7.10A, right). Recombinant CK1 has been used to probe the effect of S15 phosphorylation on T18 phosphorylation *in vitro* previously.[82] In an *in vitro* assay using recombinant CK1, pT18 levels were consistently higher across all replicates when p53 was

pre-phosphorylated at S15, compared to $p53_{rec\Delta}$. Based on a one sample t test, average normalised band intensities for $p53_{rec\Delta}$ were significantly lower than 1 when blotting against pT18 p53. Because no signal was detected in any replicates for the $p53_{rec\Delta}$ lanes when blotting for pS15 p53, statistical analysis was not carried out on these samples, however signal was consistently higher in the lanes containing $p53_{S15ph}$ (Fig 7.11).

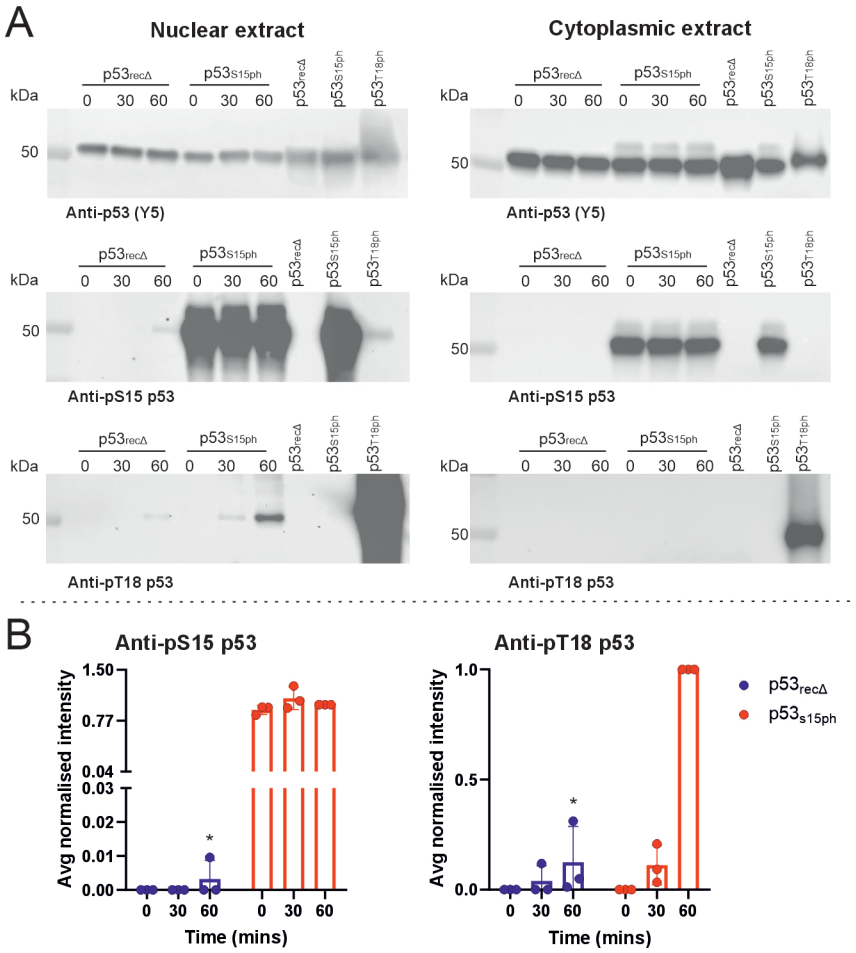

Figure 7.10: Probing the pS15-pT18 axis using unstressed extracts at 16 °C. $p53_{rec\Delta}$ or $p53_{S15ph}$ were incubated for 0, 30 or 60 minutes (indicated by 0, 30, 60) with unstressed H1299 nuclear or cytoplasmic extracts. A: Western blots against p53 (Y5, top), pS15 p53 (middle) and pT18 p53 (bottom) for assays carried out in nuclear and cytoplasmic extracts. Also included are 50 ng controls for $p53_{rec\Delta}$, $p53_{S15ph}$, and $p53_{T18ph}$. B: Band intensities were normalised by the 60 minute time point of $p53_{S15ph}$, averaged, and the means for $p53_{rec\Delta}$ at 60 minutes were analysed by one sample t test, comparing to 1. Statistically significant differences are indicated by an asterisk (*). α=0.05, n = 3. For stain-free gel images and replicates, see supplementary figures (Figs. 10.9, 10.10, and 10.11).

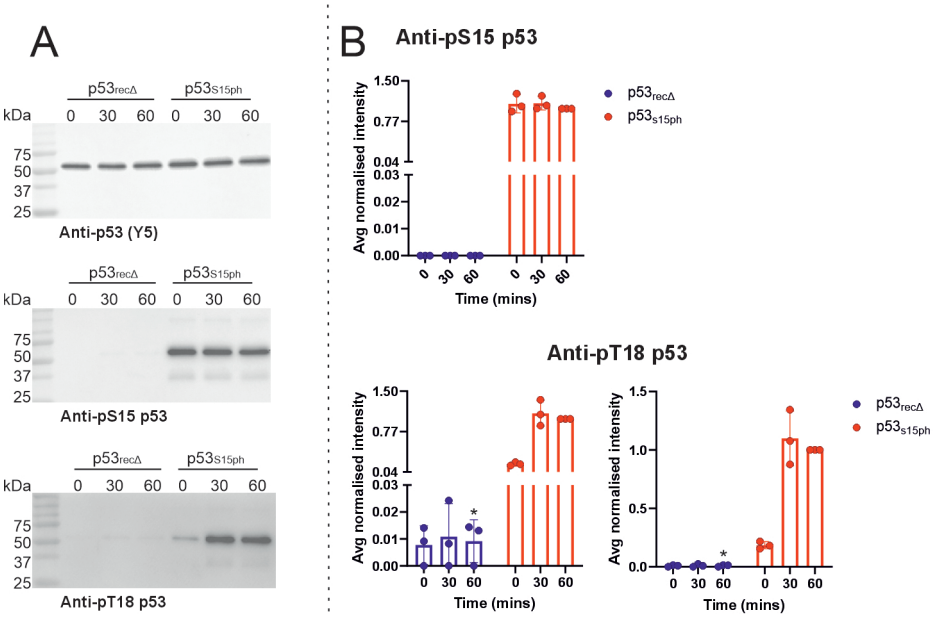

Figure 7.11: Probing the pS15-pT18 axis using purified CK1 $p53_{recΔ}$ or $p53_{S15ph}$ were incubated for 0, 30 or 60 minutes (indicated by 0, 30, 60) with recombinant CK1. A: Western blots against p53 (Y5, top), pS15 p53 (middle) and pT18 p53 (bottom). B: Band intensities were normalised by the 60 minute time point of $p53_{S15ph}$, averaged, and the means for $p53_{recΔ}$ at 60 minutes were analysed by one sample t test, comparing to 1. Statistically significant differences are indicated by an asterisk (*). Densitometric data from western blots against pT18 p53 is shown with a split axis (left) to enable visualisation of the spread of data and without a split axis (right) to enable visualisation of the time course of the reaction. α=0.05, n = 3. For stain-free gel images and replicates, see supplementary figures (Figs. 10.12 and 10.13).

Using nuclear and cytoplasmic extracts extracts prepared from unstressed H1299 cells, the effect of N-terminal phosphorylation on K373 acetylation was investigated by comparing $p53_{S15/S20ph}$ with $p53_{recΔ}$. Based on western blots carried out with a general anti-p53 antibody (Y5), p53 levels remained stable in both nuclear and cytoplasmic extracts over the course of 60 minutes. p53 band intensities were visibly lower in the cytoplasmic extract, which may have been caused by low transfer efficiency. When reactions carried out in nuclear extracts were blotted against AcK373 p53, both $p53_{recΔ}$ and $p53_{S15/S20ph}$ showed an increase in band intensity over time. $p53_{recΔ}$-containing reactions show positive bands from 0 minutes, however based on the $p53_{recΔ}$ control lane this may have been caused by non-specific binding of the primary antibody. Band intensities were consistently higher at 30 and 60 minutes for the $p53_{S15/S20ph}$-containing reactions than for those that contained $p53_{recΔ}$. Band intensities for the anti-AcK373 p53 blots were nor-

malised by the $p53_{S15/S20ph}$ band at 60 minutes on the same blots and analysed by one sample t test, comparing to 1. In nuclear extracts, normalised band intensities for $p53_{rec\Delta}$ after 60 minutes were significantly lower than 1 ($p = 0.0006$). In cytoplasmic extracts, bands were visible at all time points for both $p53_{rec\Delta}$ and $p53_{S15/S20ph}$-containing reactions when blotted with an antibody against AcK373 p53, with no visible increase over time. Signal was also observed in the control lanes, suggesting that the bands observed represent non-specific binding. Signal was visibly weaker in the $p53_{S15/S20ph}$-containing reactions and controls than those that contained $p53_{rec\Delta}$, despite the overall p53 levels being similar. This suggests that these N-terminal phosphorylation may somehow occlude antibody binding, despite the antibody targeting a C-terminal acetylation site (Fig. 7.12).

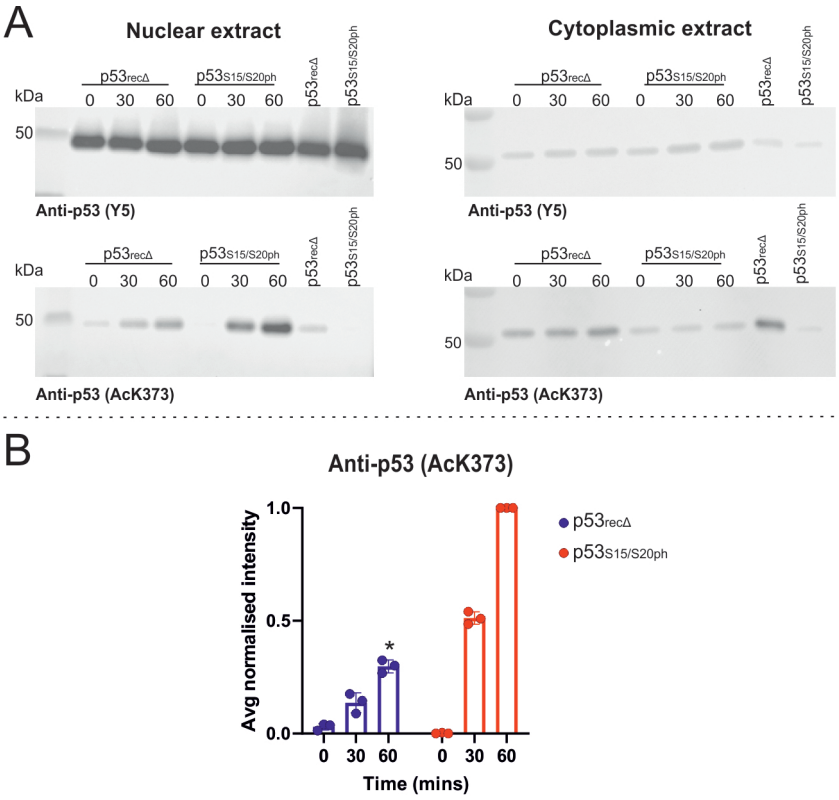

Figure 7.12: Probing the interaction between N-terminal phosphorylation and C-terminal acetylation using unstressed extracts at 16 °C. $p53_{rec\Delta}$ or $p53_{S15/S20ph}$ were incubated for 0, 30 or 60 minutes (indicated by 0, 30, 60) with unstressed H1299 nuclear or cytoplasmic extracts. A: Western blots against p53 (Y5, top) and AcK373 p53 (bottom) for assays carried out in nuclear and cytoplasmic extracts. Also included are 50 ng controls for $p53_{rec\Delta}$ and pS15/$p53_{S20ph}$. B: Band intensities were normalised by the 60 minute time point of $p53_{S15/S20ph}$, averaged, and the means for $p53_{rec\Delta}$ at 60 minutes were analysed by one sample t test, comparing to 1. Statistically significant differences are indicated by an asterisk (*). α=0.05, n = 3. For stain-free gel images and replicates, see supplementary figures (Figs. 10.14, 10.15 and 10.16).

7.2.6 Exploration of cell stress conditions

Previously, cell stress conditions were determined based on what conditions led to visible cell death under a microscope. Cell death was observed after 6 hours treatment with 1 mM cisplatin, however it was unclear to what extent this was indicative of a functional DNA-damage response leading to apoptosis. The ideal marker for p53-mediated apoptosis would ordinarily be p53, but H1299 cells are p53-negative. Though this was useful for the assays, it made it difficult to determine appropriate stress conditions.

Nuclear translocation of the kinase DYRK2 was considered as a potential marker for cell stress that would lead to p53-mediated apoptosis. DYKR2 translocation to the nucleus has been shown to occur following DNA damage. In the nucleus, DYRK2 phosphorylates p53 at S46, leading to apoptosis.[98] H1299 cells were treated with 0, 10, 100, or 1000 μM cisplatin for 0-24 hours. Nuclear extraction preparation was carried out to separate the nuclear and cytoplasmic fractions, and DYRK2 was probed in each fraction by western blotting. No evidence of DYRK2 translocation to the nucleus was found with any treatment condition (Fig. 7.13).

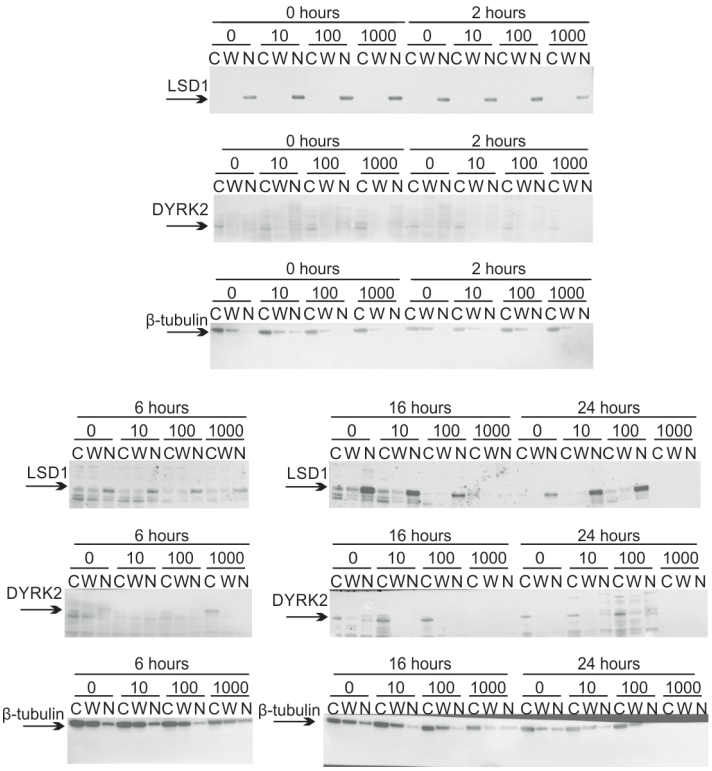

Figure 7.13: Testing for DYRK2 translocation in H1299 cells following cisplatin treatment. H1299 cells were stressed with 0, 10, 100 or 1000 μM cisplatin for 0, 2, 6, 16, or 24 hours. Fractions enriched for nuclear and cytoplasmic proteins were probed for DYRK2 (67 kDa), as well as nuclear (LSD1, 110 kDa) and cytoplasmic (β-tubulin, 50 kDa) markers. Western blotting against β-tubulin was carried out following GuHCl stripping of the DYRK2-probed membrane. Cytoplasmic extract, aliquots from a wash step, and nuclear extract are indicated by "C", "W", and "N" respectively. For stain-free gel images, see supplementary figures (Fig. 10.17).

It was considered that, potentially, the p53-negative nature of H1299 cells may be interfering with their response to DNA-damage. Though preparation of extracts from p53-positive cells would lead to extracts containing endogenous p53 and higher background signal in crosstalk assays, this may be partially mitigated through the addition of excess exogenous p53. A p53-positive cell line would offer significant advantages when validating stress conditions, as the endogenous p53 could be blotted for specific PTMs.

A549 and HCT-116 cells were treated with 0-8 μM adriamycin for 0-24 hours, and extracts were blotted for p53. In A459 cells, p53 was detected after 6 hours treatment with 8 μM adriamycin and 24 hours treatment with 0.5 μM adriamycin (Fig. 7.14). Western blotting using an antibody against pS46 p53 generated positive bands in the same lanes, and additionally the 4 μM lane after 24 hours (Fig. 7.14), however this was likely not specific to pS46 p53 as robust bands were visible in the $p53_{rec\Delta}$ p53 control lane. No p53 was detected in HCT-116. Based on these data, 6 hours treatment with 8 μM adriamycin in A549 cells was used as a stress regime to generate "stressed" nuclear extracts.

7.2.7 Using ADR-stressed A549 extracts to probe p53 "kill switches"

Nuclear and cytoplasmic extracts were prepared from A549 cells that had been treated with 8 μM adriamycin for 24 hours. Assays were carried out using nuclear extracts containing either $p53_{rec\Delta}$ or $p53_{S15/S20ph}$. In addition, a control reaction without exogenous p53 was included to measure background signal. For western blots probing K120 acetylation, $p53_{K120ac}$ produced by genetic code expansion was used as a positive control. No positive control was available for pS46 p53. After blotting for S46 phosphorylation, bands were visible at all time points for reactions containing $p53_{rec\Delta}$ and $p53_{S15/S20ph}$, and their respective controls, with no visible change in band intensity over time. It is likely these bands represent non-specific binding of the primary antibody targeting pS46 p53. No K120 acetylation was detected in reactions containing $p53_{rec\Delta}$ or $p53_{S15/S20ph}$ (Fig. 7.15).

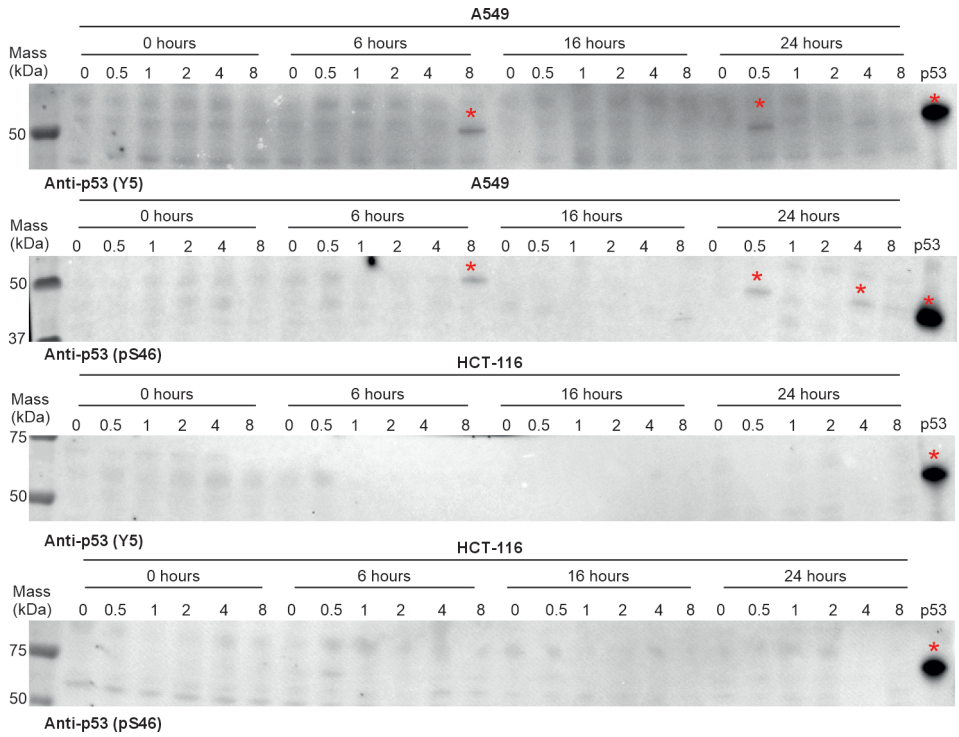

Figure 7.14: Testing for p53 accumulation in A549 and HCT-116 cells following treatment with adriamycin A549 and HCT-116 were stressed with 0 (0.008 % DMSO), 0.5, 1, 2, 4, or 8 μM adriamycin for 0, 6, 16, or 24 hours and blotted for p53 (Y5) and pS46 p53. Also shown is a $p53_{rec\Delta}$ control (50 ng). Positive p53 bands are indicated by a red asterisk (*). For stain-free gel images, see supplementary figures (Fig. 10.18).

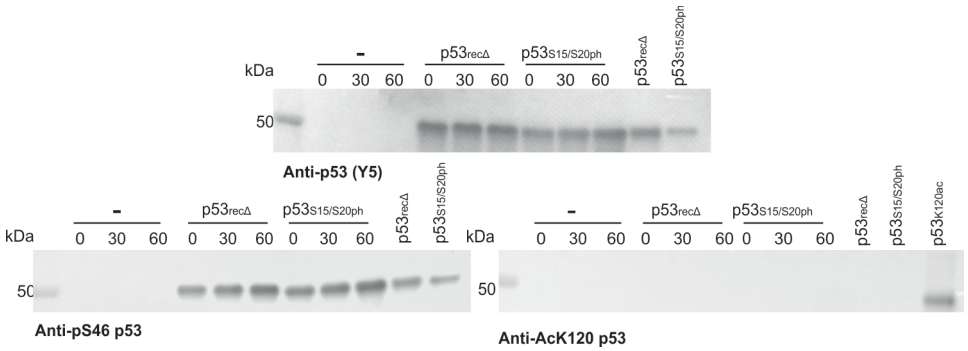

Figure 7.15: Probing for S46 phosphorylation and K120 acetylation in adriamycin-stressed A549 nuclear extracts. $p53_{rec\Delta}$ or $p53_{S15/S20ph}$ were incubated for 0, 30 or 60 minutes (indicated by 0, 30, 60) with nuclear extracts prepared from A549 cells stressed for 6 hours with 8 μM adriamycin. Also included are 50 ng controls for $p53_{rec\Delta}$, $p53_{S15/S20ph}$, and $p53_{K120ac}$ (Anti-AcK120 blot only). For stain-free gel images, see supplementary figures (Fig. 10.19).

7.3 Conclusion

The assays described here successfully reconstituted two well-known PTM crosstalk interactions using semisynthetic p53: The dependence of T18 phosphorylation on prior S15 phosphorylation and the promotion of C-terminal (K373) acetylation by N-terminal phosphorylation, the latter demonstrated using p53 double-phosphorylated at S15 and S20. This builds on previous work that used semisynthetic p53 double-phosphorylated at S15 and S20 to probe the effect of acetylation by p300 *in vitro*[168], demonstrating that this same interaction can also be reconstituted using functional nuclear extracts that more closely resemble the natural cellular environment. The ability to monitor these interactions using extracts derived from cells opens up the possibility of probing how p53 crosstalk interactions are affected by cell stress, something that cannot be studied using purified enzymes.

It was evident from the early assays that the anti-p53 (DO1) antibody did not bind as well to phosphorylated p53 variants as it did to $p53_{rec}$. This observation prompted us to systematically validate several anti-p53 antibodies against the semisynthetic variants available at the time. Serine 20 phosphorylation had a negative effect on anti-p53 (DO1) and anti-pS15 p53 antibody binding. At the time of the screen shown in Fig. 7.7, semisynthetic $p53_T18ph$ was not available, and so the anti-p53 (pT18) antibody was only screened against $p53_{rec}$, $p53_{S15ph}$, $p53_{S20ph}$, and $p53_{S15/S20ph}$, where it exhibited slight cross-binding to variants phosphorylated at S15. Subsequent assays that included positive $p53_{T18ph}$ controls, however, demonstrated that the anti-pT18 antibody binds with reasonable specificity.

The observation that anti-p53 (DO1) antibody binds very poorly to S20-phosphorylated p53 is interesting considering how frequently DO1 is used in both research and clinical settings.[236] Previous studies have shown that, under high salt conditions, the DO1 antibody only recognises p53 when S20 is not phosphorylated.[237] Because N-terminal phosphorylation occurs in conjunction with p53 accumulation, DO1 may not be optimal for studies where quantification of p53 levels is desired and S20 is phosphorylated. Anti-p53 (Y5) showed no signs of epitope occlusion, and may be a better alternative in some cases than DO1, though full characterisation against other phosphorylated variants is still required.

One aim was to be able to probe PTM crosstalk dynamics in different "stressed"

contexts. It proved difficult to find appropriate stress conditions in H1299 cells, potentially because finding appropriate stress conditions required answering a question with a hypothetical element: "If p53 were present in these cells, what stress conditions would activate it in a way that induced apoptosis?". It is surprising that none of the cisplatin treatment regimes led to positive markers for DNA damage (Akt1 phosphorylation) or p53 S46 phosphorylation (DYRK2 translocation), despite cell death being observed. The most direct marker for p53 activation is p53 itself, and so assays were performed in nuclear extracts prepared from A549 cells that had been stressed in a way confirmed to lead to p53 accumulation. These assays were also run without exogenous p53 as a negative background control for endogenous p53. No evidence of S46 phosphorylation or K120 acetylation was observed. The endogenous p53 also did not show signs of S46 phosphorylation, so it may have been that the stress was not sufficient. It is unclear why these "kill switch" modifications were not detected in cells following the stress regime employed (0-8 μM ADR for 0-24 hours). For K120 acetylation, previous work has often used other drugs and cell lines, with K120 acetylation accumulating in U20S cells from 1-13 hours treatment with 0.925 μM adriamycin[112] and after 8 hours treatment with 10 nM of the DNA-damaging agent actinomycin-D.[113,238] Previous studies using ADR to stress A549 cells showed accumulation of pS46 p53 after 4 hours treatment with 345 nM ADR, a much lower concentration than those described in this thesis.[69] For HCT116 cells, previous studies have found S46 phosphorylation following 24 hours ADR treatment, with concentrations ranging from 51 nM to 3.7 μM, again much lower than the regime described in this thesis. Despite the difficulties described in this thesis, it should be possible to find a stress regime that leads to these "kill switch" modifications occurring on endogenous p53.

Outlook

This thesis was motivated by the following question: with p53 able to induce a wide range of responses to stress, how do PTMs regulate the "decision making" process of p53? Long-term, answering this question would contribute towards a deeper understanding of what actually controls apoptosis in cells: can p53 bearing PTMs dictate cell fates independently of the broader cellular context as a "master regulator", or does the broader cellular context ultimately control what fate p53 pushes it towards by "correcting" the PTM status of p53 if it is not reflective of the stress occurring? To this end, I aimed to produce p53 site-specifically acetylated on the DNA-binding domain. I also aimed to develop assays that would assess the effect of PTMs on gene transcription and further post-translational modification of p53.

Though the production of pure, K120 acetylated p53 was not achieved, there are alternative approaches that could be taken in the future to improve yield. For example, it might be worth titrating the inducing sugars to find the optimal concentrations of arabinose and IPTG for expression. Overexpression of recombinant proteins using IPTG has been shown to lead to metabolic burden that inhibits cell growth, reducing overall protein yields.[239] Careful titration of inducing sugars may allow us to find the optimal concentration that allows for robust expression while minimising metabolic burden. One major source of protein loss occurs due to truncation at the mutated site. Use of an RF1 knockout strain could alleviate this issue, boosting the yield of the full-length modified protein by preventing truncation.[191] Whether this would boost yields enough to allow for purification from inclusion bodies and refolding is unclear, though this would be advantageous as it would allow site-specifically acetylated p53 to be produced without the stabilising mutations previously used.[197,115] It may also allow for amber suppression to be combined with protein semisynthesis to produce p53 that is both DBD-acetylated

and N-terminally phosphorylated. If p53 lacking the N-terminus were produced bearing a site-specific acetylation, it could potentially be ligated to a phosphopeptide corresponding to the N-terminus by native chemical ligation using previously described approaches.[168] Being able to produce the DBD-acetylated peptide in large yields suitable for refolding would be advantageous in this instance, as native chemical ligation conditions could be optimised without the protein needing to stay well-folded. If producing refoldable yields of acetylated p53 remains challenging, reducing the amount of truncated p53 would also boost soluble yields. It is notable that some soluble p53 was obtained while expressing at 25 °C, even without stabilising mutations. Potentially, cooling the culture further during expression may allow for more soluble p53 to be recovered. Alternative purification approaches should also be explored. For example, on-column cleavage of the H6 tag will likely lead to increased purity compared to elution with imidazole followed by cleavage in solution.[240] Using alternative purification tags is another option. GST tags have often been observed to increase the solubility of recombinant proteins, and this may be useful when expressing acetylated p53.[241] Purification using a strep-tag may lead to greater purity than purification using a H6 tag.[242] Expressing acetylated p53 with a C-terminal tag may also carry advantages as the truncated variant will not contain the tag and will therefore be purified out. One lingering question is to what extent recombinant p53, whether refolded or expressed in soluble form, is "correctly" folded. Determining this with absolute certainty is non-trivial, though techniques can be used that increase our confidence in p53 being correctly folded, including circular dichroism and western blotting with conformation-specific antibodies. In addition, assays that probe conformation-specific functions of p53, such as DNA-binding assays, transcription assays, assays probing protein-protein interactions, and assays probing quaternary structure can increase our confidence that the protein we have produced is correctly folded. Some of these assays, such as glutaraldehyde crosslinking and crosstalk assays, were employed as part of this thesis. Other assays, including pulldowns with conformation-specific antibodies, are being implemented in the lab, complementing previously carried DNA-binding experiments. Collectively, these assays will provide a quantitative measure of the fraction of correctly folded recombinant and semisynthetic p53. Where necessary, correction factors based on this measurement can be applied to downstream assays of p53 function such as transcription activation assays to enable quantitative comparisons between p53

PTM isoforms.

Of the two *in vitro* assays described in this thesis, the PTM crosstalk assay was more successful than the *in vitro* transcription assay. Because *in vitro* transcription assays have been successfully carried out in the past, it was decided that this was better achieved through collaboration. In contrast with previous *in vitro* transcription assays,[199,58,217] these assays would use site-specifically modified p53, granting full control over this part of the experiment. For crosstalk assays, having demonstrated that the assays can reconstitute well-known cascades, the next steps should focus on using the assays as a tool for discovery of new PTM crosstalk interactions. Currently, crosstalk interactions have been demonstrated using western blotting. This is useful when a specific crosstalk interaction has been hypothesised in advance, but it is less well-suited for screening with the aim of generating new hypotheses. Future work should focus on using proteomic approaches to identify differences in the accumulation of PTMs as a function of PTMs pre-loaded at the start. Potential crosstalk interactions identified in the proteomic screen may then be investigated further using western blotting and *in vitro* assays using purified enzymes. Though potential relevant enzymes may be identified based on their consensus sequence, this remains a challenge. It may also be a challenge to differentiate between "degrees" of crosstalk: if modification Y accumulates faster when p53 is pre-loaded with modification X, is that because X directly promotes Y, or does X promote a different modification that promotes Y? These questions are non-trivial, but are important to answer for a granular understanding of p53 regulation by PTMs.

No PTM removal was observed in any of the crosstalk assays described in this thesis. This was surprising, particularly as many of the assays were carried out in nuclear extracts from unstressed cells. Better characterisation of the erasers present in the nuclear extract may help ascertain whether this is an artifact of the assay or reflects a limited role for erasers in p53 regulation. It should be noted that the enzyme that dephosphorylates S15, Wip1, is a p53 target gene[80] and so may not be present in extracts from p53-negative cell lines, such as H1299.

Another remaining challenge is the generation of "stressed" nuclear extracts. The best possible marker for stress that activates p53 is p53 itself, however the presence of endogenous p53 in the nuclear extract would introduce background signal that could make analysis more difficult. Stress conditions were identified in this thesis that led to

p53 accumulation in A549 cells, however this did not lead to the installment of stress-related modifications (AcK120, pS46) when the extracts were used in crosstalk assays, nor was S46 phosphorylation detected in the endogenous p53. It is likely still possible to generate appropriately stressed nuclear extracts, and may simply require higher doses of adriamycin or longer treatment times. Though the levels of endogenous p53 were very low in the stressed A549 extracts described in this thesis, it may be that more severe stress raises endogenous p53 levels to a degree that makes interpretation of assay results difficult. Another potential approach that may alleviate this is rapidly degrading p53 post-accumulation following stress. This may be achievable using a cell line transfected with E6, an HPV protein that degrades p53 by mediating the interaction of p53 with the E3 ligase E6AP.[243] If E6 were placed under the control of an inducible promoter, p53 could be degraded prior to nuclear extract preparation. It is unclear whether residual E6 present in the nuclear extract would degrade supplemented p53 during the assay, though this may be alleviated by carrying the assays out in the presence of a proteosome inhibitor such as ALLN. It should be noted that no detectable p53 degradation was observed in the crosstalk assays described in this thesis, so it may be that the nuclear and cytoplasmic extracts do not contain a functional proteosome.

In conclusion, this thesis is an important step towards a deeper, more granular understanding of p53 PTMs, and has set the groundwork for interesting further studies. A deeper understanding of p53 may lead to the development of new therapeutic strategies. Because p53 is the most commonly mutated gene in cancer, any therapeutic strategy that works by modulating p53 function, or re-activating p53, may be applicable to a wide range of cancers.

Materials and Methods

9.1 Western blotting

Samples were loaded on to a polyacrylamide gel for SDS-PAGE. When made in-house, gels consisted of a 15 % resolving gel (15 % acrylamide, 375 mM Tris pH 8.8, 0.1 % SDS, 0.5 % TCE, 0.1 % APS and 0.1 % TEMED) and a 6 % stacking gel (15 % acrylamide, 125 mM Tris pH 6.8, 0.1 % SDS, 0.5 % TCE, 0.1 % APS and 0.1 % TEMED). 4-15 % stain-free precast gels (Bio-Rad) were also used. Gels were run at 180 V for 50-60 minutes in SDS running buffer (24.76 mM Tris base, 0.19 M glycine, 3.48 mM SDS).

After stain-free imaging with 5-minutes activation, gels were soaked in transfer buffer (24.76 mM Tris base, 0.19 M glycine, 0.06 % SDS) for 10 minutes. Extra thick filter paper (Bio-Rad) and PVDF membranes (activated in methanol for 30 seconds) were also soaked transfer buffer for 10 minutes. Transfer was carried out using the pre-defined "mixed molecular weight" method on the Trans-Blot Turbo Transfer System (Bio-Rad). When gels were imaged again post-transfer, this was achieved by stain-free imaging with no activation.

For primary antibodies targeting phosphorylated epitopes, membranes were blocked in 5 % BSA in TBST (19.8 mM Tris base, 0.15 M NaCl, 0.1 % Tween-20). For primary antibodies targeting any other epitopes, membranes were blocked in 5 % milk in TBST. Blocking was carried out at room-temperature for 1 hr. Membranes were incubated with primary antibodies, diluted in blocking solution according to manufacturer's instructions, for approximately 16 hours at 4 °C. A summary of all primary antibodies used is shown in table 9.1.

Target	Host species	Dilution	Catalogue number
p53 (DO1)	Mouse	1:1000 (Milk)	ab1101 (Abcam)
p53 (Y5)	Rabbit	1:3000 (Milk)	ab32049 (Abcam)
p53 (AcK120)	Mouse	1:1000 (Milk)	ab78316 (Abcam)
p53 (pS15)	Rabbit	1:5000 (BSA)	ab223868 (Abcam)
p53 (pT18)	Rabbit	1:1000 (BSA)	PA5-12660 (Thermo)
p53 (pS20)	Rabbit	1:1000 (BSA)	ab157454 (Abcam)
p53 (pS46)	Rabbit	1:1000 (BSA)	ab76242 (Abcam)
p53 (MetK372)	Rabbit	1:1000 (Milk)	ab16033 (Abcam)
p53 (AcK373)	Rabbit	1:5000 (Milk)	ab62376 (Abcam)
p53 (AcK382)	Rabbit	1:5000 (Milk)	ab75754 (Abcam)
Acetyllysine	Rabbit	1:1000 (Milk)	ab21623 (Abcam)
H6 tag	Mouse	1:5000 (Milk)	SAB4200620 (Sigma)
β-tubulin	Rabbit	1:1000 (Milk)	ab179513 (Abcam)
LSD1	Rabbit	1:1000 (Milk)	ab17721 (Abcam)
H3 histone	Rabbit	1:5000 (Milk)	ab18521 (Abcam)
Akt1 (pS473)	Rabbit	1:10,000 (BSA)	ab81283 (Abcam)
Cleaved PARP	Rabbit	1:1000 (Milk)	9664S (CST)
Cleaved CASP3	Rabbit	1:1000 (Milk)	5625S (CST)
DYRK2	Rabbit	1:1000 (Milk)	ab254567 (Abcam)

Table 9.1: A summary of primary antibodies used. Antibodies were diluted in 5 % (w/v) skimmed milk powder or 5 % (w/v) BSA in TBST, as indicated. CST stands for Cell Signalling Technology.

Membranes were washed with TBST for 10 minutes three times before 1 hr incubation at room-temperature with the relevant secondary antibody, diluted in TBST according to manufacturer's instructions. Membranes were then washed with TBST for 10 minutes three times. Clarity ECL substrate (Biorad) was applied to the membrane before imaging using a Chemidoc Imaging System (Bio-Rad).

9.2 Polymerase chain reaction

PCR reactions (comprising 5 μL 5x Q5 reaction buffer, 1.25 μL of each 10 μM primer, 1 μL of 10 ng/μL plasmid DNA template, 0.5 μL dNTP mix, 0.5 μL Q5 DNA polymerase, and 15.5 μL nuclease-free H_2O) were incubated according the program described in Table 9.2.

Step	**Temp (°C)**	**Time (Secs)**
1	98	30
2	98	10
3	Variable	20
4	72	180
5	72	120
6	4	Hold

Table 9.2: PCR program used. The temperature at step 3 was calculated based on the estimated melting temperature of the primers. Steps 2-4 were repeated 25 times, unless otherwise indicated:

For the agarose gel data shown in Fig. 6.2, PCR was carried out as above, with 5 μL being removed from PCR reactions after 10, 20, 25, and 30 cycles.

9.3 Plasmids and constructs

A pET3a-p53 vector, kindly provided by the Buchner group, was used for the expression of all p53 variants. PG13 and MG15 vectors bearing the luciferase were obtained from Addgene,[225] as was the pEVOL vector containing an engineered tRNA synthetase and tRNA for amber suppression.[208] The pBR322 and pACYC vectors used for amber suppression were kindly provided by Prof. Jason Chin.[114]

For HiFi DNA assembly of p53 into the pACYC vector, where myoglobin was replaced with p53, the following primers were used:
Forward: CTCAGACTGAGTTTAAACGGTAACATATGG
Reverse: TGCTGCCCATGGTTAATTCCTCCTGTTAG

For site-directed mutagensis of p53, the following primers were used:
K120* (Fwd): TGGGACAGCCTAGTCTGTGAC
K120* (Rev): GAATGCAAGAGCCCAGAC
M133L (Fwd): CCTCAACAAGCTGTTTTGCCAACTGG
M133L (Rev): GCAGGGGAGTACGTGCAA
V203A (Fwd): AAATTTGCGTGCGGAGTATTTGG
V203A (Rev): CCTTCCACTCGGATAAGATG
N239Y (Fwd): CTACATGTGTTACAGTTCCTGCATG
N239Y (Rev): TTGTAGTGGATGGTGGTAC
N268D (Fwd): ACTGGGACGGGACAGCTTTGAGG
N268D (Rev): AGATTACCACTGGAGTCTTCCAG

For HiFi DNA assembly of iSpinach into the PG13 and MG15 vectors, where luciferase was replaced by iSpinach, the following primers were used:
iSpinach (Fwd): TGTTGGTAAAGCGACTACGGTGAGGGTC
iSpinach (Rev): AGTTACATTTGCGACTACGGAGCCCAGA

The sequence of the iSpinach aptamer gene is as follows:
GCGACTACGGTGAGGGTCGGGTCCAGTAGCTTCGGCTACTGTTGAGTAGAGT
GTGGGCTCCGTAGTCGC

For PCR detection of iSpinach cDNA, the following primers were used:
iSpinach detection (Fwd): CTCATTTCAGCCTCACCAC
iSpinach detection (Rev): AGCCCACACTCTACTCAAC

The protein sequence for H6SUMO-p53 is as follows (p53 sequence is shown in bold):
MGSSHHHHHHSSGMSDSEVNQEAKPEVKPEVKPETHINLKVSDGSSEIFFKI
KKTTPLRRLMEAFAKRQGKEMDSLRFLYDGIRIQADQTPEDLDMEDNDIIEA
HREQIGG**MEEPQSDPSVEPPLSQETFSDLWKLLPENNVLSPLPSQAM**
DDLMLSPDDIEQWFTEDPGPDEAPRMPEAAPPVAPAPAAPTPAAP
APAPSWPLSSSVPSQKTYQGSYGFRLGFLHSGTAKSVTCTYSPALNK
MFCQLAKTCPVQLWVDSTPPPGTRVRAMAIYKQSQHMTEVVRRCP
HHERCSDSDGLAPPQHLIRVEGNLRVEDRNTFRHSVVVPYEPPEVGS
DCTTIHYNYMCNSSCMGGMNRRPILTYLDIITLEDSSGNLLGRNSFE
VRVCACPGRDRRTEEENLRKKGEPHHELPPGSTKRALPNNTSSSPQP
KKKPLDGEYFTLQIRGRERFEMFRELNEALELKDAQAGKEPGGSRA
HSSHLKSKKGQSTSRHKKLMFKTEGPDSD

9.4 Site-directed mutagenesis

Site-directed mutagenesis was performed using mutagenesis primers from Integrated DNA Technologies (see section 9.3) designed using NEBaseChanger and the PCR procedure described in section 9.2.

PCR reactions were analysed by 1 % agarose gel, and successful reactions were digested with 0.5 μL DpnI (New England Biolabs) overnight at 37 °C. DNA was purified with a QIAquick PCR Cleanup kit (Qiagen) and ligation was carried out by incubating 10 μL DNA with 2 μL 10 mM rATP, 1 μL 0.1M DTT, 1 μL PNK, 1 μL T4 DNA ligase, 2 μL 10x kinase buffer (New England Biolabs), 2 μL 10x T4 ligase buffer (New England Biolabs), and 1 μL nuclease-free H_2O at room temperature overnight.

3 μL of the reaction mixture was used to transform 50 μL calcium-competent Top10 cells. Following addition of the reaction mixture, Top10 cells were briefly mixed and placed on ice for 20 minutes. Cells were incubated at 42 °C for 45 seconds before 2 minutes incubation on ice. 300 μL of SOC (0.5 % (w/v) yeast extract, 2 % (w/v) tryptone, 10 mM NaCl, 2.5 mM KCl, 20mM $MgSO_4$, and 0.4 % (w/v) glucose) was added to the cells before 1 hour incubation at 37 °C. Top10 cells were spread on agar plates containing the appropriate antibiotic (Table 9.3) and incubated at 37 °C.

Individual Top10 colonies were picked and cultured overnight in LB media containing the appropriate antibiotic at 37 °C, shaking at 220 RPM. Plasmid DNA was purified from the cells using a GeneJET plasmid miniprep kit (Thermo Fisher Scientific) according to manufacturer's instructions. Sanger sequencing was carried out by Genewiz (Azenta).

Antibiotic	**Working concentration**	**Solvent for 1000x stock**
Ampicillin	100 μg/mL	Water
Kanamycin	50 μg/mL	Water
Tetracycline	10 μg/mL	Ethanol
Chloramphenicol	25 μg/mL	Ethanol

Table 9.3: Selection markers used, along with their working concentrations and solvents used to prepare 1000x stocks.

9.5 Calcium competent cell preparation

E. *coli* were plated out on to agar and incubated overnight at 16 °C. Single colonies were picked and cultured in 10 mL LB overnight, shaking at 220 RPM, 37 °C. 10 mL starter culture was added to 1 L LB media, and cells were incubated shaking at 220 RPM, 37 °C, to an OD_{600} of 0.35-0.40. Cells were chilled on ice for 20-30 minutes and centrifuged at 3000 rcf for 15 minutes at 4 °C. The supernatant was decanted and cells resuspended in 100 mL ice-cold 100 mM $MgCl_2$ before 20 minutes centrifugation at 2000 rcf, 4 °C. The supernatant was decanted and cells resuspended in 200 mL ice-cold 100 mM $CaCl_2$ before 20 minutes incubation on ice. Cells were centrifuged for 20 minutes at 2000 rcf, 4 °C. The supernatant was decanted and cells resuspended in 50 mL ice-cold 85 mM $CaCl_2$, 15 % glycerol, before 15 minutes centrifugation at 1000 rcf, 4 °C. The supernatant was decanted and cells resuspended in 2 mL ice-cold 85 mM $CaCl_2$, 15 % glycerol. 50 μL aliquots were flash-frozen in liquid N_2, and stored at -80 °C.

9.6 Expression and refolding of unmodified p53

9.6.1 p53 expression via autoinduction

BL21 (DE3) cells were transformed with a plasmid (pET3a) containing the gene for human p53 under the control of a lactose-inducible T7 promoter. 5 mL MDG media (Fig. 9.4) containing 100 μg/mL ampicillin was incubated with a single colony of transformed cells at 37 °C, shaking at 220 RPM, for 16 hours. These cells were diluted 1:1000 in TYM-5052 (Fig. 9.4) containing 100 μg/mL ampicillin and cultured for 16 hours, shaking at 220 RPM. Cell pellets were harvested by centrifugation 25 minutes centrifugation at 4200 rpm in a Beckman Coulter J6-MI centrifuge at 4 °C.

10x TY:	10 % tryptone (w/v), 5 % yeast extract (w/v)
50x 5052:	25 % glycerol (v/v), 40 % glucose (w/v), 10 % (w/v) α-lactose monohydrate
50x M:	1.25 M $Na_2HPO_4.7H_2O$, 1.25 M KH_2PO_4, 2.5 M NH_4Cl, 0.25 M Na_2SO_4
MDG:	1x M, 2 mM $MgSO_4$, 0.5 % glucose (w/v), 0.25 % pH-neutralized aspartate (w/v).
TYM-5052:	1x TY, 1x M, 1x 5052, 2 mM $MgSO_4$

Table 9.4: Stocks and media for autoinduction.

9.6.2 Inclusion body preparation

Cell pellets were resuspended in 40 mL lysis buffer (0.1 M Tris-HCl (pH 7.0 at 4 °C), 1 mM EDTA) per litre of expression culture. 1.5 mg of lysozyme was added per 1 g of cells (approximate cell dry weight, assuming a cell dry weight (g/L) to OD_{600} ratio of 0.39), and cells were incubated for 30 minutes on ice. Cells were sonicated using a

probe sonicator with an amplitude of 40 %, using cycles of 5 seconds on and 10 seconds off, for a total of 4 minutes of on-time. Cells were then passed three times through a continuous flow cell disruptor (Constant Systems) at 25 kpsi, 4 °C. DNAse was added to a final concentration of 10 μg/mL and $MgCl_2$ was added to a final concentration of 3 mM before 30 minutes incubation at room temperature, rotating. 0.5x volume of DNAse quench buffer (0.1 M Tris-HCl, 60 mM EDTA, 6 % Triton-X (v/v), 1.5 M NaCl, pH 7.0 at 4 °C) was added before 30 minutes incubation on ice. Inclusion bodies were pelleted by 60 minutes of centrifugation at 30,000 rcf at 4 °C and then washed by resuspension in wash buffer 1 (0.1 M Tris-HCl, 30 mM EDTA, 3 % (v/v) Triton-X, 0.8 M NaCl, pH 7.0 at 4 °C). Samples were centrifuged at 30,000 rcf for 20 minutes at 4 °C before being washed by resuspension in wash buffer 2 (0.1 M Tris-HCl, 20 mM EDTA, pH 7.0 at 4 °C). Inclusion bodies were centrifuged once more at 30,000 rcf for 10 minutes at 4 °C. Inclusion body pellets were stored at -80 °C until solubilization.

9.6.3 p53 purification from inclusion body

Inlcusion bodies were dissolved in IB solubilization buffer (0.1 M Tris-HCl, 6 M GuHCl, 50 mM DTT, pH 7.0 at 4 °C) and incubated for 2 hours at room temperature, rotating. The pH was reduced to 2 using 6 M HCl and the solution was centrifuged for 30 minutes at 30,000 rcf, 4 °C. The supernatant containing p53 was desalted using a PD10 column packed with Sephadex G-25 (GE Healthcare) equilibrated with 25 mL desalting buffer (30 % (v/v) acetonitrile, 0.1 % (v/v) formic acid). Samples were adjusted to 30 % (v/v) acetonitrile, centrifuged for 5 minutes at 14,000 rcf, 4 °C, and loaded on to the column. p53 was eluted in 3.5 mL desalting buffer, flash frozen in liquid N_2, and lyophilized.

9.6.4 Analytical RP-HPLC

RP-HPLC was performed using an Agilent Infinity II 1260 equipped with a C3 Zorbax column (300SB, 5 μm, 4.6x 150 mm). Buffer A was HPLC-grade H_2O with 0.1 % TFA, while buffer B was HPLC-grade acetonitrile with 0.1 % TFA. p53 was analysed using a gradient of 20-60 % buffer B over 42 minutes at 50 °C.

9.6.5 High-resolution mass spectometry

HRMS was carried out using a Waters Xevo G2-XS QTof following reverse-phase chromatography using a Waters Acquity UPLC Protein BEH C4 column (300 Å, 1.7 μm, 2.1x50 mm) and a Waters Acquity UPLC. For UPLC, solvent A was water with 0.1 % formic acid and solvent B was acetonitrile with 0.1 % formic acid. Programs were run at a flow rate of 0.2 mL/min as follows: 2 minutes of 5 % B followed by a linear gradient from 5-95 % over B over 4 minutes. HRMS spectra were analysed using Unifi (Waters).

9.6.6 p53 refolding

5-10 mg lyophilized p53 was dissolved in minimal volume IB solubilization buffer and incubated for 30 minutes at room temperature. 1 μL p53 was diluted into 29 μL acidified IB solubilization buffer (pH 2-3), centrifuged at 14,000 rcf for 10 minutes at 4 degrees, and analysed by RP-HPLC to determine p53 concentration. For refolding, seven falcon tubes, each containing 45 mL of refolding buffer (50 mM sodium diphosphate, 1 M L-arginine, 0.2 mM $ZnCl_2$, 50 mM DTT, pH 8.0), were pre-cooled to 15 °C. p53 was diltued to 5-10 μM in acidic IB solubilization buffer. 450 μL of p53 was added quickly to each falcon tube at 4 °C and the solution was incubated at 15 °C, rocking gently at 50 rpm. Every 90 minutes, 450 μL more p53 was added to each falcon, each followed by incubation at 15 °C, rocking at 50 rpm. Six 450 μL additions of p53 were made to each falcon tube in total. The solutions were then dialysed overnight at 4 °C against 50 mM sodium diphosphate, 5 % glycerol, 4 mM DTT (pH 8) using Spectrum^{TM} Spectra/Por^{TM} 4 RC Dialysis Membrane Tubing (12,000 to 14,000 MWCO). Samples were then dialysed against fresh dialysis buffer for 4 hours at 4 °C.

A 5 mL HiTrap Heparin column (Cytiva) was washed with ddH_2O and equilibrated with IEX low salt buffer (30 mM sodium diphosphate, 100 mM KCl, 4 mM DTT, 3 % glycerol, pH 7.5). Dialysed p53 was loaded onto the column using a peristaltic pump at an approximate flow rate of 1 mL/min. The sample was loaded for approximately 20 hours, with the flow through continuously being loaded back on to the column. p53 was eluted using an Äkta Pure FPLC system (Cytivia) as described in table 9.5.

Protein concentration of each fraction was determined by Bradford assay, and fractions containing protein were merged. Protein was concentrated to a volume of 1 mL using 50

Column volumes	% A	% B
1.0	100	0
1.5	90	10
4.0	45	55
1.5	0	100
1.5	100	0

Table 9.5: Program for eluting refolded p53 from the heparin column. Buffer A was IEX low salt buffer (30 mM sodium diphosphate, 100 mM KCl, 4 mM DTT, 3 % glycerol, pH 7.5). Buffer B was the same, but with 1 M KCl. 1 mL fractions were collected.

% ammonium sulfate precipitation, carried out at 4 °C: the sample was divided into 1.5 mL aliquots, and to each aliquot a total of 0.45 μg of ammonium sulfate was added across three batches, ensuring the previous batch was completely dissolved before addition of the next batch. The samples were rotated slowly (approximately 11 RPM) at 4 °C for 1 hour. Precipitated protein was centrifuged at 10,000 rcf for 20 minutes at 4 °C, and the pellet was dissolved in 1 mL SEC buffer (30 mM sodium diphosphate, 300 mM KCl, 3 % (v/v) glycerol, 4 mM DTT, pH 7.5). The sample was centrifuged at 10,000 rcf for 10 minutes at 4 °C, and the supernatant was injected on to a Superose 6 Increase 10/300 GL column that had been equilibrated with SEC buffer. p53 was eluted in 1.5 column volumes of SEC buffer, collecting fractions of 0.5 mL. Fractions containing p53 tetramers were merged and concentrated with 50 % ammonium sulfate precipitation as before, redissolving the precipitate to 1/5 of their original volume in SEC buffer. Samples were dialysed overnight against 1 L p53 storage buffer (30 mM sodium diphosphate, 50 mM KCl, 5 % (v/v) glycerol, 2 mM DTT, pH 7.5) using Slide A Lyzer Mini Dialysis Devices (10-100 uL, 10 kDa MWCO, Thermo Fisher) at 4 °C. Refolded p53 was flash frozen in liquid N_2 and stored at -80 °C.

9.6.7 Glutaraldehyde crosslinking

p53 was diluted to 1.5 μM in p53 storage buffer. Glutaraldehyde dilutions of 2.5, 0.75, 0.25, 0.075 and 0.025 % (v/v) in 0.2 M phosphate buffer were prepared and used to prepare reactions containing final glutaraldehyde concentrations of 0, 0.1, 0.03, 0.01, 0.003, 0.001 % (v/v) and a final p53 concentration of 0.06 μM. Reactions were incubated

at 37 °C for 3 minutes, then quenched by addition of 10 μL 1 M Tris-base (pH 8.0).

9.7 Ulp1 expression and refolding

BL21 cells were transformed with a pET30 vector containing H6-tagged Ulp1 under the control of a T7 promoter by 45 seconds heat-shock at 42 °C and plated onto agar containing 50 μg/mL kanamycin. Expression was carried out by autoinduction as described for p53 in section 9.6.1. Cells were pelleted by 15 minutes centrifugation at 6000 rcf, 4 °C. Cells were resuspended in 5 mL lysis buffer (50mM Tris, 150mM NaCl, 1 % Triton X-100, 5 % Glycerol, 0.1mM EDTA, 5mM 2-mercaptoethanol, pH 7.9) per gram of wet pellet and sonicated using a probe sonicator at 40 % amplitude for 4 minutes "on time", using cycles of 5 seconds on and 10 seconds off. The pellets were then passed through a OneShot cell disruptor (Constant Systems) twice, with the lysate clarified by 15 minutes centrifugation at 15,000 rcf, 4 °C. The pellet was washed with 5 mL of lysis buffer per gram of original pellet and subjected to 15 minutes centrifugation at 15,000 rcf, 4 °C. The wash and centrifugation was carried out again, but without Triton X-100 and the resulting pellet was dissolved in 2.5 mL binding buffer (50 mM Tris, 100 mM NaCl, 6M GuHCl, 5 % glycerol, 5 mM imidazole, pH 7.9) per gram of original pellet and rocked at room temperature for 60 minutes. This was centrifuged by 15 minutes centrifugation at 15,000 rcf, 4 °C, and the supernatant was loaded onto a pre-equilibrated 5 mL HisTrap HP column using a peristaltic pump at an approximate flow rate of 2 mL/min. The column was washed twice with 3 CV binding buffer, followed by one wash with 1 CV binding buffer containing 10 mM imidazole. Washes were carried out at a flow rate of 3.5 mL/min. Elution was carried out by applying 1 CV of elution buffer (37.5 mM Tris, 112.5 mM NaCl, 4.5 M urea, 500 mM imidazole, pH 7.9) five times, collecting the flow-through after each elution. The protein concentrations of each fraction were assessed by Bradford assay. Fractions containing protein were merged and diluted to a protein concentration of 4 mg/mL.

For refolding, ulp1 was combined with 2 x volumes of 2 M L-arginine (pH 7.9) and 1 x volume of glycerol (25 % final), mixed, and incubated on ice for 2 hours. The solution was dialysed against 4 L of 50mM Tris, 150mM NaCl, 1mM DTT (pH 8.2) using 12-14 kDa MWCO dialysis tubing for approximately 16 hours. Dialysis was carried out again using

fresh dialysis buffer for 4 hours. Refolded protein was centrifuged for 15 min at 15000 rcf, 4 °C and the supernatant was concentrated to 0.5 mg/mL protein using Vivaspin 10 kDa MWCO concentrators (GE Healthcare). Ulp1 was aliquoted, flash frozen in liquid N_2, and stored at -80 °C.

9.8 Expression of $p53_{K120ac}$ inclusion bodies in DH10B cells

DH10B cells were double-transformed with a pBR322 vector containing an Nϵ-acetyllysyl-tRNA-synthetase and a pACYC vector containing the corresponding tRNA and p53 mutated to have TAG at position 120. The presence of correctly mutated p53 was confirmed using Sanger sequencing with pBAD forward and reverse primers provided by Azenta. Double-transformation was achieved as followed: each plasmid was diluted to 2 ng/μL and 1 μL of each diluted plasmid was added to 50 μL calcium-competent DH10B cells, mixing gently by flicking the tube. The cells were placed on ice for 20 minutes before undergoing 45 seconds heat-shock at 42 °C. After heat shock, the cells were immediately placed on ice for 2 minutes, then incubated at 37 °C for 1 hour following addition of 350 μL SOC media (0.5 % yeast extract, 2 % tryptone, 10 mM NaCl, 2.5 mM KCl, 10 mM $MgCl_2$, 10 mM $MgSO_4$, 20 mM glucose). Cells were plated out on agar containing 50 μg/mL kanamycin and 10 μg/mL tetracycline (from a 10 mg/mL stock in ethanol) and incubated for about 16 hours at 37 °C. Single colonies were picked and cultured overnight in LB containing 50 μg/mL kanamycin and 10 μg/mL tetracycline shaking at 220 RPM at 37 °C. These cells were diluted 1:1000 in TYM-5052 containing 50 μg/mL kanamycin, 10 μg/mL tetracycline, 0.2 % L-arabinose, and 5 mM acetyllysine and cultured for 16 hours, shaking at 220 RPM. Cell pellets were harvested by centrifugation 25 minutes centrifugation at 4200 rpm in a Beckman Coulter J6-MI centrifuge at 4 °C. Inclusion body purification was carried out as described in section 9.6.2.

9.9 Expressing $p53_{K120ac}$ inclusion bodies in BL21 cells

BL21 cells were double-transformed with a pEVOL vector containing an Nϵ-acetyllysyl-tRNA-synthetase and the corresponding tRNA, and a pET vector containing the p53

mutated to contain TAG at position 120. Mutation of p53 was confirmed using Sanger sequencing with T7 and T7-term primers provided by Azenta. Double-transformation was achieved as followed: 1 μL of pEVOL (tRNA synthetase/tRNA) plasmid was added to 50 μL calcium-competent BL21 cells, mixing gently by flicking the tube. The cells were placed on ice for 20 minutes before undergoing 45 seconds heat-shock at 42 °C. After heat shock, the cells were immediately placed on ice for 2 minutes, then incubated at 37 °C for 1 hour following addition of 350 μL SOC media (0.5 % yeast extract, 2 % tryptone, 10 mM NaCl, 2.5 mM KCl, 10 mM $MgCl_2$, 10 mM $MgSO_4$, 20 mM glucose). Cells were plated out on agar containing 25 μg/mL chloramphenicol (from a 25 mg/mL stock in ethanol) and incubated for about 16 hours at 37 °C. Cells were cultured and made calcium-competent again as described in section 9.5, with volumes scaled appropriately and all LB supplemented with 25 μg/mL chloramphenicol. The calcium-competent pEVOL-transformed BL21 cells were stored at -80 °C. Transformation of the pEVOL-transformed BL21 cells with the pET (p53) vector was carried out as described for pEVOL, with all media (except SOC) supplemented with both 25 μg/mL chloramphenicol and 100 μg/mL ampicillin. After transformation with pET, cells were plated out onto agar containing 25 μg/mL chloramphenicol and 100 μg/mL ampicillin.

Single colonies were picked and cultured overnight in LB containing 25 μg/mL chloramphenicol and 100 μg/mL ampicillin, shaking at 220 RPM at 37 °C. These cells were diluted 1:1000 in TYM-5052 containing 25 μg/mL chloramphenicol, 100 μg/mL ampicillin, 0.2 % L-arabinose, and 5 mM acetyllysine (added as a solid) and cultured for 24 hours, shaking at 220 RPM. Cell pellets were harvested by centrifugation 25 minutes centrifugation at 4200 rpm in a Beckman Coulter J6-MI centrifuge at 4 °C. Inclusion body purification was carried out as described in section 9.6.2.

9.9.1 Expression trial comparing "bulk" and "spike" acetyllysine addition

Transformation and expression was carried out as described in section 9.9 with the following changes: when diluting pre-cultured cells 1:1000 in TYM-5052, solid acetyllysine was added to a final concentration of 0, 5, 10, or 20 mM in the cells designated as receiving "bulk" acetyllysine. These cells were incubated shaking at 220 RPM, 37 °C for 48 hours, with aliquots taken every 24 hours. For cells designated as receiving "spike" acetyllysine,

solid acetyllysine was added to a final concentration of 0, 2.5, 5, or 10 mM at the point of dilution with TYM-5052. After 24 hours, the same mass of acetyllysine was added to the culture flasks again. "Spike" samples were also incubated shaking at 220 RPM, 37 °C, for 48 hours, with aliquots taken every 24 hours.

9.10 Expression and purification of soluble p53$_{K120ac}$

9.10.1 Expression

Transformation was carried out as described in section 9.8 using a pEVOL vector containing the tRNA synthetase and tRNA genes, and a pET vector containing H6SUMO p53 carrying four stabilising mutations (M133L/V203A/N239Y/N268D) and position 120 of p53 mutated to TAG. Incorporation of stabilizing mutations was confirmed using Sanger sequencing with T7 and T7-term primers provided by Azenta. Double-transformed BL21 cells were plated on to agar supplemented with 100 μg/mL ampicillin and 25 μg/mL chloramphenicol (from a 1000x stock, dissolved in EtOH) and incubated overnight at 37 °C. Single colonies were picked and cultured in LB to an OD_{600} of 1.0. Cells were diluted to an OD_{600} of 0.1 in 3 L LB and incubated shaking at 220 RPM, 37 °C. Acetyllysine, freshly dissolved in ddH_2O and filter sterilised, was added to the culture once it reached an OD_{600} of 0.3 to a final concentration of 10 mM, along with nicotinamide to a final concentration of 50 mM. Cells were cultured to an OD_{600} of 0.6-0.8 and induced with 0.2 % L-arabinose and 1 mM IPTG, both freshly dissolved in LB. Cells were incubated shaking at 220 RPM, 25 °C for at least 20 hours before harvesting.

9.10.2 Purification

Cells were harvested by centrifugation for 30 minutes at 4200 RPM, 4 °C, in a Beckman Coulter J6-MI centrifuge. The supernatant was discarded and the cell pellet was resuspended in 30 mL AS lysis buffer (50 mM phosphate buffer, 300 mM NaCl, 0.01 % (v/v) NP-40, 1 mM PMSF, 0.1 mM DTT, pH 8.0) before sonication using a probe sonicator with an amplitude of 40 %, using cycles of 5 seconds on and 10 seconds off, for a total of 4 minutes of on time. Cells were then lysed by two passages through a OneShot cell disruptor (Constant Systems). The lysate was clarified by 20 minutes centrifugation at

15,000 rcf, 4 °C. The clarified supernatant was applied to a pre-equilibrated 5 mL HisTrap at a flow rate of approximately 2 mL/min using a peristaltic pump at 4 °C. The HisTrap was then washed twice with 5 column volumes lysis buffer. Elution was achieved using a gradient of 0-100 % B over 25 column volumes, where buffer B comprised 50 mM phosphate buffer, 150 mM NaCl, 0.01 % (v/v) NP-40, 0.1 mM DTT, and 1 M imidazole, pH 8.0. Buffer A was the same, except with 20 mM imidazole. Elution was carried out using an Äkta Pure (Cytivia).

The protein-containing peak was collected and Ulp1 was added to a final concentration of 0.02 mg/L. Reactions were transferred to Spectrum^{TM} Labs Spectra/Por^{TM} 3.5 kD MWCO dialysis tubing and dialysed overnight against a buffer the same as buffer B, but without imidazole. The sample was applied to a pre-equilibrated 5 mL HiTrap Heparin HP column (GE Healthcare) using a peristaltic pump by passing through the column once at an approximate flow rate of 1 mL/min, 4 °C. An aliquot was taken of the flow through, and the sample was left passing through the column overnight, recycling the flow-through back into the same tube to enable multiple passes through. The heparin column was washed twice with 25 column volumes of dialysis buffer. Elution was achieved using a gradient of 0-100 % B over 25 column volumes, where buffer B comprised 50 mM phosphate buffer, 1 M NaCl, 0.01 % (v/v) NP-40, and 0.1 mM DTT. Buffer A was the same, except with no NaCl. Elution was carried out using an Äkta Pure (Cytivia). The sample was passed once through a pre-equilibrated 5 mL HisTrap to remove cleaved H6SUMO tag and Ulp1, retaining the flow-through. Protein was flash frozen in liquid N_2 and stored at -80 °C.

9.11 Expression trial comparing arabinose addition before or with IPTG addition

The following three expression protocols were carried out using both wild-type and superstable mutants:

9.11.1 H6SUMO-p53 and H6SUMO-p53$_{SS}$, non-amber suppressed

Expression was carried out as described in section 9.10 with the following changes: BL21 cells were transformed with a single pET vector containing either the H6SUMO-p53 or H6SUMO-p53$_{SS}$ gene. After dilution to an OD_{600} of 0.1 in 100 mL LB, cells were cultured shaking at 220 RPM, 37 °C, until they reached an OD_{600} of 0.6-0.8. Cells were then induced with 10 mM IPTG and incubated for 16-48 hours shaking at 220 RPM, 25 °C. Aliquots were taken pre-expression and at 16, 18, 20, 22, 24, and 36 hours post-induction for SDS-PAGE and western blot analysis.

9.11.2 H6SUMO-p53$_{K120ac}$, amber suppressed, arabinose added before IPTG

Expression was carried out as described in section 9.10 using the pEVOL vector and a pET vector containing either the H6SUMO-p53$_{K120ac}$ or H6SUMO-p53$_{SSK120ac}$ gene. The protocol was changed as follows: After dilution of the culture from an OD_{600} of 1.0 to 0.1 in 100 mL LB, L-arabinose was added to 0.2 %. Acetyllysine and nicotinamide was added once the culture reached an OD_{600} of 0.3, as described in section 9.10, and once the culture reached an OD_{600} of 0.6-0.8, expression was induced by the addition of 10 mM IPTG.

9.11.3 H6SUMO-p53$_{K120ac}$, amber suppressed, arabinose added with IPTG

Expression was carried out as described in section 9.10 in 100 mL LB using the pEVOL vector and a pET vector containing the H6SUMO-p53$_{K120ac}$ or H6SUMO-p53$_{SSK120ac}$ gene. Aliquots were taken pre-expression and at 16, 18, 20, 22, 24, and 36 hours post-induction for SDS-PAGE and western blot analysis.

9.12 Expression trial comparing the solubility of H6SUMO-p53$_{K120ac}$ versus H6SUMO-p53$_{SSK120ac}$

H6SUMO-p53 and H6SUMO-p53$_{SS}$ were expressed in non-amber suppressed BL21 cells as described in section 9.11.1. H6SUMO p53$_{K120ac}$ and H6SUMO p53$_{SSK120ac}$ were expressed as described in section 9.11.3. Expression was carried out in 100 mL LB. Lysis was carried out as described in section 9.10 using 5 x pellet volume AS lysis buffer. After lysis, supernatant was clarified by 20 minutes centrifugation at 15,000 rcf, 4 °C, and an aliquot was taken of the supernatant. The pellet was resuspended in 5 x pellet volume AS lysis buffer and centrifuged again, with an aliquot being taken of the supernatant as before. The pellet was resuspended in 5 x pellet volume AS lysis buffer without centrifugation, and an aliquot was taken of the resuspension. All aliquots were analysed by SDS-PAGE and western blotting.

9.13 Human cell culture

H1299, HCT116, and HeLa cells were generously provided by the Tavassoli lab at King's College London, while A549 cells were generously provided by the Parsons lab at King's College London. Cells were grown at 37 °C and 5 % CO_2 in DMEM supplemented with 100 U/mL penicillin, 100 μg/mL streptomycin and 1 mM sodium pyruvate.

9.13.1 Cell treatment with cisplatin or adriamycin

Cisplatin solutions were prepared by dissolving solid cisplatin directly into DMEM to the desired concentration. For adriamycin, a 100 mM stock solution was prepared by dissolving solid adriamycin in DMSO. A working stock solution was prepared by diluting the 100 mM ADR to 0.5 mM using DMEM. Adriamycin treatments were prepared by diluting the working stock to the desired concentration in DMEM.

Cells (H1299, HCT116, or A549) were grown to 50-60 % confluency. The DMEM was removed by aspiration and replaced with media containing the prepared cisplatin, adriamycin, or DMSO treatment, as appropriate. Cells were incubated for the indicated time points, after which they were harvested as described in section 9.13.2.

9.13.2 Human cell harvesting

Cells were washed once with PBS and trypsinised by the addition of 1 x trypsin-EDTA (Sigma-Aldrich) in PBS and incubation at 37 °C. Once cells were detached, double the trypsin volume of DMEM was added to quench the trypsin. Cells were transferred to a separate tube, and flasks were washed with ice cold PBS, which was then added to the tube. When necessary, a 10 μL aliquot of cell suspension was combined with 10 μL trypan blue and cells were counted using a haemocytometer. Cells were harvested by 10 minutes centrifugation at 400 rcf, 4 °C. supernatants were removed by aspiration and pellets were resuspended in ice cold PBS. Cells were centrifuged as before, and supernatant was removed by aspiration. Cells were either lysed directly with 1 x loading dye for western blotting or carried forward for nuclear and cytoplasmic extract preparation.

9.13.3 Nuclear and cytoplasmic extract preparation

Cell pellets were resuspended in 5x pellet-volume CE buffer (10 mM HEPES (pH 7.6), 60 mM KCl, 1 mM EDTA, 0.075 % (v/v) NP-40, 1 mM DTT, and 1 mM PMSF), placed on ice for 3 minutes, then centrifuged for 5 minutes at 0.4 rcf, 4 °C. The supernatant (cytoplasmic extract) was removed and the pellet washed with wash buffer (10 mM HEPES, 60 mM KCl, 1 mM EDTA, 1 mM DTT, and 1 mM PMSF, pH 7.6) twice by gentle resuspention in 5x pellet-volume and 5 minutes centrifugation at 0.4 rcf, 4 °C, discarding the supernatant each time. The remaining pellet was resuspended in 1x pellet volume NE buffer (20 mM Tris-base, 800 mM NaCl, 1.5 mM $MgCl_2$, 0.2 mM EDTA, 1 mM PMSF, 20 % (v/v) glycerol, pH 8.0) and incubated for one hour on ice, briefly vortexing every 20 minutes. Remaining nuclei in the nuclear and cytoplasmic extracts were pelleted by 10 minutes centrifugation at 2000 rcf, 4 °C. The cytoplasmic extract was adjusted to 20 % (v/v) glycerol, flash frozen in liquid N_2 and stored in aliquots at -80 °C. Nuclear extracts were dialized overnight in buffer D (20 mM HEPES, 100 mM KCl, 1.5 mM $MgCl_2$, 0.2 mM EDTA, 1 mM PMSF, 20 % (v/v) glycerol, pH 8.0), flash frozen in liquid N_2 and stored in aliquots at -80 °C.

9.14 *In vitro* transcription using T7 RNA polymerase

MG15 and PG13 DNA templates were linearized using PflMI (New England Biolabs). 50 μL reactions containing 0.02 μg DNA, 1x NEBuffer^{TM} r3.1 (New England Biolabs) and 10 U PflMI were incubated for 15 minutes at 37 °C before 20 minutes heat-inactivation at 65 °C. DNA was purified using a PCR purification kit (QIAGEN) according to manufacturer's instructions and DNA concentration was measured via NanoDrop.

Transcription reactions were carried out using a HiScribe® T7 Quick High Yield RNA Synthesis Kit (New England Biolabs). Briefly, 30 μL transcription reactions containing 1 μg DNA, 6.7 mM each of rATP, rGTP, rCTP and rUTP; and 2 μL RNA polymerase mix were incubated at 37 °C for 4 hours. RNA was purified from the reaction using a Monarch RNA purification kit (New England Biolabs) according to the manufacturer's instructions, eluting in 26 μL RNAse-free (DEPC-treated) ddH_2O. 3 μL 10x DNAse 1 buffer (New England Biolabs) and 1 μL DNAse 1 (New England Biolabs) were added to the purified RNA and the reactions were incubated for two hours at 30 °C. Reactions were purified again using the Monarch RNA purification kit (New England Biolabs) according to the manufacturer's instructions. Purified aptamers were heated for 2 minutes at 85 °C before being left to cool at room temperature for 5 minutes. Purified aptamers were diluted 100 x in 1x KCl buffer (20 mM Tris-HCl, 2 mM $MgCl_2$, 100 mM KCl, pH 7.5), while DFHBI was diluted to 20 μM in 1x KCl buffer from a 20 mM stock in DMSO. Diluted aptamer and DFHBI were combined at 1 1:1 ratio and fluorescence was measured with a Hidex Multimode Microplate Reader using an excitation of 444 nm and an emission of 520 nm.

9.15 *In vitro* transcription using HeLa nuclear extracts

51 μL reactions containing 10 μL nuclear extract, 14 μL dilution buffer (20 mM HEPES (pH 7.9), 50 mM KCl, 1 mM DTT, 0.2 mM EDTA, 10 % glycerol), 0.5 μL of 1 μg/μL MG15 or PG13 DNA template, 0.5 μL RNAse inhibitor (New England Biolabs), and 1μL 10 ng/μL p53 were incubated at 30 °C for two hours. RNA was purified from the reaction using a Monarch RNA purification kit (New England Biolabs) according to the

manufacturer's instructions, eluting in 26 μL RNAse-free (DEPC-treated) ddH_2O. 3 μL 10x DNAse 1 buffer (New England Biolabs) and 1 μL DNAse 1 (New England Biolabs) were added to the purified RNA and the reactions were incubated for two hours at 30 °C. Reactions were purified again using the Monarch RNA purification kit (New England Biolabs) according to the manufacturer's instructions. Purified transcripts were heated for 2 minutes at 85 °C before being left to cool at room temperature for 5 minutes. DFHBI was diluted to 20 μM in 2x KCl buffer (40 mM Tris-HCl, 4 mM $MgCl_2$, 200 mM KCl, pH 7.5) from a 20 mM stock in DMSO. Transcription reactions and DFHBI were combined at 1 1:1 ratio and fluorescence was measured with a Hidex Multimode Microplate Reader (Ex: 444 nm, Em 520 nm).

9.16 Reverse transcription

Reverse transcription following *in vitro* transcription was carried out using a High-Capacity cDNA Reverse Transcription kit (Thermo Fisher Scientific) according to manufacturer's instructions, following RNA purification using the Monarch RNA purification kit (New England Biolabs).

9.17 Agarose gel electrophoresis of RNA

A 1 % agarose gel comprising 20 mM MOPS, 5 mM sodium acetate, 1 mM EDTA, 10 mg/mL agarose, 0.0074 % (v/v) formaldehyde, 0.009 % (v/v) SYBR^{TM} Gold (Thermo Fisher Scientific) was prepared using RNAse-free (DEPC-treated) ddH_2O. 4 μL RNA samples were mixed with 2 μL formaldehyde loading buffer (Thermo Fisher Scientific) and incubated at 65 °C for 15 minutes. Gels were run at 100 V for 45 minutes.

9.18 Agarose gel electrophoresis of DNA

Agarose gels were prepared as 1 % or 2 % agarose gels. Gels comprised of 40 mM Tris-base, 20 mM acetic acid, 1 mM EDTA, 0.01 % SYBR^{TM} Safe and either 10 mg/mL or 20 mg/mL agarose for 1 % and 2 % agarose gels respectively. Samples were prepared by adding 1 μL 6x purple gel loading dye (New England Biolabs) to 5 μL sample. Gels were run at 100 V for one hour.

9.19 Optimised crosstalk assay

Aliquots of nuclear/cytoplasmic extract and p53 were thawed on ice. Nuclear and cytoplasmic extracts were diluted to 3 mg/mL protein, and p53 was diluted to 200 ng/μL. All dilutions were made in their respective storage buffers. For p53, storage buffer comprised 30 mM sodium diphosphate, 50 mM KCl, 5 % (v/v) glycerol and 2 mM DTT (pH 7.5). For cytoplasmic extract, storage buffer comprised 10 mM HEPES, 60 mM KCl, 1 mM EDTA, 0.075 % (v/v) NP-40, 1 mM DTT, 20 % glycerol (v/v), and 1 mM PMSF (pH 7.6). For nuclear extract, storage buffer comprised 20 mM HEPES, 100 mM KCl, 1.5 mM $MgCl_2$, 0.2 mM EDTA, 1 mM PMSF, and 20 % (v/v) glycerol (pH 8.0). Mixes were prepared on ice containing 1.6 mg/mL nuclear/cytoplasmic extract, 500 μM ATP, 10 μM Acetyl-CoA, 10 μM SAM, 10 mM $MgCl_2$ and 0.1 mM DTT. 51.6 μL aliquots were prepared from the mixes, to which p53 was added to a final concentration of 10 ng/μL. Immediately, 16 μ was removed from the reactions and quenched with 5.3 μL 4x SDS loading dye. Reactions were incubated at 16 °C for 1 hour, with 16 μL removed and quenched with 5.3 μL 4x SDS loading dye every 30 minutes.

9.20 Initial crosstalk assay

The results shown in Fig. 7.2 were generated from assays carried out as described in section 9.19, except reactions contained 833 μM ATP, were incubated at 37 °C, and aliquots were taken every 15 minutes.

9.21 Broad crosstalk screen

The results shown in Figs. 7.4 and 7.5 were generated from assays carried out as described in section 9.19, except reactions contained 833 μM ATP and were incubated at 37 °C. During western blotting, membranes were stripped and re-probed using three methods, detailed below. After stripping, membranes were blocked with 5 % milk or 5 % BSA, as appropriate, and probed with a different antibody.

9.21.1 Mild stripping

Probed PVDF membranes were incubated with mild stripping buffer (199.8 mM glycine, 0.1 % SDS, 1 % Tween-20, pH 2.2) rocking for 5-10 minutes twice, washed with PBS for 10 minutes twice, and washed with TBST for 5 minutes twice.

9.21.2 Harsh stripping

Probed PVDF membranes were incubated with harsh stripping buffer (62.5 mM Tris-HCl, 10 % SDS, 0.8 % β-mercaptoethanol, pH 6.8) for 45 minutes at 50 °C, rocking. The membrane was rinsed under a running water tap for 1-2 minutes, then washed for 5 minutes with TBST.

9.21.3 GuHCl stripping

Probed PVDF membranes were incubated with GuHCl stripping buffer (20 mM Tris-HCl, 6M GuHCl, 0.2 % NP-40, 100 mM β-mercaptoethanol, pH 7.5), rocking for 5 minutes, twice. The membrane was then washed for 5 minutes with TBST four times.

9.22 Optimising cofactor concentrations for crosstalk assays

Crosstalk assays were carried out described in section 9.19 using $p53_{rec\Delta}$. ATP concentrations tested were 0, 10, 25, 50, 100, 250, 500, and 833 μM. Acetyl-CoA concentrations tested were 0, 5, 10, 20, and 40 μM. SAM concentrations tested were 0, 6.5, 10, 26, 104.2, and 416.7 μM.

9.23 *In vitro* kinase assay using CK1

Aliquots of $p53_{rec\Delta}$ or $p53_{S15ph}$, were thawed on ice and diluted to 50 ng/μL. Reactions were prepared, on ice, containing 10 mM HEPES, 10 ng/μL p53, 500 μL ATP, 0.01 μg/mL CK1 (Abcam, ab103955), 10 mM $MgCl_2$, 50 mM KCl, 0.1 mM EDTA, 10 % glycerol (v/v), and 0.002 % BSA (w/v), pH 7.5.

Immediately, 12 μL of each reaction was quenched in 4 μL 4x SDS loading dye. The reactions were then incubated at 30 °C for 1 hour. Every 30 minutes, 12 μL were removed and quenched in 4 μL 4x SDS loading dye.

9.24 Densitometric and statistical analysis

Densitometric analysis of stain-free gels and western blots was carried out using ImageJ or Image Lab (Bio-Rad). Statistical analysis was carried out using Graphpad Prism. Triplicate data from crosstalk assays, including assays using recombinant CK1, was normalised as indicated in results, checked for normal distribution and analysed one sample t test, comparing to 1, $\alpha = 0.05$.

Supplementary Materials

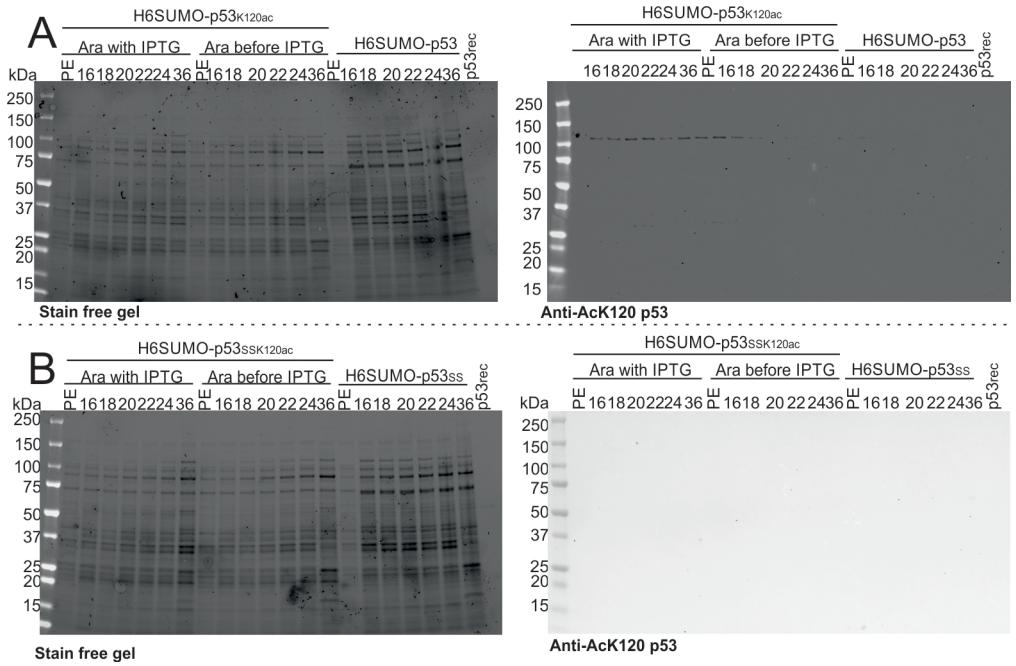

Figure 10.1: Expression trial with different timings of arabinose addition. H6SUMO $p53_{K120ac}$ was expressed at 25 °C using amber suppression and the pEVOL/pET system in BL21 cells. Arabinose was added either simultaneously with IPTG (Ara with IPTG) or at the start of growth culture (Ara before IPTG). Aliquots were taken pre-expression (PE) and at time points indicated, shown in hours (16-36). A 50 ng $p53_{rec}$ is also shown running at 53 kDa. Full-length H6SUMO-p53 runs at 75 kDa, the truncated variant falls around 37 kDa. Shown are stain free gels and western blots against AcK120 p53 for H6SUMO-$p53_{K120ac}$ (A) and H6SUMO-$p53_{SSK120ac}$ (B).

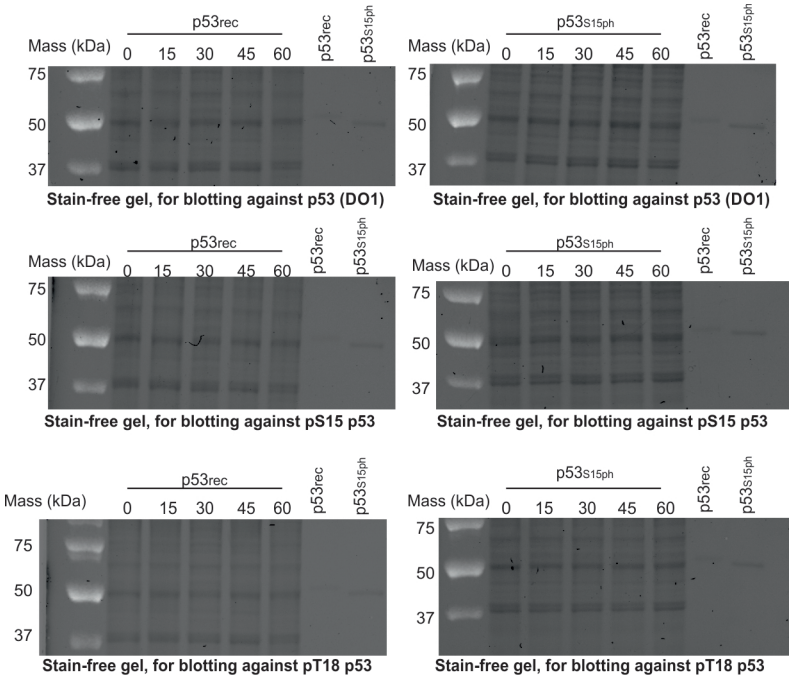

Figure 10.2: p53 phosphorylation occurs in nuclear extracts. Crosstalk assays were carried out over the course of 1 hour, with reactions quenched at 0, 15, 30, 45, and 60 minutes (indicated by numbers). Shown are stain free gels corresponding to western blots shown in Fig. 7.2.

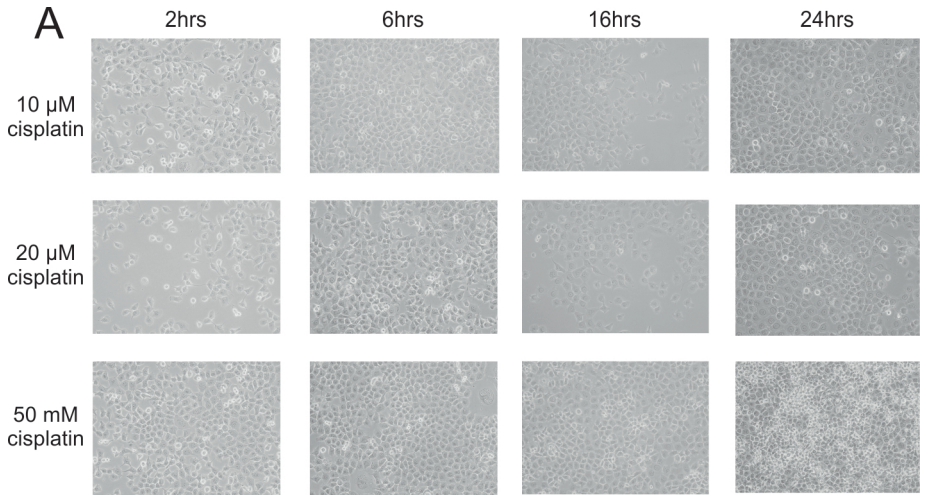

Figure 10.3: Cisplatin treatment screen. H1299 cells were treated with 0-1 mM cisplatin for 24 hours. Shown are cell images taken at 2, 6, 16, and 24 hours for 10 μM, 20 μM, and 50 μM cisplatin.

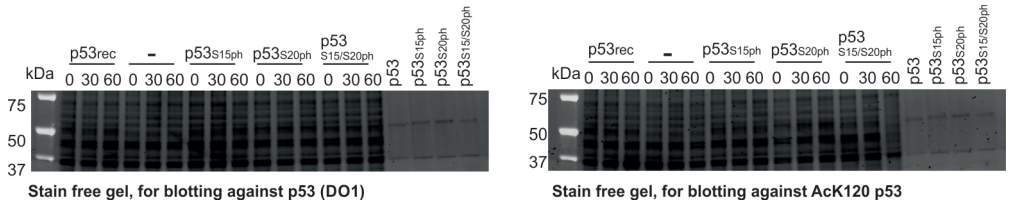

Figure 10.4: Broad PTM screen in unstressed nuclear extracts. $p53_{rec}$, $p53_{S15ph}$, $p53_{S20ph}$, and $p53_{S15/S20ph}$, as well as a negative control with no p53 were incubated for 0, 30 or 60 minutes (indicated by 0, 30, 60) with nuclear extracts derived from unstressed H1299 cells. Shown are the stain free gels that were blotted using a generic anti-p53 antibody (DO1) and an antibody targeting AcK120 p53.

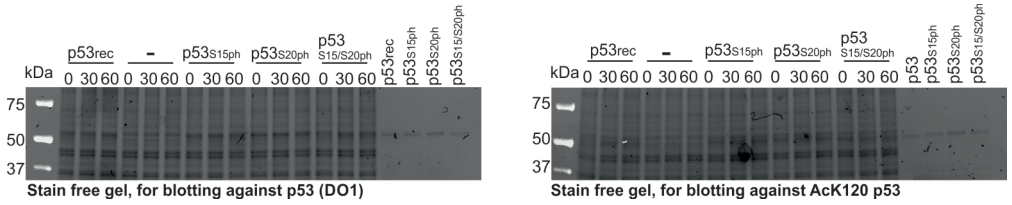

Figure 10.5: Broad PTM screen in nuclear extracts derived from 1 mM-cisplatin stressed cells. $p53_{rec}$, $p53_{S15ph}$, $p53_{S20ph}$, and $p53_{S15/S20ph}$, as well as a negative control with no p53 were incubated for 0, 30 or 60 minutes (indicated by 0, 30, 60) with nuclear extracts derived from H1299 cells that had been stressed for 2 hours with 1 mM cisplatin. Shown are the stain free gels that were blotted using a generic anti-p53 antibody (DO1) and an antibody targeting AcK120 p53.

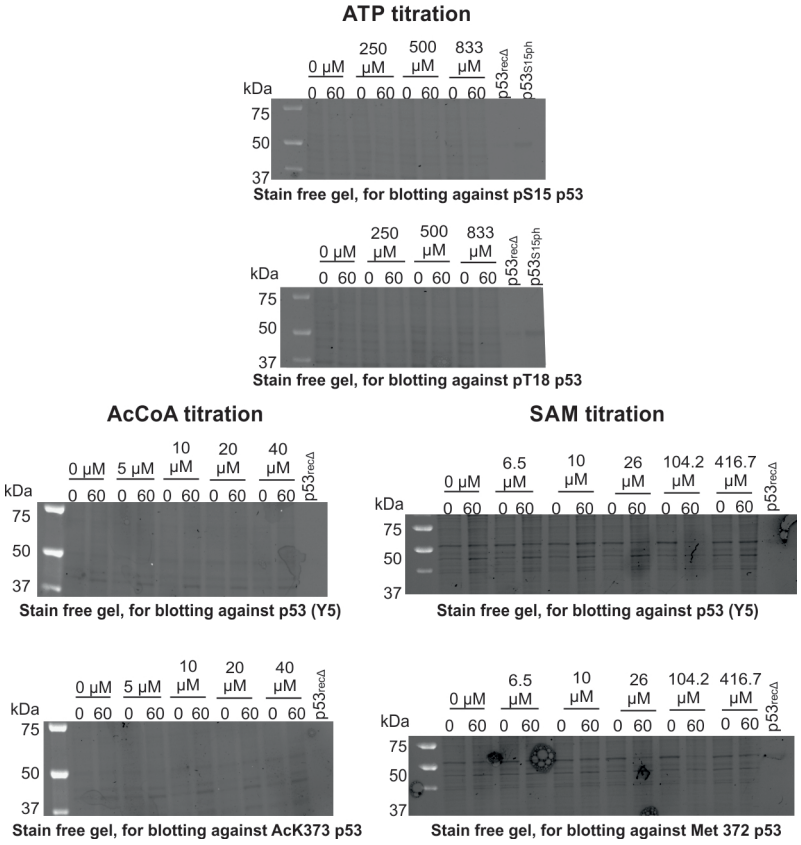

Figure 10.6: Cofactor titration Assays were performed using p53 in nuclear extracts, supplementing PTM cofactors at different concentrations. ATP titration assays were carried out using $p53_{S15ph}$, blotting for T18 phosphorylation. AcCoA and SAM titration assays were carried out using $p53_{rec\Delta}$, blotting for AcK373 and Met372 p53 respectively. Shown are stain free gels for western blots shown in Fig. 7.8. Time points (0, 60) are shown in minutes. Also loaded are 50 ng p53 controls. Overall p53 levels in the ATP titration assays were determined using an anti-p53 (pS15) antibody. ATP titration data were collected by Maria Hancu.

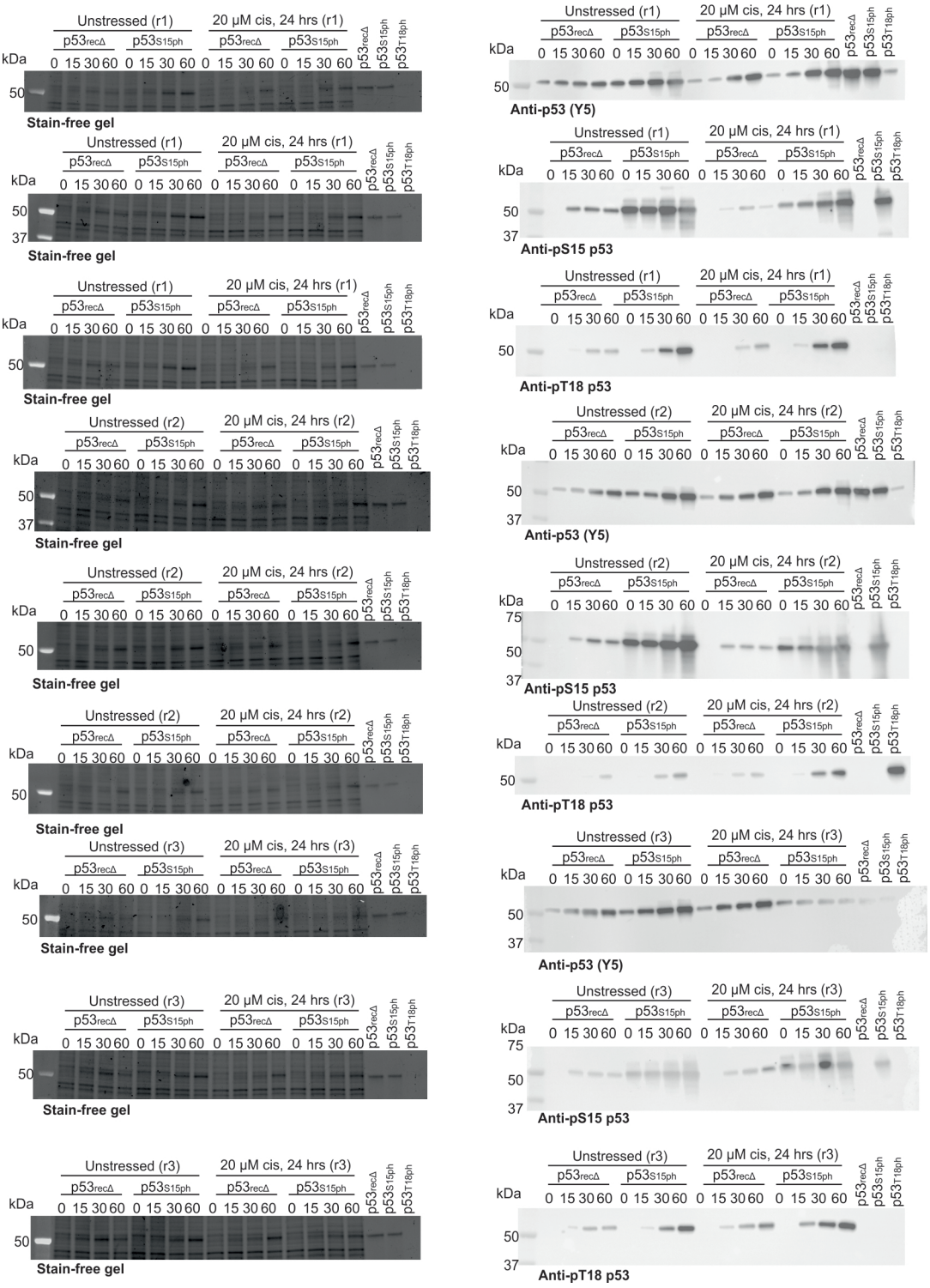

Figure 10.7: Probing the pS15-pT18 axis using unstressed or 20 μM cisplatin-stressed extracts at 30 °C. p53$_{recΔ}$ or p53$_{S15ph}$ were incubated for 0, 15, 30 or 60 minutes (indicated by 0, 15, 30, 60) with nuclear extracts derived from either unstressed or 20 μM cisplatin-stressed H1299 cells. Western blots from all replicates (r1, r2, r3) are shown with their corresponding stain-free gels adjacent. Also shown are 50 ng positive controls for p53$_{recΔ}$, p53$_{S15ph}$, and p53$_{T}$18ph. Data collected by Maria Hancu.

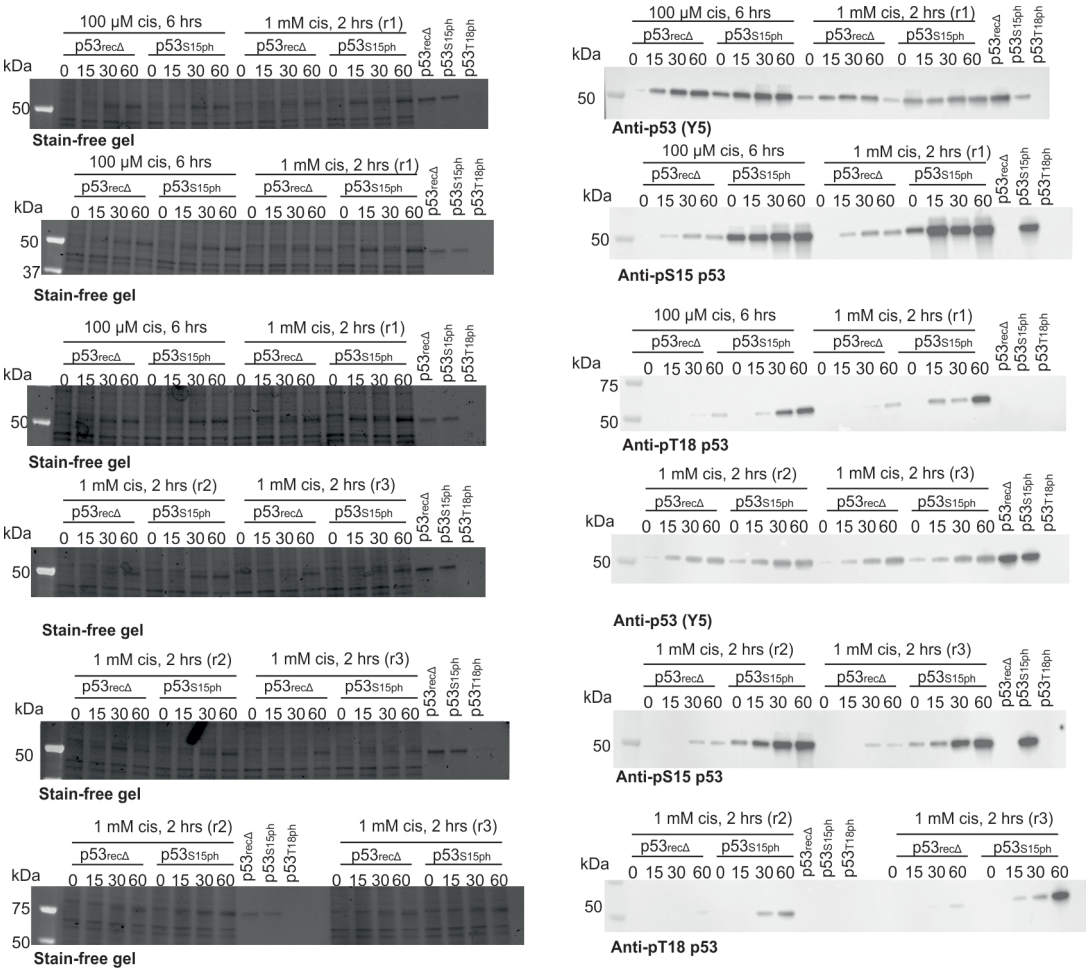

Figure 10.8: Probing the pS15-pT18 axis using 100 μM or 1 mM cisplatin-stressed extracts at 30 °C. $p53_{rec\Delta}$ or $p53_{S15ph}$ were incubated for 0, 15, 30 or 60 minutes (indicated by 0, 15, 30, 60) with nuclear extracts derived from either 100 μM or 1 mM cisplatin-stressed H1299 cells. Western blots from all replicates (r1, r2, r3) are shown with their corresponding stain-free gels adjacent. Also shown are 50 ng positive controls for $p53_{rec\Delta}$, $p53_{S15ph}$, and $p53_T18ph$. Data collected by Maria Hancu.

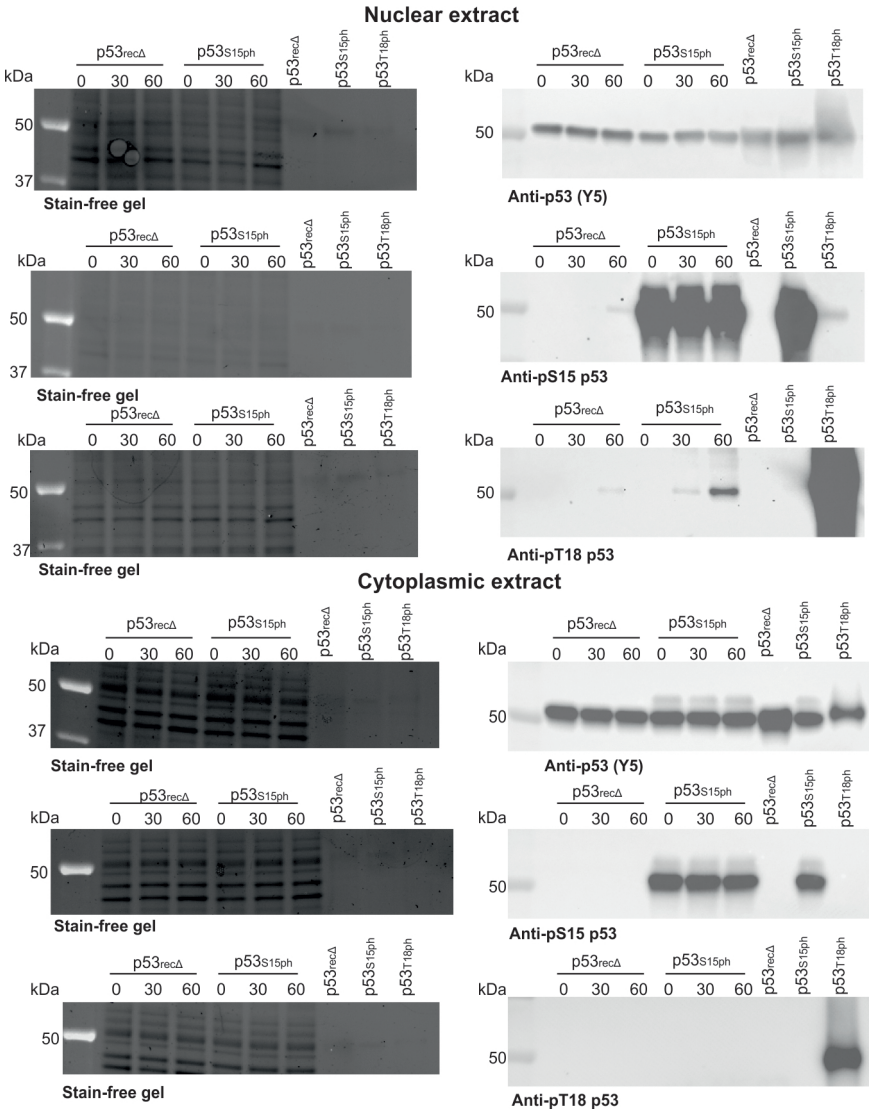

Figure 10.9: Probing the pS15-pT18 axis using unstressed extracts at 16 °C (replicate 1). $p53_{rec\Delta}$ or $p53_{S15ph}$ were incubated for 0, 30 or 60 minutes (indicated by 0, 30, 60) with unstressed H1299 nuclear or cytoplasmic extracts. Shown are western blots and corresponding stain free gels (adjacent) for assays carried out in nuclear and cytoplasmic extracts. Also included are 50 ng controls for $p53_{rec\Delta}$, $p53_{S15ph}$, and $p53_T18ph$.

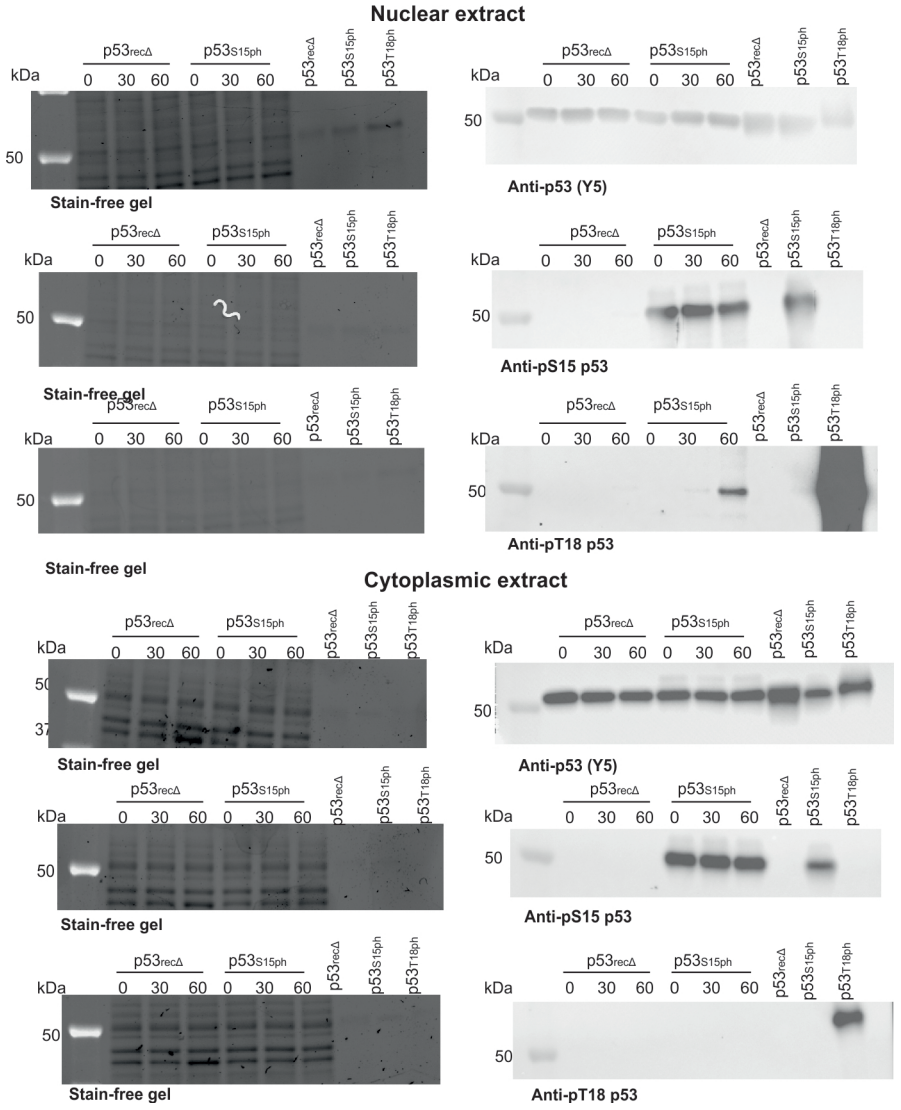

Figure 10.10: Probing the pS15-pT18 axis using unstressed extracts at 16 °C (replicate 2). $p53_{rec\Delta}$ or $p53_{S15ph}$ were incubated for 0, 30 or 60 minutes (indicated by 0, 30, 60) with unstressed H1299 nuclear or cytoplasmic extracts. Shown are western blots and corresponding stain free gels (adjacent) for assays carried out in nuclear and cytoplasmic extracts. Also included are 50 ng controls for $p53_{rec\Delta}$, $p53_{S15ph}$, and $p53_T18ph$.

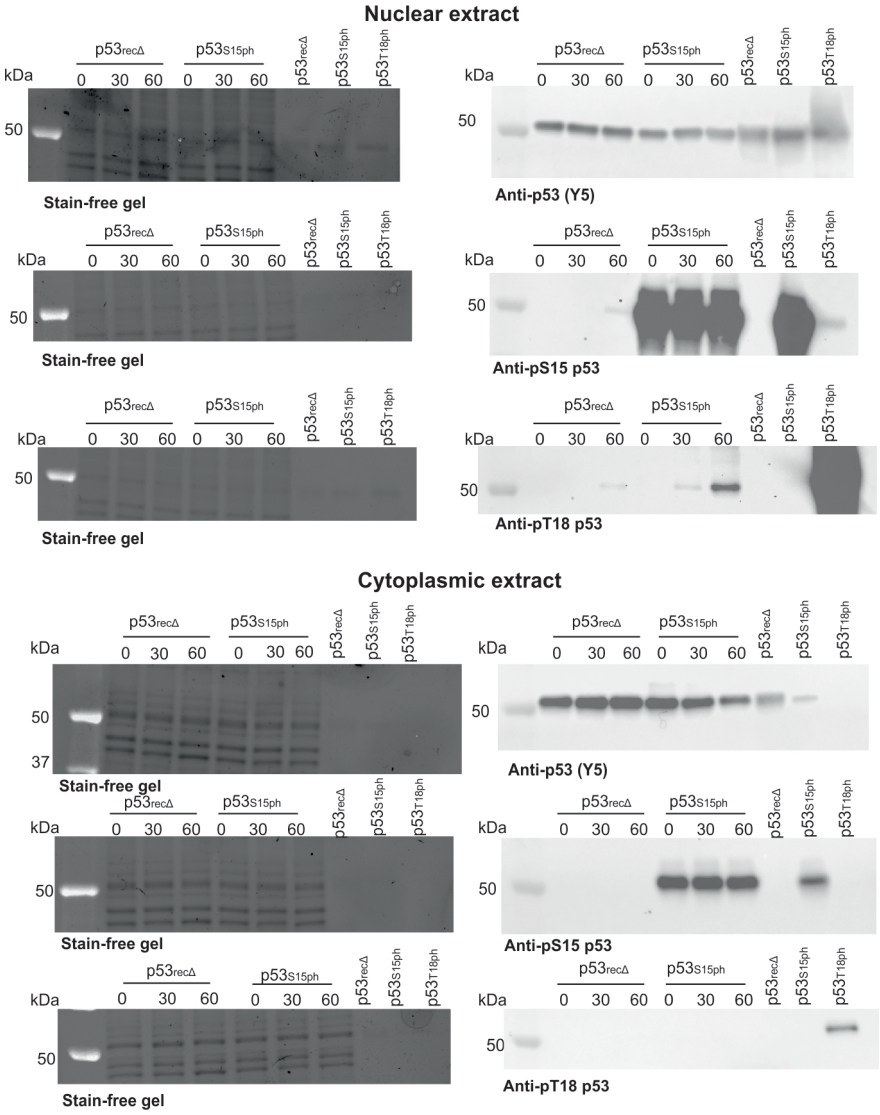

Figure 10.11: Probing the pS15-pT18 axis using unstressed extracts at 16 °C (replicate 3). $p53_{rec\Delta}$ or $p53_{S15ph}$ were incubated for 0, 30 or 60 minutes (indicated by 0, 30, 60) with unstressed H1299 nuclear or cytoplasmic extracts. Shown are western blots and corresponding stain free gels (adjacent) for assays carried out in nuclear and cytoplasmic extracts. Also included are 50 ng controls for $p53_{rec\Delta}$, $p53_{S15ph}$, and $p53_T18ph$.

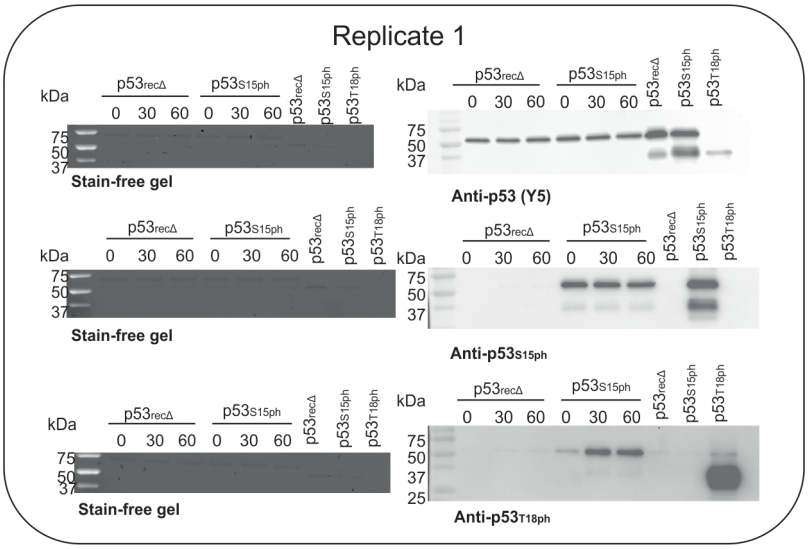

Figure 10.12: Probing the pS15-pT18 axis using purified CK1 (replicate 1) $p53_{rec\Delta}$ or $p53_{S15ph}$ were incubated for 0, 30 or 60 minutes (indicated by 0, 30, 60) with recombinant CK1. Shown are western blots and corresponding stain free gels (adjacent) for assays carried out in nuclear and cytoplasmic extracts. Also included are 50 ng controls for $p53_{rec\Delta}$, $p53_{S15ph}$, and $p53_T18ph$.

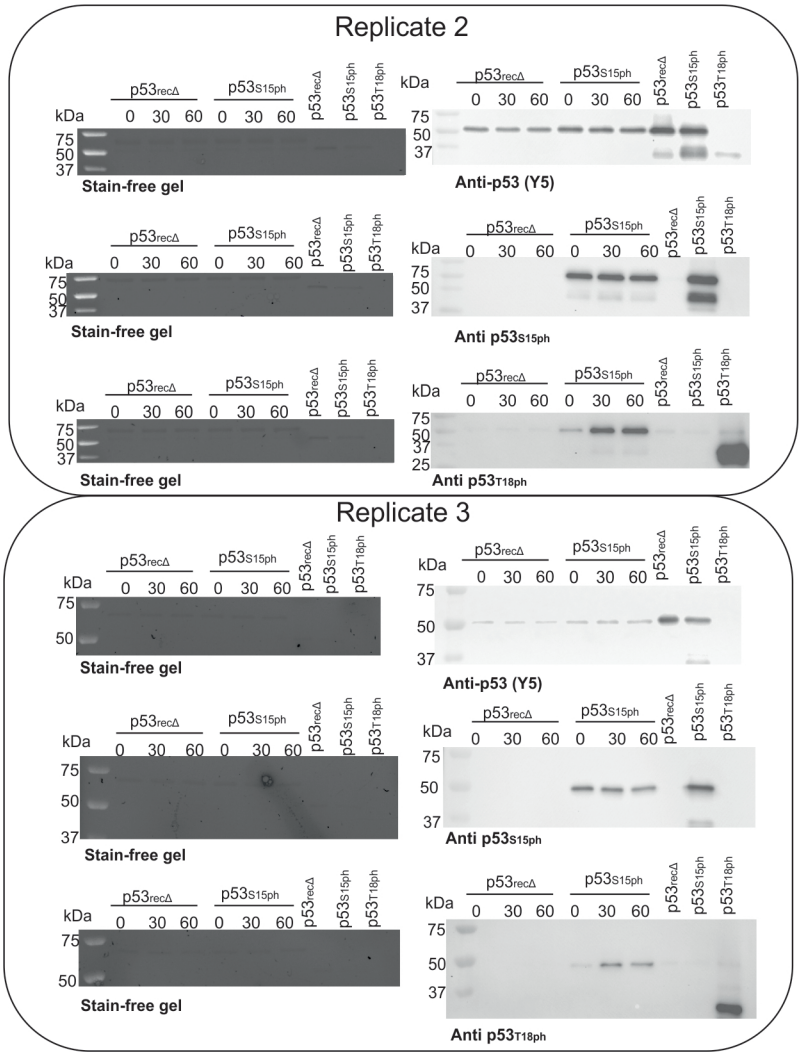

Figure 10.13: Probing the pS15-pT18 axis using purified CK1 (replicates 2 and 3) $p53_{rec\Delta}$ or $p53_{S15ph}$ were incubated for 0, 30 or 60 minutes (indicated by 0, 30, 60) with recombinant CK1. Shown are western blots and corresponding stain free gels (adjacent) for assays carried out in nuclear and cytoplasmic extracts. Also included are 50 ng controls for $p53_{rec\Delta}$, $p53_{S15ph}$, and $p53_{T}18ph$.

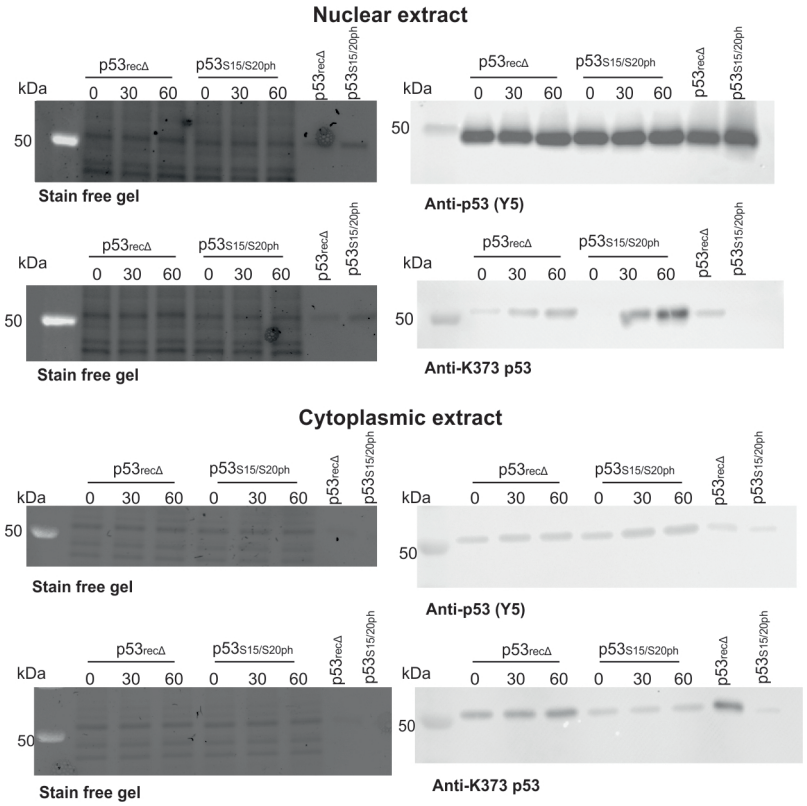

Figure 10.14: Probing the interaction between N-terminal phosphorylation and C-terminal acetylation using unstressed extracts at 16 °C (replicate 1). $p53_{rec\Delta}$ or $p53_{S15/S20ph}$ were incubated for 0, 30 or 60 minutes (indicated by 0, 30, 60) with unstressed H1299 nuclear or cytoplasmic extracts. Shown are western blots and corresponding stain free gels (adjacent) for assays carried out in nuclear and cytoplasmic extracts. Also included are 50 ng controls for $p53_{rec\Delta}$ and $p53_{S15/S20ph}$.

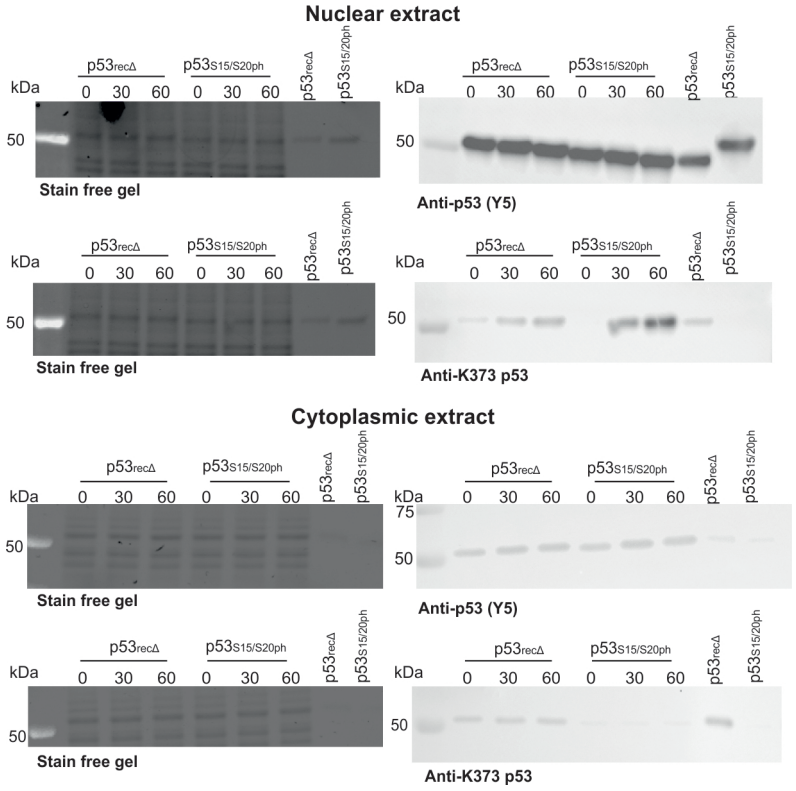

Figure 10.15: Probing the interaction between N-terminal phosphorylation and C-terminal acetylation using unstressed extracts at 16 °C (replicate 2). $p53_{rec\Delta}$ or $p53_{S15/S20ph}$ were incubated for 0, 30 or 60 minutes (indicated by 0, 30, 60) with unstressed H1299 nuclear or cytoplasmic extracts. Shown are western blots and corresponding stain free gels (adjacent) for assays carried out in nuclear and cytoplasmic extracts. Also included are 50 ng controls for $p53_{rec\Delta}$ and $p53_{S15/S20ph}$.

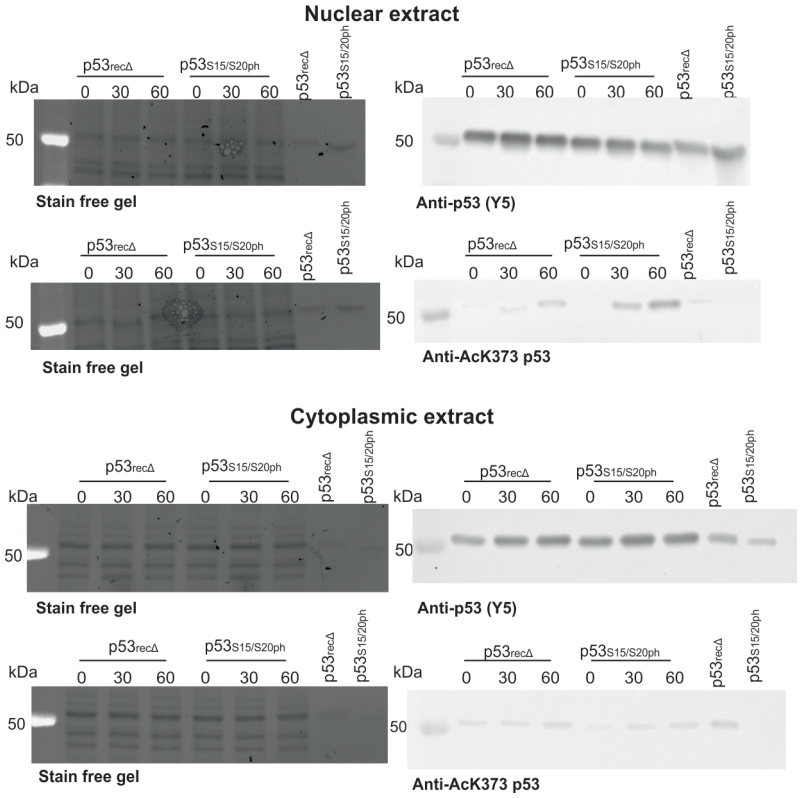

Figure 10.16: Probing the interaction between N-terminal phosphorylation and C-terminal acetylation using unstressed extracts at 16 °C (replicate 3). $p53_{rec\Delta}$ or $p53_{S15/S20ph}$ were incubated for 0, 30 or 60 minutes (indicated by 0, 30, 60) with unstressed H1299 nuclear or cytoplasmic extracts. Shown are western blots and corresponding stain free gels (adjacent) for assays carried out in nuclear and cytoplasmic extracts. Also included are 50 ng controls for $p53_{rec\Delta}$ and $p53_{S15/S20ph}$.

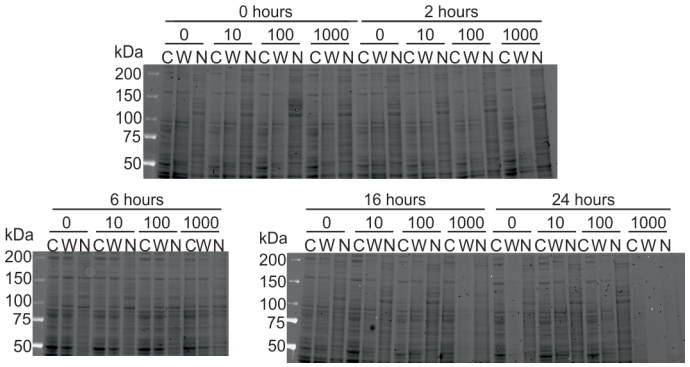

Figure 10.17: Testing for DYRK2 translocation in H1299 cells following cisplatin treatment. H1299 cells were stressed with 0, 10, 100 or 1000 μM cisplatin for 0, 2, 6, 16, or 24 hours. Fractions enriched for nuclear and cytoplasmic proteins were probed for DYRK2 (67 kDa), as well as nuclear (LSD1, 110 kDa) and cytoplasmic (β-tubulin, 50 kDa) markers. Shown are the stain free gels that correspond to the western blots shown in Fig. 7.13.

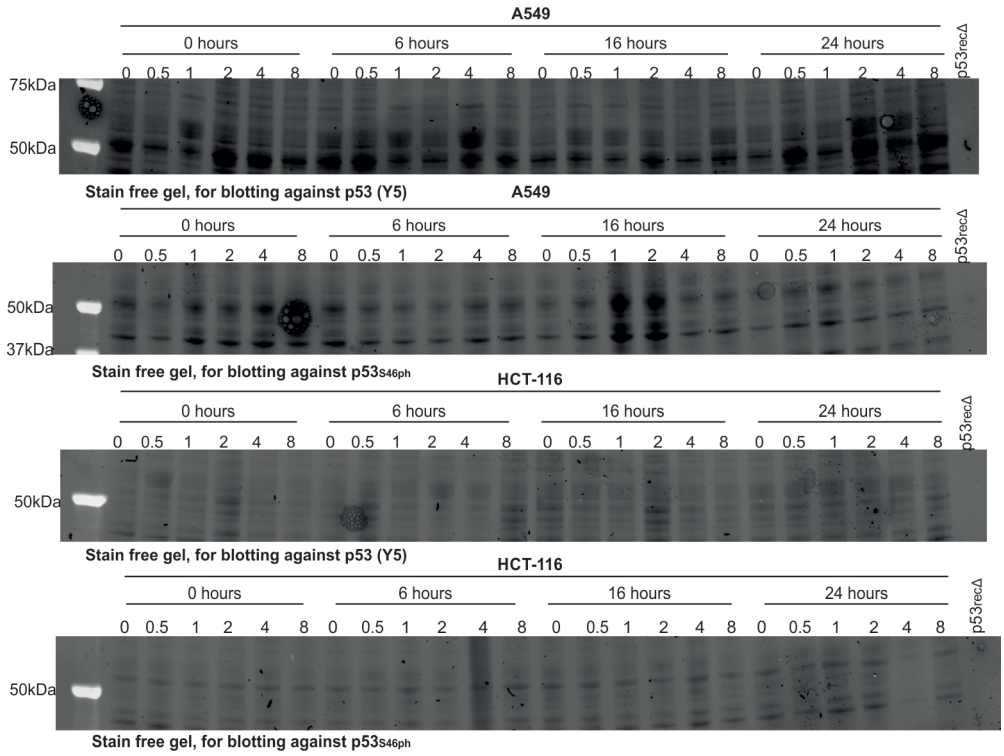

Figure 10.18: Testing for p53 accumulation in A549 and HCT-116 cells following treatment with adriamycin. A549 and HCT-116 were stressed with 0 (0.008 % DMSO), 0.5, 1, 2, 4, or 8 μM adriamycin for 0, 6, 16, or 24 hours and blotted for p53 (Y5) and pS46 p53. Shown are the stain free gels that correspond to the western blots shown in Fig. 7.14.

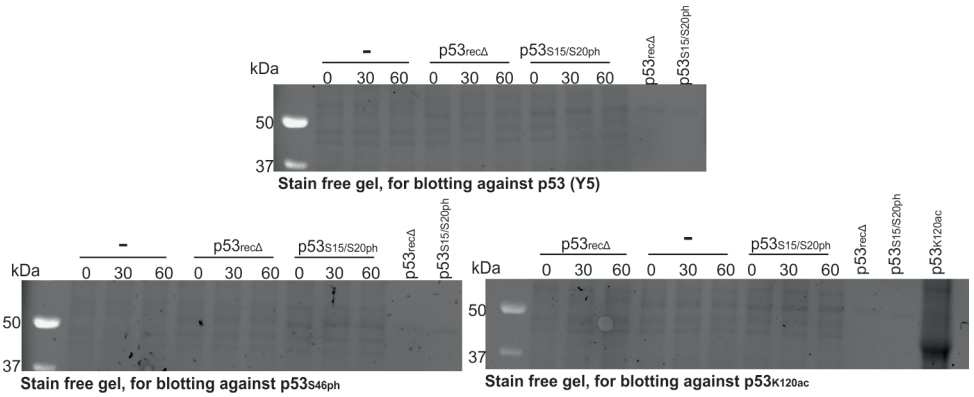

Figure 10.19: Probing for S46 phosphorylation and K120 acetylation in adriamycin-stressed A549 nuclear extracts. $p53_{rec\Delta}$ or $p53_{S15/S20ph}$ were incubated for 0, 30 or 60 minutes (indicated by 0, 30, 60) with nuclear extracts prepared from A549 cells stressed for 6 hours with 8 μM adriamycin. Shown are the stain free gels that correspond to the western blots shown in Fig. 7.15.

Bibliography

[1] Edward Kastenhuber and Scott Lowe. "Putting p53 in context". In: *Cell* 170.6 (2018), pp. 1062–1078.

[2] Tanya Guha and David Malkin. "Inherited TP53 Mutations and the Li–Fraumeni Syndrome". In: *Cold Spring Harbour Perspectives in Medicine* 7.4 (2017).

[3] A J Levine and Moshe Oren. "The first 30 years of p53: growing ever more complex". In: *Nature Reviews Cancer* 9 (2009), pp. 749–758.

[4] Y Haupt et al. "Mdm2 promotes the rapid degradation of p53". In: *Nature* 387.6630 (1997), pp. 296–299.

[5] Christopher L. Brooks and Wei Gu. "p53 Regulation by Ubiquitin". In: *FEBS Lett.* 585.18 (2011), pp. 2803–2809.

[6] S P Jackson N D Lakin. "Regulation of p53 in response to DNA damage". In: *Oncogene* 8 (1999), pp. 7644–7655.

[7] Ashley B. Williams and Björn Schumacher. "p53 in the DNA-Damage-Repair Process". In: *Cold Spring Harbour Perspectives in Medicine* 6.5 (2016), a026070.

[8] Brandon J Aubrey et al. "How does p53 induce apoptosis and how does this relate to p53-mediated tumour suppression?" In: *Cell Death and Differentiation* 25 (2017), pp. 104–113.

[9] Amato J Giaccia Ester M Hammond. "The role of p53 in hypoxia-induced apoptosis". In: *Biochem Biophys Res Commun.* 331.3 (2005), pp. 718–725.

[10] Krishna P Bhat et al. "Essential role of ribosomal protein L11 in mediating growth inhibition-induced p53 activation". In: *EMBO J* 23.12 (2004), pp. 2402–2412.

[11] J. Grossman. "Molecular mechanisms of "detachment-induced apoptosis—Anoikis"". In: *Apoptosis* 7 (2002), pp. 247–260.

[12] Jerry E. Chipuk and Douglas R. Green. "p53's Believe It or Not: Lessons on Transcription-Independent Death". In: *Journal of Clinical Immunology* 23 (2003), pp. 355–361.

[13] Andreas C. Joerger and Alan R. Fersht. "Structural Biology of the Tumor Suppressor p53". In: *Annual Review of Biochemistry* 77 (2003), pp. 557–582.

[14] A Keith Dunker et al. "Flexible nets. The roles of intrinsic disorder in protein interaction networks". In: *FEBS J* 272.20 (2005), pp. 5129–5148.

[15] Jiangang Liu et al. "Intrinsic disorder in transcription factors". In: *Biochemistry* 45.22 (2006), pp. 6873–6888.

[16] Paul H. Kussie et al. "Structure of the MDM2 Oncoprotein Bound to the p53 Tumor Suppressor Transactivation Domain". In: *Science* 274.5289 (1996), pp. 948–953.

[17] Grzegorz M. Popowicz et al. "Molecular Basis for the Inhibition of p53 by Mdmx". In: *Cell Cycle* 6.19 (2007), pp. 2386–2392.

[18] Kazuyasu Sakaguchi et al. "Damage-mediated Phosphorylation of Human p53 Threonine 18 through a Cascade Mediated by a Casein 1-like Kinase: EFFECT ON Mdm2 BINDING". In: *J Biol Chem* 275.13 (2000), pp. 9278–9283.

[19] Daniel P. Teufel et al. "Four domains of p300 each bind tightly to a sequence spanning both transactivation subdomains of p53". In: *Proc Natl Acad Sci USA* 104.17 (2007), pp. 7009–7014.

[20] Daniel P. Teufel, Mark Bycroft, and Alan R. Fersht. "Regulation by phosphorylation of the relative affinities of the N-terminal transactivation domains of p53 for p300 domains and Mdm2". In: *Oncogene* 28.20 (2009), pp. 2112–2118.

[21] Feng Wang, Christopher B Marshall, and Mitsuhiko Ikura. "Transcriptional/epigenetic regulator CBP/p300 in tumorigenesis: structural and functional versatility in target recognition". In: *Cell Mol Life Sci.* 70.21 (2013), pp. 3989–4008.

[22] Yanqing Liu, Omid Tavana, and Wei Gu. "p53 modifications: exquisite decorations of the powerful guardian". In: *J Mol Cell Biol.* 11.7 (2019), pp. 564–577.

[23] H Lu and A J Levine. "Human TAFII31 protein is a transcriptional coactivator of the p53 protein". In: *Proc Natl Acad Sci USA.* 92.11 (1995), pp. 5154–5158.

[24] C J Thut et al. "p53 transcriptional activation mediated by coactivators TAFII40 and TAFII60". In: *Science* 267.5194 (1995), pp. 100–104.

[25] Paola Di Lello et al. "Structure of the Tfb1/p53 complex: Insights into the interaction between the p62/Tfb1 subunit of TFIIH and the activation domain of p53". In: *Mol Cell* 22.6 (2006), pp. 731–740.

[26] Chris D Nicholls et al. "Biogenesis of p53 involves cotranslational dimerization of monomers and posttranslational dimerization of dimers. Implications on the dominant negative effect". In: *J Biol Chem.* 15 (2002), pp. 12937–12945.

[27] P D Jeffrey, S Gorina, and N P Pavletich. "Crystal structure of the tetramerization domain of the p53 tumor suppressor at 1.7 angstroms". In: *Science* 267.5203 (1995), pp. 1498–1502.

[28] M G Mateu, M M Sánchez Del Pino, and A R Fersht. "Mechanism of folding and assembly of a small tetrameric protein domain from tumor suppressor p53". In: *Nature Struc Biol.* 6.2 (1999), pp. 191–198.

[29] M G Mateu and A R Fersht. "Nine hydrophobic side chains are key determinants of the thermodynamic stability and oligomerization status of tumour suppressor p53 tetramerization domain". In: *EMBO J.* 17.10 (1998), pp. 2748–2758.

[30] K G McLure and P W Lee. "How p53 binds DNA as a tetramer". In: *EMBO J.* 17.12 (1998), pp. 3342–3350.

[31] J M Stommel et al. "A leucine-rich nuclear export signal in the p53 tetramerization domain: regulation of subcellular localization and p53 activity by NES masking". In: *EMBO J.* 18.6 (1999), pp. 1660–1672.

[32] Nicholas W. Fischer et al. "p53 oligomerization status modulates cell fate decisions between growth, arrest and apoptosis". In: *Cell Cycle* 15.23 (2016), pp. 3210–3219.

[33] Sridharan Rajagopalan et al. "14-3-3 activation of DNA binding of p53 by enhancing its association into tetramers". In: *Nucleic Acids Res.* 36.18 (2008), pp. 5983–5991.

[34] Stefan Bell et al. "p53 contains large unstructured regions in its native state". In: *J Mol Biol.* 322.5 (2002), pp. 917–927.

[35] R R Rustandi, D M Baldisseri, and D J Weber. "Structure of the negative regulatory domain of p53 bound to S100B(betabeta)". In: *Nat Struc Biol.* 7.7 (2000), pp. 570–574.

[36] Oleg Laptenko et al. "The Tail That Wags the Dog: How the Disordered C-Terminal Domain Controls the Transcriptional Activities of the p53 Tumor-Suppressor Protein". In: *Trends Biochem Sci* 41.12 (2016), pp. 1022–1034.

[37] Anahita Tafvizi et al. "A single-molecule characterization of p53 search on DNA". In: *Proc Natl Acad Sci USA.* 108.2 (2011), pp. 563–568.

[38] Alessio Di Ianni et al. "Structural assessment of the full-length wild-type tumor suppressor protein p53 by mass spectrometry-guided computational modeling". In: *Scientific Reports* 13 (2023), p. 8497.

[39] Yanqing Liu, Omid Tavana, and Wei Gu. "p53 modifications: exquisite decorations of the powerful guardian". In: *J Mol Cell Biol.* 11.7 (2019), pp. 564–577.

[40] Y Cho et al. "Crystal structure of a p53 tumor suppressor-DNA complex: understanding tumorigenic mutations". In: *Science* 265.5170 (1994), pp. 346–355.

[41] Ying Wang, Anja Rosengarth, and Hartmut Luecke. "Structure of the human p53 core domain in the absence of DNA". In: *Acta Crystallogr D Biol Crystallogr.* 63.Pt 3 (2007), pp. 276–281.

[42] José Manuel Pérez Cañadillas et al. "Solution structure of p53 core domain: structural basis for its instability". In: *Proc. Natl. Acad. Sci. USA* 103.7 (2006), pp. 2109–2114.

[43] W S el-Deiry et al. "Definition of a consensus binding site for p53". In: *Nat Genet.* 1.1 (1992), pp. 45–49.

[44] Jennifer J. Jordan et al. "Noncanonical DNA Motifs as Transactivation Targets by Wild Type and Mutant p53". In: *PLOS Genetics* 4.6 (2008), e1000104.

[45] Malka Kitayner et al. "Structural Basis of DNA Recognition by p53 Tetramers". In: *Molecular Cell* 22.6 (2006), pp. 741–753.

[46] Krassimira Botcheva. "p53 binding to human genome: crowd control navigation in chromatin context". In: *Frontiers in Genetics* 5.447 (2014).

[47] Fangjie Zhu et al. "The interaction landscape between transcription factors and the nucleosome". In: *Nature* 562.7725 (2018), pp. 76–81.

[48] R D Kornberg and Y Lorch. "Chromatin Structure and Transcription". In: *Annu Rev Cell Biol.* 8 (1992), pp. 563–587.

[49] Gregory D Bowman and Michael G Poirier. "Post-translational modifications of histones that influence nucleosome dynamics". In: *Chem Rev.* 115.6 (2015), pp. 2274–2295.

[50] Suehyb G. Alkhatib and Joseph W. Landry. "The Nucleosome Remodeling Factor". In: *FEBS Lett.* 585.20 (2016), pp. 3197–3207.

[51] Andrew J. Bannister et al. "Selective recognition of methylated lysine 9 on histone H3 by the HP1 chromo domain". In: *Nature* 410.6824 (2001), pp. 120–124.

[52] Yingming Zhao and Benjamin A. Garcia. "Comprehensive Catalog of Currently Documented Histone Modifications". In: *Cold Spring Harb Perspect Biol.* 7.9 (2015), a025064.

[53] Morgan A Sammons et al. "TP53 engagement with the genome occurs in distinct local chromatin environments via pioneer factor activity". In: *Genome Research* 25.2 (2014), pp. 179–188.

[54] Efrat Lidor Nili et al. "p53 binds preferentially to genomic regions with high DNA-encoded nucleosome occupancy". In: *Genome Res.* 20.10 (2010), pp. 1361–1368.

[55] Dan Su et al. "Interactions of Chromatin Context, Binding Site Sequence Content, and Sequence Evolution in Stress-Induced p53 Occupancy and Transactivation". In: *PLoS Genet* 11.1 (2015), e1004885.

[56] R Murr et al. "Orchestration of chromatin-based processes: mind the TRRAP". In: *Nature* 26 (2007), pp. 5358–5372.

[57] Nickolai A. Barlev et al. "Acetylation of p53 Activates Transcription through Recruitment of Coactivators/Histone Acetyltransferases". In: *Molecular Cell* 8.6 (2001), pp. 1243–1254.

[58] Joequim E. Espinosa and Beverly M. Emerson. "Transcriptional Regulation by p53 through Intrinsic DNA/Chromatin Binding and Site-Directed Cofactor Recruitment". In: *Molecular Cell* 8.1 (2001), pp. 57–69.

[59] Geetaram Sahu et al. "p53 Binding to Nucleosomal DNA Depends on the Rotational Positioning of DNA Response Element". In: *Journal of Biological Chemistry* 285.2 (2010), pp. 1321–1332.

[60] William C Ho, Mary X Fitzgerald, and Ronen Marmorstein. "Structure of the p53 core domain dimer bound to DNA". In: *Journal of Biological Chemistry* 281.29 (2006), pp. 20494–20502.

[61] S.A. Forbes et al. "COSMIC: High-Resolution Cancer Genetics Using the Catalogue of Somatic Mutations in Cancer". In: *Current Protocols in Human Genetics* (2018).

[62] COSMIC. *COSMIC - Catalogue of Somatic Mutations in Cancer*. https://cancer.sanger.ac.uk/cos [Accessed 16.01.2024].

[63] Liacine Bouaoun et al. "TP53 Variations in Human Cancers: New Lessons from the IARC TP53 Database and Genomics Data". In: *Hum Mutat.* 37.9 (2016), pp. 865–876.

[64] Evan H Baugh et al. "Why are there hotspot mutations in the TP53 gene in human cancers?" In: *Cell Death & Differentiation* 25 (2018), pp. 154–160.

[65] Magali Olivier, Monica Hollstein, and Pierre Hainaut. "TP53 Mutations in Human Cancers: Origins, Consequences, and Clinical Use". In: *Cold Spring Harb Perspect Biol.* 2.1 (2009), a001008.

[66] Catherine Vaughan et al. "p53: its mutations and their impact on transcription". In: *Subcell Biochem.* 85 (2014), pp. 71–90.

[67] Jae-Cheol Lee et al. "Protein L-isoaspartyl methyltransferase regulates p53 activity". In: *Nature Communications* 3 (2012), p. 927.

[68] Xian Zhang et al. "TRAF6 restricts p53 mitochondrial translocation, apoptosis and tumor suppression". In: *Mol Cell* 64.4 (2016), pp. 803–814.

[69] Shin'ichi Saito et al. "Phosphorylation site interdependence of human p53 post-translational modifications in response to stress". In: *J Biol Chem.* 278.39 (2003), pp. 37536–37544.

[70] Kazuyasu Sakaguchi et al. "DNA damage activates p53 through a phosphorylation–acetylation cascade". In: *Genes Dev.* 12.18 (1998), pp. 2831–2841.

[71] Thomas Buschmann et al. "Jun NH2-Terminal Kinase Phosphorylation of p53 on Thr-81 Is Important for p53 Stabilization and Transcriptional Activities in Response to Stress". In: *Mol Cell.* 21.8 (2001), pp. 2743–2754.

[72] Y Higashimoto et al. "Human p53 is phosphorylated on serines 6 and 9 in response to DNA damage-inducing agents". In: *J Biol Chem* 275.30 (2000), pp. 23199–23203.

[73] Heng-Hong Li et al. "Phosphorylation on Thr-55 by TAF1 mediates degradation of p53: a role for TAF1 in cell G1 progression". In: *Mol Cell.* 13.6 (2004), pp. 867–78.

[74] Heng-Hong Li et al. "A specific PP2A regulatory subunit, B56gamma, mediates DNA damage-induced dephosphorylation of p53 at Thr55". In: *EMBO J* 26.2 (2007), pp. 402–411.

[75] Yong Wu et al. "Phosphorylation of p53 by TAF1 inactivates p53-dependent transcription in the DNA damage response". In: *Mol Cell.* 53.1 (2014), pp. 63–74.

[76] Linda M. Smith Jayne Loughery Miranda Cox and David W. Meek. "Critical role for p53-serine 15 phosphorylation in stimulating transactivation at p53-responsive promoters". In: *Nucleic Acids Research* 42.12 (2014), pp. 7666–7680.

[77] Ashley L Craig et al. "ΔNp63 transcriptionally regulates ATM to control p53 Serine-15 phosphorylation". In: *Mol Cancer* 9.195 (2010).

[78] Bianca M. Sirbu et al. "ATR-p53 Restricts Homologous Recombination in Response to Replicative Stress but Does Not Limit DNA Interstrand Crosslink Repair in Lung Cancer Cells". In: *PLoS One* 6.8 (2011).

[79] Paul F. Lambert et al. "Phosphorylation of p53 Serine 15 Increases Interaction with CBP". In: *Journal of Biological Chemistry* 273.49 (1998), pp. 33048–33053.

[80] Michele Fiscella et al. "Wip1, a novel human protein phosphatase that is induced in response to ionizing radiation in a p53-dependent manner". In: *PNAS* 94.12 (1997), pp. 6048–6053.

[81] D W-C Li et al. "Protein serine/threonine phosphatase-1 dephosphorylates p53 at Ser-15 and Ser-37 to modulate its transcriptional and apoptotic activities". In: *Oncogene* 25.21 (2006), pp. 3006–3022.

[82] David W Meek Nicolas Dumaz Diane M Milne. "Protein kinase CK1 is a p53-threonine 18 kinase which requires prior phosphorylation of serine 15". In: *FEBS Letters* 463.3 (2000), pp. 312–316.

[83] Oliver Schon et al. "Molecular Mechanism of the Interaction between MDM2 and p53". In: *Journal of Molecular Biology* 323.3 (2009), pp. 491–501.

[84] S Y Shieh et al. "The human homologs of checkpoint kinases Chk1 and Cds1 (Chk2) phosphorylate p53 at multiple DNA damage-inducible sites". In: *Genes Dev* 14.3 (2000), pp. 289–300.

[85] Gaetan A Turenne1 and Brendan D Price. "Glycogen synthase kinase3 beta phosphorylates serine 33 of p53 and activates p53's transcriptional activity". In: *BMC Cell Biol.* 2.12 (2001).

[86] D M Milne et al. "Phosphorylation of the p53 tumour-suppressor protein at three N-terminal sites by a novel casein kinase I-like enzyme". In: *Oncogene* 7.7 (1992), pp. 1361–1369.

[87] Shigeki Arai et al. "Novel homeodomain-interacting protein kinase family member, HIPK4, phosphorylates human p53 at serine 9". In: *FEBS Lett.* 581.21 (2000), pp. 5649–5657.

[88] Senthil K. Radhakrishnan and Andrei L. Gartel. "CDK9 Phosphorylates p53 on Serine Residues 33, 315 and 392". In: *Cell Cycle* 5.5 (2006), pp. 519–521.

[89] Kathleen M Dohoney et al. "Phosphorylation of p53 at serine 37 is important for transcriptional activity and regulation in response to DNA damage". In: *Oncogene* 23.1 (2006), pp. 49–57.

[90] X Shang et al. "Dual-specificity phosphatase 26 is a novel p53 phosphatase and inhibits p53 tumor suppressor functions in human neuroblastoma". In: *Oncogene* 29.35 (2010), pp. 4938–4946.

[91] Paola Zacchi et al. "The prolyl isomerase Pin1 reveals a mechanism to control p53 functions after genotoxic insults". In: *Nature* 419.6909 (2002), pp. 853–857.

[92] Hongwu Zheng et al. "The prolyl isomerase Pin1 is a regulator of p53 in genotoxic response". In: *Nature* 419.6909 (2002), pp. 849–853.

[93] Yang Chen et al. "Prolyl isomerase Pin1: a promoter of cancer and a target for therapy". In: *Cell Death Dis.* 9.9 (2018), p. 883.

[94] Gerburg M Wulf et al. "Role of Pin1 in the regulation of p53 stability and p21 transactivation, and cell cycle checkpoints in response to DNA damage". In: *J Biol Chem* 277.50 (2002), pp. 47976–47979.

[95] Eric R. Wolf et al. "Mutant and wild-type p53 complex with p73 in response to JNK phosphorylation". In: *Sci Signal* 11.524 (2018), eaao4170.

[96] K Oda et al. "p53AIP1, a potential mediator of p53-dependent apoptosis, and its regulation by Ser-46-phosphorylated p53". In: *Cell* 102.6 (2000), pp. 849–862.

[97] Leonie Smeenk et al. "Role of p53 serine 46 in p53 target gene regulation". In: *PLoS One* 6.3 (2011), e17574.

[98] Naoe Taira et al. "DYRK2 Is Targeted to the Nucleus and Controls p53 via Ser46 Phosphorylation in the Apoptotic Response to DNA Damage". In: *Mol Cell.* 25.5 (2007), pp. 725–738.

[99] Cinzia Rinaldo et al. "MDM2-Regulated Degradation of HIPK2 Prevents p53Ser46 Phosphorylation and DNA Damage-Induced Apoptosis". In: *Mol Cell.* 25.5 (2007), pp. 739–750.

[100] Kiyotsugu Yoshida 1, Hanshao Liu, and Yoshio Miki. "Protein kinase C delta regulates Ser46 phosphorylation of p53 tumor suppressor in the apoptotic response to DNA damage". In: *J Biol Chem.* 281.9 (2006), pp. 5734–5740.

[101] Shin'ichi Saito et al. "ATM mediates phosphorylation at multiple p53 sites, including Ser(46), in response to ionizing radiation". In: *J Biol Chem.* 277.15 (2002), pp. 12491–12494.

[102] Jean-Luc Perfettini et al. "Protein kinase C delta regulates Ser46 phosphorylation of p53 tumor suppressor in the apoptotic response to DNA damage". In: *J Exp Med* 201.2 (2005), pp. 279–289.

[103] Dana W Aswad, Mallik V Paranandi, and Brandon T Schurter. "Isoaspartate in peptides and proteins: formation, significance, and analysis". In: *J Pharm Biomed Anal.* 21.6 (2000), pp. 1129–1136.

[104] Bech-Otschir D et al. "COP9 signalosome-specific phosphorylation targets p53 to degradation by the ubiquitin system". In: *EMBO J* 20 (2001), pp. 1630–1639.

[105] Lykke-Andersen K et al. "Disruption of the COP9 signalosome CSN2 subunit in mice causes deficient cell proliferation, accumulation of p53 and cyclin E, and early embryonic death". In: *Mol Cell Biol* 23.19 (2003), pp. 6790–6797.

[106] Qiyuan Liu et al. "Aurora-A abrogation of p53 DNA binding and transactivation activity by phosphorylation of serine 215". In: *Journal of Biological Chemistry* 279.50 (2004), pp. 52175–52182.

[107] Jennifer A Fraser, Borivoj Vojtesek, and Ted R Hupp. "A novel p53 phosphorylation site within the MDM2 ubiquitination signal: I. phosphorylation at SER269 in vivo is linked to inactivation of p53 function". In: *Journal of Biological Chemistry* 285.48 (2010), pp. 37762–3772.

[108] Jennifer A Fraser et al. "A novel p53 phosphorylation site within the MDM2 ubiquitination signal: II. a model in which phosphorylation at SER269 induces a mutant conformation to p53". In: *Journal of Biological Chemistry* 285.48 (2010), pp. 37773–37786.

[109] Yi-Fu Huang et al. "Isg15 controls p53 stability and functions". In: *Cell Cycle* 13.14 (2014), pp. 2199–2209.

[110] Yi-Fu Huang and Dmitry V Bulavin. "Oncogene-mediated regulation of p53 ISGylation and functions". In: *Oncotarget* 5.14 (2014), pp. 5808–5818.

[111] Kai-Wei Hsueh et al. "A novel Aurora-A-mediated phosphorylation of p53 inhibits its interaction with MDM2". In: *Biochem Biophys Acta* 1834.2 (2013), pp. 508–515.

[112] Stephen M Sykes et al. "Acetylation of the p53 DNA-binding domain regulates apoptosis induction". In: *Mol Cell* 24.6 (2006), pp. 841–851.

[113] Yi Tang et al. "Tip60-dependent acetylation of p53 modulates the decision between cell-cycle arrest and apoptosis". In: *Mol Cell* 24.6 (2006), pp. 827–839.

[114] Heinz Neumann, Sew Y Peak-Chew, and Jason W Chin. "Genetically encoding N(epsilon)-acetyllysine in recombinant proteins". In: *Nat Chem Biol* 4.4 (2008), pp. 232–234.

[115] Eyal Arbely et al. "Acetylation of lysine 120 of p53 endows DNA-binding specificity at effective physiological salt concentration". In: *PNAS* 108.20 (2011), pp. 8251–8256.

[116] Radion Vainer et al. "Structural Basis for p53 Lys120-Acetylation-Dependent DNA-Binding Mode". In: *Journal of Molecular Biology* 428.15 (2016), pp. 3013–3025.

[117] Yi Tang et al. "Acetylation is indispensable for p53 activation". In: *Cell* 133.4 (2008), pp. 612–626.

[118] Tongyuan Li et al. "Tumor suppression in the absence of p53-mediated cell-cycle arrest, apoptosis, and senescence". In: *Cell* 149.6 (2012), pp. 1269–1283.

[119] Shang-Jui Wang et al. "Acetylation Is Crucial for p53-mediated Ferroptosis and Tumor Suppression". In: *Cell Rep* 17.2 (2017), pp. 366–373.

[120] Dong Hwan Ho et al. "Leucine-Rich Repeat Kinase 2 (LRRK2) phosphorylates p53 and induces p21WAF1/CIP1 expression". In: *Mol Brain* 8.54 (2015).

[121] Olivier Pluquet et al. "Endoplasmic reticulum stress accelerates p53 degradation by the cooperative actions of Hdm2 and glycogen synthase kinase 3beta". In: *Mol Cell Biol* 25.21 (2005), pp. 9392–9405.

[122] Laurent Le Cam et al. "E4F1 Is an Atypical Ubiquitin Ligase that Modulates p53 Effector Functions Independently of Degradation". In: *Cell* 127.4 (2009), pp. 775–788.

[123] Wassim M. Abida et al. "FBXO11 Promotes the Neddylation of p53 and Inhibits Its Transcriptional Activity". In: *J Biol Chem.* 282.3 (2007), pp. 1797–1804.

[124] Yan-Hsiung Wang et al. "Identification and Characterization of a Novel p300-mediated p53 Acetylation Site, Lysine 305". In: *J Biol Chem.* 278.28 (2003), pp. 25568–25576.

[125] L Liu et al. "p53 sites acetylated in vitro by PCAF and p300 are acetylated in vivo in response to DNA damage". In: *Mol Cell Biol* 19.2 (1999), pp. 1202–1209.

[126] Chad D. Knights et al. "Distinct p53 acetylation cassettes differentially influence gene-expression patterns and cell fate". In: *J Cell Biol* 173.4 (2006), pp. 533–544.

[127] Connie Chao et al. "Acetylation of mouse p53 at lysine 317 negatively regulates p53 apoptotic activities after DNA damage". In: *Mol Cell Biol* 26.18 (2006), pp. 6859–69.

[128] Se-In Lee et al. "HDAC6 preserves BNIP3 expression and mitochondrial integrity by deacetylating p53 at lysine 320". In: *Biochem Biophys Res Commun* 691 (2024), p. 149320.

[129] Yanlu Xiong et al. "SIRT3 deacetylates and promotes degradation of P53 in PTEN-defective non-small cell lung cancer". In: *J Cancer Res Clin Oncol* 144.2 (2018), pp. 189–198.

[130] Jovanka Gencel-Augusto and Guillermina Lozano. "p53 tetramerization: at the center of the dominant-negative effect of mutant p53". In: *Cell Cycle* 15.11 (2020), pp. 1425–1438.

[131] Martin Jansson et al. "Arginine methylation regulates the p53 response". In: *Nature Cell Biology* 10.12 (2008), pp. 1431–1439.

[132] Jan-Philipp Kruse and Wei Gu. "MSL2 Promotes Mdm2-independent Cytoplasmic Localization of p53". In: *Journal of Biological Chemistry* 284.5 (2009), pp. 3250–3263.

[133] Wei Gu and Robert G. Roeder. "Activation of p53 Sequence-Specific DNA Binding by Acetylation of the p53 C-Terminal Domain". In: *Cell* 90.4 (1997), pp. 595–606.

[134] Zhangchuan Xia et al. "Deciphering the acetylation code of p53 in transcription regulation and tumor suppression". In: *Oncogene* 41.22 (2022), pp. 3039–3050.

[135] M S Rodriguez et al. "Multiple C-terminal lysine residues target p53 for ubiquitin-proteasome-mediated degradation". In: *Mol Cell Biol* 20.22 (2000), pp. 8458–8467.

[136] Masha V Poyurovsky et al. "The C terminus of p53 binds the N-terminal domain of MDM2". In: *Nat Struct Mol Biol* 17.8 (2010), pp. 982–989.

[137] Lijin Feng et al. "Functional Analysis of the Roles of Posttranslational Modifications at the p53 C Terminus in Regulating p53 Stability and Activity". In: *Mol Cell Biol* 25.13 (2005), pp. 5389–5395.

[138] Pierre-Jacques Hamard et al. "The C terminus of p53 regulates gene expression by multiple mechanisms in a target- and tissue-specific manner in vivo". In: *Genes Dev.* 27.17 (2013), pp. 1868–1885.

[139] Iva Simeonova et al. "Mutant mice lacking the p53 C-terminal domain model telomere syndromes". In: *Cell Rep.* 3.6 (2013), pp. 2046–2058.

[140] Donglai Wang et al. "Acetylation-regulated interaction between p53 and SET reveals a widespread regulatory mode". In: *Nature* 538.7623 (2016), pp. 118–122.

[141] Ning Kon et al. "Robust p53 stabilization is dispensable for its activation and tumor suppressor function". In: *Cancer Res.* 81.4 (2021), pp. 935–944.

[142] Takao Fujisawa and Panagis Filippakopoulos. "Functions of bromodomain-containing proteins and their roles in homeostasis and cancer". In: *Nature Reviews Molecular Cell Biology* 18 (2017), pp. 246–262.

[143] Shiraz Mujtaba et al. "Structural Mechanism of the Bromodomain of the Coactivator CBP in p53 Transcriptional Activation". In: *Mol Cell.* 13.2 (2004), pp. 251–263.

[144] Andrew G. Li et al. "An Acetylation Switch in p53 Mediates Holo-TFIID Recruitment". In: *Mol Cell.* 28.3 (2007), pp. 408–421.

[145] Weijia Cai et al. "PBRM1 acts as a p53 lysine-acetylation reader to suppress renal tumor growth". In: *Nat Commun.* 10 (2019), p. 5800.

[146] Sara M. Reed and Dawn E. Quelle. "p53 Acetylation: Regulation and Consequences". In: *Cancers (Basel)* 7.1 (2015), pp. 30–69.

[147] Xiaobing Shi et al. "Modulation of p53 function by SET8-mediated methylation at lysine 382". In: *Mol Cell* 27.4 (2022), pp. 636–466.

[148] Jing Huang et al. "Repression of p53 activity by Smyd2-mediated methylation". In: *Nature* 444 (2006), pp. 629–632.

[149] Gleb S. Ivanov et al. "Methylation-Acetylation Interplay Activates p53 in Response to DNA Damage". In: *Mol Cell Biol* 27.19 (2007), pp. 6756–6769.

[150] Julia K. Kurash et al. "Methylation of p53 by Set7/9 Mediates p53 Acetylation and Activity In Vivo". In: *Mol Cell.* 29.3 (2008), pp. 392–400.

[151] Bernhard Lehnertz et al. "p53-dependent transcription and tumor suppression are not affected in Set7/9-deficient mice". In: *Mol Cell* 43.4 (2011), pp. 673–860.

[152] Stefano Campaner et al. "Methylation-Acetylation Interplay Activates p53 in Response to DNA Damage". In: *Mol Cell* 43.4 (2011), pp. 681–688.

[153] Jing Huang et al. "p53 is regulated by the lysine demethylase LSD1". In: *Nature* 449.7158 (2007), pp. 5983–5991.

[154] Shwu-Yuan Wu and Cheng-Ming Chiang. "Crosstalk between sumoylation and acetylation regulates p53-dependent chromatin transcription and DNA binding". In: *EMBO J.* 28.9 (2009), pp. 1246–1259.

[155] Stephanie Carter et al. "C-terminal modifications regulate MDM2 dissociation and nuclear export of p53". In: *Nature Cell Biology* 9 (2007), pp. 428–435.

[156] M J Waterman et al. "ATM-dependent activation of p53 involves dephosphorylation and association with 14-3-3 proteins". In: *Nat Genet* 19.2 (1998), pp. 175–178.

[157] Benjamin Schumacher et al. "Structure of the p53 C-terminus bound to 14-3-3: Implications for stabilization of the p53 tetramer". In: *FEBS Lett.* 584.8 (2010), pp. 1443–1448.

[158] I Takenaka et al. "Regulation of the sequence-specific DNA binding function of p53 by protein kinase C and protein phosphatases". In: *Mol Brain* 270.10 (1995), pp. 5405–5411.

[159] K Sakaguchi et al. "Effect of phosphorylation on tetramerization of the tumor suppressor protein p53". In: *J Protein Chem* 16.5 (1997), pp. 553–556.

[160] Mari B. Ishak Gabra et al. "IKKβ activates p53 to promote cancer cell adaptation to glutamine deprivation". In: *Oncogenesis* 7.11 (2018), p. 93.

[161] Aimee I. Badeaux and Yang Shi. "Emerging roles for chromatin as a signal integration and storage platform". In: *Nature Reviews Molecular Cell Biology* 14 (2013), pp. 211–224.

[162] Uwe Knippschild et al. "The CK1 Family: Contribution to Cellular Stress Response and Its Role in Carcinogenesis". In: *Front Oncol* 4.96 (2014).

[163] Lorna J. Warnock et al. "Role of phosphorylation in p53 acetylation and PAb421 epitope recognition in baculoviral and mammalian expressed proteins". In: *The FEBS Journal* 272.7 (2005), pp. 1669–1675.

[164] L J Warnock et al. "Crosstalk between site-specific modifications on p53 and histone H3". In: *Oncogene* 27.11 (2008), pp. 1639–1644.

[165] Dmitry V. Bulavin et al. "Phosphorylation of human p53 by p38 kinase coordinates N-terminal phosphorylation and apoptosis in response to UV radiation". In: *The EMBO Journal* 18.23 (1999), pp. 6845–6854.

[166] L Kim and A R Kimmel. "GSK3, a master switch regulating cell-fate specification and tumorigenesis". In: *Curr Opin Genet Dev.* 10.5 (2000), pp. 508–514.

[167] Yi-Hung Ou et al. "p53 C-Terminal Phosphorylation by CHK1 and CHK2 Participates in the Regulation of DNA-Damage-induced C-Terminal Acetylation". In: *Mol Biol Cell.* 16.4 (2005), pp. 1684–1695.

[168] Sofia Margiola, Karola Gerecht, and Manuel M. Müller. "Semisynthetic 'designer' p53 sheds light on a phosphorylation–acetylation relay". In: *Chem Sci.* 12.24 (2021), pp. 8563–8570.

[169] Xin Liu et al. "The structural basis of protein acetylation by the p300/CBP transcriptional coactivator". In: *Nature* 451.7180 (2008), pp. 846–850.

[170] Manuela Delvecchio et al. "Structure of the p300 catalytic core and implications for chromatin targeting and HAT regulation". In: *Nature Structural and Molecular Biology* 20 (2013), pp. 1040–1046.

[171] Josephine C. Ferreon et al. "Cooperative regulation of p53 by modulation of ternary complex formation with CBP/p300 and HDM2". In: *PNAS* 106.16 (2009), pp. 6591–6596.

[172] Lisa M Miller Jenkins et al. "Two distinct motifs within the p53 transactivation domain bind to the Taz2 domain of p300 and are differentially affected by phosphorylation". In: *Biochemistry* 48.6 (2009), pp. 1244–1255.

[173] Hanqiao Feng et al. "Structural Basis for p300 Taz2/p53 TAD1 Binding and Modulation by Phosphorylation". In: *Structure* 17.2 (2010), pp. 202–210.

[174] Smarajit Polley et al. "Differential recognition of phosphorylated transactivation domains of p53 by different p300 domains". In: *J Mol Biol* 376.1 (2008), pp. 8–12.

[175] Chul Won Lee et al. "Graded enhancement of p53 binding to CREB-binding protein (CBP) by multisite phosphorylation". In: *PNAS* 107.45 (2010), pp. 19290–19295.

[176] Susumu Rokudai et al. "Monocytic Leukemia Zinc Finger (MOZ) Interacts with p53 to Induce p21 Expression and Cell-cycle Arrest". In: *Journal of Biological Chemistry* 248.1 (2009), pp. 237–244.

[177] Aneta Kozeleková et al. "Phosphorylated and Phosphomimicking Variants May Differ—A Case Study of 14-3-3 Protein". In: *Front. Chem* 10 (2022), e835733.

[178] Manuel Müller. "Chemical Protein Synthesis: Strategies and Biological Applications". In: *Chemical and Biological Synthesis: Enabling Approaches for Understanding Biology*. Ed. by Nick J Westwood and Adam Nelson. London: The Royal Society of Chemistry, 2018. Chap. 13.

[179] Irene Coin, Michael Beyermann, and Michael Bienert. "Solid-phase peptide synthesis: from standard procedures to the synthesis of difficult sequences". In: *Nature protocols* 2 (2007), pp. 3247–3256.

[180] P E Dawson et al. "Synthesis of proteins by native chemical ligation". In: *Science* 266.5186 (1994), pp. 776–779.

[181] Duhee Bang, Brad L. Pentelute, and Stephen B. H. Kent. "Kinetically controlled ligation for the convergent chemical synthesis of proteins". In: *Angew Chem Int Ed Engl.* 45.24 (2006), pp. 3985–3988.

[182] Tom W. Muir, Dolan Sondhi, and Philip A. Cole. "Expressed protein ligation: A general method for protein engineering". In: *PNAS* 95.12 (1998), pp. 6705–6710.

[183] Hao Wang et al. "Protein Splicing of Inteins: A Powerful Tool in Synthetic Biology". In: *Front Bioeng Biotechnol* 10 (2022), p. 810180.

[184] Mia A. Shandell, Zhongping Tan, and Virginia W. Cornish. "Genetic Code Expansion: A Brief History and Perspective". In: *Biochemistry* 60.46 (2021), pp. 3455–3469.

[185] Miguel Angel Rubio Gomez and Michael Ibba. "Aminoacyl-tRNA synthetases". In: *RNA* 26.8 (2020), pp. 910–936.

[186] Yasukazu Nakamura, Takashi Gojobori, and Toshimichi Ikemura. "Codon usage tabulated from international DNA sequence databases: status for the year 2000". In: *Nucleic Acids Research* 28.1 (2000), p. 292.

[187] Gayathri Srinivasan, Carey M James, and Joseph A Krzycki. "Pyrrolysine encoded by UAG in Archaea: charging of a UAG-decoding specialized tRNA". In: *Science* 296.5572 (2002), pp. 1459–1462.

[188] Bing Hao et al. "A new UAG-encoded residue in the structure of a methanogen methyltransferase". In: *Science* 296.5572 (2002), pp. 1462–1466.

[189] Abhishek Chatterjee et al. "A versatile platform for single- and multiple-unnatural amino acid mutagenesis in Escherichia coli". In: *Biochemistry* 52.10 (2003), pp. 1828–1837.

[190] Jianming Xie and Peter G. Schultz. "An expanding genetic code". In: *Methods* 36.3 (2005), pp. 227–238.

[191] David B.F. Johnson et al. "RF1 Knockout Allows Ribosomal Incorporation of Unnatural Amino Acids at Multiple Sites". In: *Nat Chem Biol.* 7.11 (2011), pp. 779–786.

[192] Sviatlana Smolskaya and Yaroslav A. Andreev. "Site-Specific Incorporation of Unnatural Amino Acids into Escherichia coli Recombinant Protein: Methodology Development and Recent Achievement". In: *Biomolecules.* 9.7 (2019), a255.

[193] Xiaozhou Luo et al. "Genetically encoding phosphotyrosine and its nonhydrolyzable analog in bacteria". In: *Nat Chem Biol.* 13.8 (2017), pp. 845–849.

[194] Duy P. Nguyen et al. "Genetically Encoding Nϵ-Methyl-l-lysine in Recombinant Histones". In: *J. Am. Chem. Soc.* 131.40 (2009), pp. 14194–14195.

[195] Alexandra Julier et al. "Generation and Characterization of Site-Specifically Mono-Ubiquitylated p53". In: *Chembiochem* 23.6 (2022), e202100659.

[196] Zhipeng A. Wang et al. "A Genetically Encoded Allysine for the Synthesis of Proteins with Site-specific Lysine Dimethylation". In: *Angew Chem Int Ed Engl.* 56.1 (2017), pp. 212–216.

[197] P V Nikolova et al. "Semirational design of active tumor suppressor p53 DNA binding domain with enhanced stability". In: *Proc Natl Acad Sci U S A.* 95.25 (1998), pp. 14675–14680.

[198] Tom J Petty et al. "Structural Basis for p53 Lys120-Acetylation-Dependent DNA-Binding Mode". In: *EMBO J* 30.11 (2011), pp. 2167–2176.

[199] George Farmer et al. "Wild-type p53 activates transcription in vitro". In: *Nature* 358.6381 (1992), pp. 83–86.

[200] Heinz Neumann et al. "A method for genetically installing site-specific acetylation in recombinant histones defines the effects of H3 K56 acetylation". In: *Mol Cell* 36.1 (2009), pp. 153–163.

[201] Stefan Bell, Silke Hansen, and Johannes Buchner. "Refolding and structural characterization of the human p53 tumor suppressor protein". In: *Biophysical Chemistry* 96.2-3 (2001), pp. 243–257.

[202] Boris Görke and Jörg Stülke. "Isoaspartate in peptides and proteins: formation, significance, and analysis". In: *J Pharm Biomed Anal.* 21.6 (2000), pp. 1129–1136.

[203] F. William Studier. "Protein production by auto-induction in high-density shaking cultures". In: *Protein Expression and Purification* 41.1 (2005), pp. 207–234.

[204] Jared T Hammill et al. "Preparation of site-specifically labeled fluorinated proteins for 19F-NMR structural characterization". In: *Nat Protoc.* 2.10 (2007), pp. 2601–2607.

[205] Jennifer C Peeler and Ryan A Mehl. "Site-specific incorporation of unnatural amino acids as probes for protein conformational changes". In: *Methods Mol Biol* 794 (2012), pp. 125–134.

[206] Michael Muzika et al. "Chemically-defined lactose-based autoinduction medium for site-specific incorporation of non-canonical amino acids into proteins". In: *RSC Adv* 8.45 (2018), pp. 2601–2607.

[207] Simone Balzer et al. "A comparative analysis of the properties of regulated promoter systems commonly used for recombinant gene expression in Escherichia coli". In: *Microbial Cell Factories* 12 (2013), p. 26.

[208] Wesley Wei Wang et al. "A Click Chemistry Approach Reveals the Chromatin-Dependent Histone H3K36 Deacylase Nature of SIRT7". In: *J Am Chem Soc* 141.6 (2019), pp. 2462–2473.

[209] Sung Kuk Lee et al. "Directed Evolution of AraC for Improved Compatibility of Arabinose- and Lactose-Inducible Promoters". In: *Appl Environ Microbiol* 73.18 (2007), pp. 5711–5715.

[210] Justin J Lin and Michael Carey. "In vitro transcription and immobilized template analysis of preinitiation complexes". In: *Curr Protoc Mol Biol* 12 (2012).

[211] J D Dignam, R M Lebovitz, and R G Roeder. "Accurate transcription initiation by RNA polymerase II in a soluble extract from isolated mammalian nuclei". In: *Nucleic Acids Research* 11.5 (1983), pp. 1475–1489.

[212] Jill Bargonetti et al. "Wild-Type but Not Mutant p53 lmmunopurified Proteins Bind to Sequences Adjacent to the SV40 Origin of Replication". In: *Cell* 65 (1991), pp. 1063–1091.

[213] Xuan Liu and Arnold J. Berk. "Reversal of In Vitro p53 Squelching by both TFIIB and TFIID". In: *Molecular And Cellular Biology* 15.11 (1995), pp. 6474–6478.

[214] Tae Kook Kim. "In Vitro Transcriptional Activation of p21 Promoter by p53". In: *Biochemical and Biophysical Research Communications* (1997).

[215] M Mundt et al. "Protein interactions at the carboxyl terminus of p53 result in the induction of its in vitro transactivation potential". In: *Oncogene* 15.2 (1997), pp. 237–244.

[216] I Chesnokov et al. "p53 inhibits RNA polymerase III-directed transcription in a promoter-dependent manner". In: *Mol Cell Biol* 16.12 (1996), pp. 7084–7088.

[217] Hyunjung Kim et al. "p53 Requires an Intact C-Terminal Domain for DNA Binding and Transactivation". In: *J Mol Biol.* 415.5 (2012), pp. 843–854.

[218] Jeong Hyeon Park and Natisha Magan. "Reverse Transcriptase-Coupled Quantitative Real Time PCR Analysis of Cell-Free Transcription on the Chromatin-Assembled p21 Promoter". In: *PLoS One* 6.8 (2021), e23617.

[219] Jeremy S. Paige, Karen Wu, and Samie R. Jaffrey. "RNA mimics of green fluorescent protein". In: *Science* 333.6042 (2011), pp. 642–646.

[220] Grigory S. Filonov et al. "Broccoli: Rapid Selection of an RNA Mimic of Green Fluorescent Protein by Fluorescence-Based Selection and Directed Evolution". In: *J. Am. Chem. Soc.* 136.46 (2014), pp. 16299–16308.

[221] Saskia Neubacher and Sven Hennig. "RNA Structure and Cellular Applications of Fluorescent Light-Up Aptamers". In: *Angew Chem Int Ed Engl.* 58.5 (2019), pp. 1266–1279.

[222] Shinsuke Sando et al. "Transcription monitoring using fused RNA with a dye-binding light-up aptamer as a tag: a blue fluorescent RNA". In: *Chem Commun (Camb)* 7.3 (2008), pp. 3858–3860.

[223] Weitong Qin et al. "High-throughput iSpinach fluorescent aptamer-based real-time monitoring of in vitro transcription". In: *Bioresources and Bioprocessing* 9 (2022), a112.

[224] Alexis Autour, Eric Westhof, and Michael Ryckelynck. "iSpinach: a fluorogenic RNA aptamer optimized for in vitro applications". In: *Nucleic Acids Res.* 44.6 (2016), pp. 2491–2500.

[225] W S el-Deiry et al. "WAF1, a potential mediator of p53 tumor suppression". In: *Cell* 75.4 (1993), pp. 817–825.

[226] Martin Fischer, Lydia Steiner, and Kurt Engeland. "The transcription factor p53: Not a repressor, solely an activator". In: *Cell Cycle* 13.19 (2014), pp. 3037–3058.

[227] Jung-Shin Lee, Edwin Smith, and Ali Shilatifard. "The language of histone crosstalk". In: *Cell* 142.5 (2010), pp. 682–685.

[228] Mario Leutert, Samuel W. Entwisle, and Judit Villén. "Decoding Post-Translational Modification Crosstalk With Proteomics". In: *Mol Cell Proteomics* 20 (2021).

[229] Uyen T. T. Nguyen et al. "Accelerated Chromatin Biochemistry Using DNA-Barcoded Nucleosome Libraries". In: *Nat Methods* 11.8 (2015), pp. 834–840.

[230] Masami Kodama et al. "Requirement of ATM for Rapid p53 Phosphorylation at Ser46 without Ser/Thr-Gln Sequences". In: *Mol Cell Biol* 30.7 (2010), pp. 1620–1633.

[231] Danrui Cui et al. "The Cross Talk Between p53 and mTOR Pathways in Response to Physiological and Genotoxic Stresses". In: *Front. Cell Dev. Biol* 9 (2021), p. 775507.

[232] J Böhm, E J Schlaeger, and R Knippers. "Acetylation of nucleosomal histones in vitro". In: *Eur J Biochem.* 112.2 (1980), pp. 353–362.

[233] Shai Duchin et al. "A continuous kinetic assay for protein and DNA methyltransferase enzymatic activities". In: *Epigenetics Chromatin.* 8.56 (1980).

[234] Hongbiao Huang et al. "Physiological levels of ATP negatively regulate proteasome function". In: *Cell Research* 20 (2010), pp. 1372–1385.

[235] Fiona M. Gribble et al. "A Novel Method for Measurement of Submembrane ATP Concentration". In: *The Journal of Biological Chemistry* 275.39 (2000), pp. 30046–30049.

[236] Kanaga Sabapathy and David P Lane. "Understanding p53 functions through p53 antibodies". In: *J Mol Cell Biol* 11.4 (2019), pp. 317–329.

[237] Nabil H. Chehab et al. "Phosphorylation of Ser-20 mediates stabilization of human p53 in response to DNA damage". In: *Proc Natl Acad Sci U S A.* 96.24 (1999), pp. 13777–13782.

[238] Xiaofeng Liu et al. "NAT10 regulates p53 activation through acetylating p53 at K120 and ubiquitinating Mdm2". In: *EMBO Rep.* 17.3 (2016), pp. 349–366.

[239] Zhaopeng Li and Ursula Rinas. "Recombinant protein production-associated metabolic burden reflects anabolic constraints and reveals similarities to a carbon overfeeding response". In: *Biotechnology and bioengineering* 118.1 (2021), pp. 94–105.

[240] Sandra Harper and David W. Speicher. "Purification of proteins fused to glutathione S-tranferase". In: *Methods Mol Biol* 681 (2011), pp. 259–280.

[241] Frank Schäfer et al. "Purification of GST-Tagged Proteins". In: *Methods Enzymol* 559 (2015), pp. 127–139.

[242] Jordan J. Lichty et al. "Comparison of affinity tags for protein purification". In: *Protein Expression and Purification* 41.1 (2005), pp. 98–105.

[243] Xavier Bernard et al. "Proteasomal Degradation of p53 by Human Papillomavirus E6 Oncoprotein Relies on the Structural Integrity of p53 Core Domain". In: *PLoS One* 6.10 (2011), e25981.